IN-1314

IN-1314

October 1969

CHEMICAL TECHNOLOGY BRANCH ANNUAL REPORT
FISCAL YEAR 1969

IDAHO NUCLEAR CORPORATION
NATIONAL REACTOR TESTING STATION
IDAHO FALLS, IDAHO

U. S. ATOMIC ENERGY COMMISSION

DISCLAIMER

Printed in the United States of America
Available from
Clearinghouse for Federal Scientific and Technical Information
National Bureau of Standards, U. S. Department of Commerce
Springfield, Virginia 22151
Price: Printed Copy $3.00; Microfiche $0.65

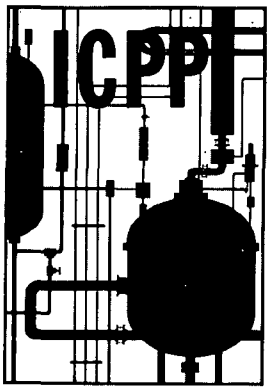

IN-1314
Issued: October 1969
General, Miscellaneous, and Progress Reports
TID-4500

MASTER

CHEMICAL TECHNOLOGY BRANCH ANNUAL REPORT FISCAL YEAR 1969

D. R. de Boisblanc
MANAGER
NUCLEAR AND CHEMICAL TECHNOLOGY DIVISION

J. A. Buckham
MANAGER
CHEMICAL TECHNOLOGY BRANCH

J. R. Bower
EDITOR

IDAHO NUCLEAR CORPORATION
A Jointly Owned Subsidiary of
AEROJET GENERAL CORPORATION
ALLIED CHEMICAL CORPORATION
PHILLIPS PETROLEUM COMPANY

U. S. Atomic Energy Commission Research and Development Report
Issued Under Contract AT(10-1)-1230
Idaho Operations Office

THIS PAGE

WAS INTENTIONALLY

LEFT BLANK

SUMMARY

The ICPP fuel processing facilities were essentially on standby during FY-1969 while the Waste Calcining Facility was being operated full time. Minor quantities of uranium were recovered from several fuel and scrap processing operations.

A feed clarification centrifuge is being installed to remove solids from dissolver solutions prior to introduction to the extraction process; laboratory studies indicate that separation, washing, and transfer of expected solids should proceed readily with no significant loss of uranium. Polymerized silica solids are minimized by coprocessing of high-silica aluminum fuel solutions with fluoride solutions from zirconium fuel dissolution. In solutions free of fluoride, gelatin or chemically inert solids were shown to ease handling by accelerating gel formation in high-acid silica-containing solutions, but no new coagulating agents were discovered. Uranium aluminide in fuel cores formed by powder metallurgy techniques was shown to dissolve more slowly than aluminum of the cladding or matrix material, and precautions will be taken to avoid carrying undissolved uranium out of the dissolver system when processing such materials. Descriptions of test reactor fuel elements (components, alloys, compositions, etc) have been summarized, and expected behavior during reprocessing has been projected. In additional plant support studies, it has been determined (a) that traces of fluoride from the first cycle scrubbing column should not cause corrosion in the zirconium process headend evaporator, (b) that no reagent superior to 0.5 M Na_2CO_3 has been found for scrubbing dibutyl phosphoric acid from the TBP-solvent stream, and (c) that no single-cycle process yet considered would satisfactorily remove plutonium and fission product contamination from the neptunium concentrate being recovered at the ICPP.

Design and safety analysis of the fluidized-bed denitration facility for converting recovered uranyl nitrate solutions to solid UO_3 are discussed, together with performance of the pilot-plant development unit.

Development of the fluidized-bed combustion process for graphite fuels is continuing with design of a concentric-chambered burner which greatly improves heat transfer capability and reliability of the system; pilot-plant tests to date indicate reliable performance over a wide range of operating conditions and indicate control over combustion conditions which, if not properly controlled, in theory could result in temperatures capable of melting stainless steel. Leaching studies of the product ash with nitric acid have demonstrated at least 99.8% recovery of uranium from niobium-containing fuels and 99.99% recovery of uranium from niobium-free fuels. Conceptual material balance flowsheets are presented for the combined combustion-leaching-solvent extraction process.

Design of the ICPP electrolytic dissolution system for EBR-II fuels is nearing completion: summaries presented include general aspects of the dissolver design, a process description, a proposed material balance flowsheet, results of pilot-plant studies on dissolution of actual EBR-II fuel elements, and results of varied laboratory studies involving chemical behavior of system components. Additional laboratory studies indicate that, while irradiation history and composition of stainless steel and aluminum alloy cladding materials

affect galvanostatic responses, all of these materials should dissolve readily in the electrolytic dissolver. Solids resulting from electrolytic dissolution were removed from the recycled dissolvent in varying degrees of effectiveness, ranging from 95% removal for stainless steel grains to 10% removal for fissium alloy residues, by use of experimental hydroclones.

During 7000 hours of operation of the Waste Calcining Facility in FY-1969, an 89% on-stream time was achieved. Approximately 312,000 gallons of high-level zirconium waste and 17,000 gallons of high-level aluminum waste were calcined to 4500 and to 230 ft^3 of solids, respectively -- an average volume reduction factor of 10. Process performance was generally satisfactory; corrosion problems that did occur were attributable to periods of excessive carryover of solids to the scrubbing system, which was caused by an excess of calcium added to the feed. Limiting the calcium nitrate addition to that required to combine with available fluoride prevented excessive carryover and alleviated corrosion problems. In the course of this scrubbing system study, solubility isotherms for calcium fluoride in nitric acid were determined and are reported.

Storage of solid calcined wastes in stainless steel bins housed in underground concrete vaults has been reviewed and the containment at the ICPP has been judged capable of withstanding natural phenomena such as earthquakes and flooding; with proper design allowing for local conditions, the concept is considered an acceptable approach to permanent disposal of highly radioactive waste in other locations as well. Design features of the third WCF solids storage facility at the ICPP are summarized; through simplification of the system which distributes solids to the bins, approximately one-third more solids will be stored in the same size vault as used in the second storage facility. Two-year laboratory corrosion tests indicate that the present Type 304 stainless steel bins are suitable for very long-term storage of calcine from zirconium process wastes. Leaching tests of zirconia-type calcine indicate that Cs-137 and Sr-90 are leachable in water, but that Pu-239, Ce-144, and Ru-106 are resistant to leaching. Migration of Cs-137 through a calcine bed at elevated temperatures is shown to be controlled by transport through intra- or interparticle voids, and diffusivity values are reported.

Pilot plant studies have demonstrated the feasibility of using in-bed combustion of fuel for heating a fluidized-bed calciner; studies related to safety indicate ready control of temperature under conditions of feed or oxygen flow interruption. Detailed designs are being prepared for conversion of the WCF to this form of heating during FY-1970. Purex-type wastes were successfully calcined in a 12-inch diameter fluidized-bed calciner using in-bed combustion of fuel: good agreement was obtained between calculated and experimental compositions of off-gases and solids; compounds of sodium formed in the calcination reaction were the thermally stable $Na_3Al(SO_4)_3$ and $NaFe(SO_4)_2$. Corrosion tests indicate that only modest corrosion should occur in the gas phase region of the WCF during in-bed combustion operations at 450°C.

Additional waste management studies reported included use of organic cation exchange resins for final decontamination of low-level waste evaporation condensates, and demonstration that rhodium-alumina catalyst used for decomposition of N_2O in the rare gas plant feed stream was not degraded by overheating. Loss of catalyst activity on overheating was found to be due to surface sintering and channeling; when broken up, the catalyst was still active.

LOFT assistance studies show that the use of chemically removable coating systems offer a rapid, effective method for remotely decontaminating surfaces. Further decontamination studies show that molecular iodine cannot be removed from coated and carbon steel surfaces at reagent temperatures less that 40°C, but that stainless steel surfaces can be decontaminated at temperatures as low as 20°C with low-pressure sprays. Methyl iodide was shown to penetrate deeply into surface coatings and was not leached from the coatings by decontamination spraying. Tests of the Continuous Sampler-Monitor (CSM) for the containment atmosphere indicate that elemental iodine detection agrees to within 10% of the values determined by Maypack samplers, but that methyl iodide values may vary by 50%; temperature greatly affects absorption of methyl iodide in the scrubbing solution. The gross activity monitors on the CSM streams give satisfactory and rapid response to changes in the containment atmosphere. In the area of waste management, the proposed LOFT waste handling system has been studied and recommendations have been made for handling all anticipated liquid waste streams.

Additional reactor technology support programs reported include (a) an outline of a conceptual HTGR reference fuel process; (b) a report of testing procedures to determine the applicability of coating systems for reactor containment buildings; (c) a procedure for treating test reactor fuel elements to minimize formation of boehmite film on the surfaces; (d) developments in the process for manufacture of uranium aluminide fuel material by a fluidized-bed technique; and (e) a study of fission product release from heated bulk uranium aluminide fuel.

CONTENTS

FIGURES

TABLES

CHEMICAL TECHNOLOGY BRANCH ANNUAL REPORT FISCAL YEAR 1969

I. FUEL REPROCESSING

1. PERFORMANCE OF ICPP FUEL RECOVERY PROCESSES

The ICPP fuel recovery processes were essentially on standby during FY-1969 while the Waste Calcining Facility was being operated full time. Only minor quantities of uranium were recovered from miscellaneous sources.

1.1 Miscellaneous and Custom Fuel Reprocessing (W. J. Venable, G. F. Offutt; Process Engineering Section)

Small quantities of uranium were recovered from several sources at ICPP. These included uranium from (a) three batches of zirconium fuel, (b) Vycor glass from the EBR-II fuel molding operation, and (c) the leaching of residue from graphite fuel used in pilot plant tests. The zirconium fuel was dissolved, processed through first cycle extraction, and combined with uranium-bearing leachate from the Vycor glass and graphite fuel in intercycle storage. Then the blended solutions were processed through the second, third, and fourth cycles of solvent extraction. Operation of all four cycles of extraction was satisfactory, and about 41 kg of total uranium were recovered.

1.2 Recovery of Uranium from EBR-II Vycor Glass Molds (M. E. Jacobson; Chemistry Section)

During the year about 13.8 kg of 50%-enriched uranium were recovered from broken Vycor glass mold tubes that are used to cast fuel pins at EBR-II Fuel Cycle Facility. Uranium was leached from the glass following the procedures described in the previous annual report, IN-1201[1]. The leachate was transferred to the ICPP solvent extraction system for uranium recovery. To date there have been five campaigns, involving 63 batches of glass, executed in a semiroutine manner and without exceptional problems.

2. SUPPORT STUDIES FOR CURRENT ICPP FUEL RECOVERY PROCESSES

2.1 Clarification of Solvent Extraction Feed

A number of the fuels being reprocessed at ICPP generate considerable quantities of solids during their dissolution. In the past, undissolved solids in the dissolver product solutions have caused line blockage and contributed to interface crud accumulation in the first-cycle extraction equipment at ICPP; therefore, a centrifuge has been installed to remove solids from the dissolver solutions before they are fed into the extraction columns. A brief

description of the centrifuge and of the process installation is presented. The centrifuge will be operated for the first time during FY-1970.

Also reported is a laboratory study directed toward estimation of the quantities of solids which may be encountered in the ICPP centrifuge, determination of their behavior during centrifuge operation, and estimation of the uranium losses associated with the solids.

2.11 The ICPP Centrifuge. (G. F. Offutt; Process Engineering Section). The centrifuge is a belt driven, imperforate basket type manufactured by Bird Machine Company. The bowl is 26 inches in diameter and 16 inches deep. A "doughnut" as shown in Figure 1, plated internally with cadmium and filled with Santowax[a], was installed inside the bowl to guarantee nuclear safety. The "doughnut" does not rotate during operation.

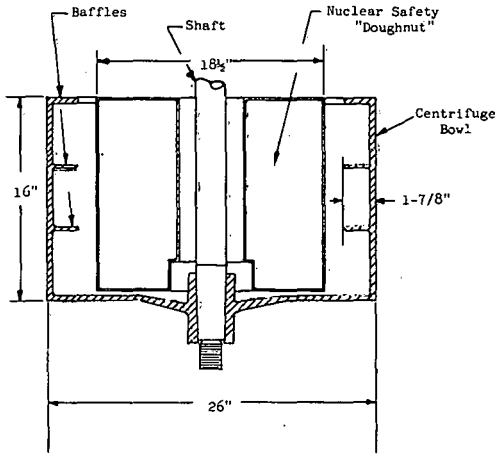

Fig. 1 Cutaway view of centrifuge bowl.

The centrifuge will operate at about 1760 rpm and will create a centrifugal force of about 1000 times gravity. It also has a low speed (870 rpm) for use during the skimming operation where excess liquid is removed from the cake. The unit has an automatic washing cycle which will go through a sequence of five steps -- slowing to 10 rpm then speeding up to 150 rpm -- and will then stop. This jogging with alternating speed will tend to free any solids stuck to the bowl and mix them with the wash solution. The solids capacity of the bowl is about 1.0 ft^3 and the total volume, less the "doughnut", is 2.6 ft^3.

Feed will be introduced to the centrifuge from several sources: (a) aluminum fuel dissolver product, (b) complexed dissolver product from zirconium fuels, (c) complexed solution from blending of aluminum fuel and zirconium fuel dissolver products during coprocessing, and (d) from the electrolytic dissolution of stainless steel clad or ceremet fuels. The flow rates and estimated quantities of solids in the various feed solutions are shown in Table I. When 1/3 to 2/3 ft^3 of solids have been collected, the solids will be washed and slurried to the process equipment waste system.

[a] Monsanto trademark for a high boiling aromatic mixture.

TABLE I

ESTIMATED SOLIDS IN FEED SOLUTIONS

Process	Flow Rate l/hr	Solids Content g/liter	Volume Collected Per Day (ft^3)
Aluminum Fuel	480	0.2	0.07
Zirconium Fuel	600	0.03	0.01
Coprocessing of Al and Zr Fuels	470	0.1	0.04
EBR-II Fuel, Electrolytic Dissolution	280	0.6	0.13

2.12 Laboratory Investigation of Extraction Feed Centrifugation (B. E. Paige and T. L. Evans; Chemistry Section). The purpose of this study was to provide a frame of reference for operation of the plant centrifuge by estimating the quantities of solids to be encountered in the ICPP centrifuge, determining their behavior during centrifuge operation, and estimating the uranium losses associated with the solids collection and washing operation.

Description and Scale of Laboratory Centrifuge

The laboratory basket centrifuge[a] used for these experiments was operated at 1000 times the force of gravity (x G) to simulate the centrifuge installed in the ICPP process. A hand-operated skimmer was developed to remove liquid while the centrifuge is operating. The bowl holdup capacity is rated at 0.3 liters, but laboratory measurements indicate this volume varies with the nature of the material in the bowl. The plant scale centrifuge installed at ICPP has an estimated holdup capacity of 42 liters. Thus, the laboratory centrifuge, at a scale-down factor of 140, requires a throughput of 60 ml/min to produce the average five-minute residence time expected in the plant centrifuge. In continuous operation, the feed is introduced through a plastic tube to the bottom of the centrifuge and the supernatant liquid overflows the top lip of the bowl into the draining chamber in a manner similar to that of the plant centrifuge.

Types and Quantities of Solids in Dissolver Product Solutions

The silicon solids generated from dissolution of aluminum alloy fuel were of primary interest in this study, and the ETR fuel was used as a basis for the quantity of solids used. In all studies, complete dissolution of the

[a] International Chemical Centrifuge (No. 1399) developing a force of 1150 x G at 4000 rpm; solid-type stainless steel basket (No. 1341), five-inch diameter and 2-1/2 inches deep; stainless steel draining chamber (No. 1320) permitting operation in a continuous mode.

aluminum-uranium alloy is assumed. ETR elements are clad with 1100 aluminum which contains up to 0.1 wt% silicon according to actual alloy analysis from fuel fabricators, and the side plates are 6061-T6 aluminum which contains up to 0.6 wt% silicon. This could result in a total of up to 12.3 g of insoluble elemental silicon per element. A second insoluble material present in important quantities is boron carbide. Boron content varies for different elements with a maximum of 5.8 g of boron carbide per element being used to date.

Another type of silicon solid which may be generated during dissolution of aluminum fuel is polymerized silica, a gelatinous and voluminous material. Extensive studies of aluminum-uranium-silicon alloys [2] have shown that silicon associated with the aluminum-uranium alloy in a ratio of <1 atom of silicon per atom of uranium will dissolve in nitric acid; this dissolved silicon may polymerize and agglomerate during the dissolution, or with the passing of time, and form a gelatinous precipitate which will centrifuge from the solution. On the other hand, aluminum alloy fuels produced by powder metallurgy do not contain silicon which will dissolve and, therefore, will not produce polymerized silica. However, current aluminum fuel production includes ETR elements prepared by alloying aluminum and uranium metals, and these elements will contain as much as 45.4 g of silicon which will dissolve. Very little is known about the kinetics of the polymerization of dissolved silicon in a continuous dissolver, and the quantity of this type of solid which may form with different process conditions is not known. Complete polymerization of the dissolved silicon from some ETR aluminum alloy fuels could produce several volume percent of the gelatinous solid; however, the quantity of dissolved silicon which will convert to gelatinous solids prior to leaving the dissolver is expected to be small. For the purpose of this study, the quantity of gelantinous precipitate was estimated to represent the polymerization of about 0.25 wt% of the dissolved silicon for one day.

During the last processing campaign for Zircaloy-clad fuel at ICPP, considerable zirconium oxide solids were encountered. An extensive literature survey revealed that the corrosion product of Zircaloy in either high temperature water or steam is entirely ZrO_2. The effect of irradiation upon corrosion is reported to be small. The amount of corrosion film is, of course, highly dependent upon the reactor history; Table II presents the estimated ZrO_2 buildup for various reactor temperatures and fuel burnups. Assuming a neutron flux of 4×10^{13} n/cm^2-sec, 30% burnup is produced in 150 days, 50% burnup is produced in 300 days, and 70% burnup is produced in 500 days. At 550°F, the most realistic temperature for estimating corrosion for extended periods, the amount of oxide does not vary widely over a wide range of burnup. If we assume 60 to 70 mg of ZrO_2 per dm^2 of fuel surface for Zircaloy-clad fuel processes at ICPP, the total ZrO_2 produced per day at ICPP probably will be about one-half the quantity of undissolved elemental silicon expected from dissolution of ETR fuel for the same period.

Observations on Centrifugation of Solids from Aluminum Alloy Fuel Dissolver Solutions

Solutions with Average Solids Distribution. An aluminum dissolver solution containing 1.6 M aluminum, 5.6 g/liter of uranium, 1.1 M nitric acid, and proportional quantities of the solids described above (elemental silicon, boron carbide, and polymerized silica) was centrifuged in a batch mode for 30 minutes

TABLE II

ZrO_2 COATING FORMED ON ZIRCALOY-2

Temperature of Water	Length of Time at Reactor Temperature		
	150 Days	300 Days	500 Days
	(ZrO_2 coating as mg/dm^2)		
550°F	56	66	74
600°F	82	97	113
680°F	188	420	728

in the basket centrifuge. The quantity of solids used represented a scale-down factor of 140 from the ICPP centrifuge, assuming 24-hour operation at full plant capacity and 0.25% polymerization of the dissolved silicon from an ETR fuel with an aluminum-uranium alloy containing 3% silicon. The following observations of process interest were made: (a) after five minutes (estimated residence time for the ICPP centrifuge) the supernatant liquid was not entirely clear, but additional centrifugation did not remove a measurable quantity of residue; (b) the gelatinous silica and the powdered solids were mixed throughout the cake, and they contributed jointly to the volume of the cake; (c) the cake adhered nicely to the stainless steel basket, as did the solids from a solution containing no gelatinous silica; (d) in either case, it was possible to skim off the clear supernatant liquid until the skimmer contacted the cake.

Solutions Containing Unusually High Polymerized Silica. In a separate experiment, the centrifuge was filled by continuous operation to about 40% of its holdup capacity with polymerized silica. Significant observations in this experiment included the following: (a) the cake was gelatinous and some tendency to sag was observed; (b) continued centrifugation removed additional supernatant liquid from the cake; and (c) the apparent volume of the gelatinous silica decreased with extended centrifugation time. The final volume of the cake in the basket centrifuge was about half the volume predicted on the basis of direct centrifugation of the solution in a clinical centrifuge tube.

Solutions Treated with Gelatin. The aluminum dissolver solution is sometimes treated with gelatin to prevent emulsion formation in the extraction columns[3]; gelatin has also been used as a flocculant prior to centrifugation to remove silica[4]. In the current work, treating the solution with 100 μg of gelatin/ml at the boil for 10 minutes did not appear to help the centrifugation of the silica which had already polymerized. On the contrary, data obtained for identical solutions indicated that the volume of the solids obtained from gelatin treated solution was slightly higher, possibly due to additional polymerization of silica in the presence of gelatin.

Solutions from Coprocessing of Aluminum and Zirconium Fuels. Coprocessing of solutions of Zircaloy-clad fuel in hydrofluoric acid using the aluminum alloy dissolver solution as the complexer will proceed this year at ICPP[1]. To test the effect of this blending, a dissolver product solution containing 0.9 M zirconium, 0.4 g/liter of uranium, 7.5 M fluoride, and 3 M in hydrogen ion was combined with aluminum dissolver solution containing a high concentration of polymerized silica in flowsheet proportions (a volume ratio of approximately two to one); the gelatinous solids containing polymerized silica disappeared. Disappearance of the gelatinous precipitate was not instantaneous; a holdup of 5 to 10 minutes should be allowed to destroy this undesirable solid prior to introduction of the combined dissolver solutions into the centrifuge. The elemental silicon and boron carbide solids from the coprocess solution were the same in appearance and nature as when no gelatinous silica was present, but data indicate that some of these solids also may be dissolved. This observation may be used to advantage by scheduling coprocessing of wrought aluminum fuel containing soluble silica with zirconium-hydrofluoric solution to destroy the gelatinous silica and avoid possible overloading of the centrifuge.

Centrifuge Cake Volume and Liquid Retention. The skimming technique apparently left the cake dry, and the liquid retained after centrifugation was held in the cake itself. The volumes of the cake and the retained liquid are given in Table III for three processing modes. The volume of the retained liquid was calculated using the quantity of uranium recovered in a subsequent wash and the concentration of the uranium in the original solution. The volume of liquid retained is greatest for the solutions containing the gelatinous silica and least for the coprocess solution, reflecting the absence of the gelatinous precipitate in this solution. The bulk density of the cake is approximately one, according to these data.

TABLE III

VOLUME OF CENTRIFUGE CAKE

(Cake Volume from 16g B_4C Plus 6g Elemental Si)

PROCESSING MODE	Wet Cake Volume (ml)	Retained Liquid Volume (ml)
Aluminum Fuel -- No Gelatin Treatment	18 to 21	13
Aluminum Fuel -- Gelatin Treated	22 to 23	16
Aluminum and Zirconium Fuel Coprocessed	12 to 13	8

Uranium Loss to Solids from Aluminum Alloy Processes

The quantity of uranium remaining in the solids and the effect of washing the solids with water and with dilute nitric acid were examined for the aluminum process solution with no treatment, the aluminum process solution with gelatin treatment, and the aluminum process solution with zirconium dissolver product added in coprocess flowsheet proportions. In all cases the cake was removed from the walls of the centrifuge easily by a small stream of water or by alternately rotating and stopping the bowl. The volume of wash used in these studies was one-third of the holdup volume of the centrifuge and about five to eight times the volume of the cake being washed. All solids reslurried readily with water and transferred easily from the centrifuge bowl.

In Table IV, the uranium recovered by the washing procedure is compared for the three aluminum processes on the basis of the percent of the total uranium in each experiment. The quantity of aluminum dissolver solution and the quantity of suspended solids were the same in all three experiments. To keep the solids uniform in all experiments, zirconium oxide was not added to the coprocess study; however, the uranium concentration in solution was lower in the coprocess experiment due to the dilution by the zirconium dissolver solution.

TABLE IV

URANIUM RECOVERED FROM SOLIDS AFTER CENTRIFUGATION OF ALUMINUM DISSOLVER SOLUTION

PROCESSING MODE	PERCENT OF TOTAL URANIUM IN THE SOLUTION			
	1st Wash with H_2O	2nd Wash with H_2O	3rd Wash with 0.1 M HNO_3	Dissolution of Washed Precipitate
Aluminum Fuel -- No Gelatin Treatment	6.2	0.59	0.1	0.013
Aluminum Fuel -- Gelatin Treated	7.1	1.2	0.19	0.014
Aluminum and Zirconium Coprocessed	1.6	0.21	0.03	0.045

In all cases uranium recovery was in direct proportion to the volumetric ratio of wash solution used per retained liquid volume, indicating that dilution and displacement of free liquid containing uranium was the only factor of significance in recovery of the uranium. Further washing decreased the uranium in successive increments as would be expected, and no additional gains in uranium recovery were made using 0.1 M nitric acid as the wash. In all cases, only a small amount of uranium remained in the precipitate after three washes. These data show that the gelatinous silica can be successfully washed with water.

The uranium losses reported in Table V were estimated for ICPP assuming one day at full rate for the aluminum process. Using a scale-down factor of 140, these data were calculated for the insoluble solids (boron carbide and elemental silicon) collected from ETR fuel in one day using the total quantity of uranium processed during the same period of operation. The uranium losses may be sufficiently low to omit washing of the solids removed from powder-metallurgy fuel or coprocess solutions. In the case of alloyed fuel containing soluble silicon, the degree of polymerization prior to centrifugation must be somewhat less than 1% (0.25% assumed here) to eliminate washing. Higher levels of polymerization will produce greater quantities of gelatinous silica and correspondingly higher retention of uranium, thus requiring adequate washing to recover the uranium. Further studies are being made to determine the degree of polymerization associated with different conditions during continuous dissolution of aluminum-uranium-silicon alloy fuel in nitric acid.

TABLE V

ESTIMATED URANIUM LOSS TO SOLIDS BASED ON CPP THROUGHPUT FOR ONE DAY AT FULL CAPACITY WITH ALUMINUM FUEL

PROCESSING MODE	LOSS AS PERCENT OF URANIUM PROCESSED	
	No Washing	With Three Washes
Aluminum Fuel -- No Gelatin Treatment	2.0×10^{-2}	4.1×10^{-5}
Aluminum Fuel -- Gelatin Treated	2.7×10^{-2}	4.7×10^{-5}
Aluminum and Zirconium Fuel Coprocess	5.9×10^{-3}	1.5×10^{-5}

Centrifugation of Solids from Zircaloy-Clad Fuel

The centrifugal force required to remove zirconium oxide solids from a synthetic complexer solution was determined experimentally in a calibrated clinical centrifuge. Highly radioactive solids were obtained from the complexing tank, E-102, during the reprocessing of Zircaloy-clad fuel in ICPP. The solids were suspended in a solution containing 0.5 M zirconium, 0.8 M aluminum, and 1.7 M hydrogen ion with a specific gravity of 1.22 at 25°C, simulating the actual process solution. Visual examination of the sample in the centrifuge tube was used to determine if the bulk of the solids had been removed. Since the length of time of centrifugation was very short, the data were corrected for the startup and slowdown of the centrifuge.

A centrifugal force of 100 x G removed the bulk of the solids from solution in less than one minute. Fine particles, detected by a Tyndall beam, were still present after three minutes at 100 x G or one minute at 500 x G, but were removed in three minutes at 500 x G. Since the rate of sedimentation

is approximately inversely proportional to the centrifugal force, 1000 x G should remove even the fine particles in less than 1-1/2 minutes, and therefore, the ICPP centrifuge should easily remove the zirconium oxide solids from the complexer matrix.

Determination of uranium loss to the solids was not attempted because the solids were highly radioactive. However, upon dissolution of Zircaloy-clad fuel, the zirconium oxide coating produces an inert finely divided solid which should resemble rather closely the inert boron carbide and elemental silicon in washing characteristics.

2.2 Factors Influencing the Rate of Silica Gel Formation in High Acid Solutions (D. Cranney and B. C. Musgrave; Chemistry Section)

The chemical or electrochemical dissolution of silicon-containing nuclear fuel alloys generates silicic acid in solution; this in turn polymerizes to polysilicic acid and may ultimately form a gel [2]. The polymers and gels can lead to line plugging throughout the plant and emulsion stabilization in the solvent extraction columns of the reprocessing plant. Several possible methods of controlling this problem were studied, including (a) preventing or slowing the polymerization and (b) using additives to accelerate the rate of polymerization so that the gel could be readily removed from solution. To study the effects of acid, temperature, salt concentration, and additives on this reaction, the gel times of solutions containing exaggerated concentrations of silicon were measured as a function of the variables. Finally, the effects were verified by measurements made with solutions containing silicon concentrations typical of ICPP streams.

It was shown that the presence of chemically inert solids or gelatin in the solution accelerated gel formation by various mechanisms and would facilitate removal of the gel by centrifugation. Hydrogen bonding agents, which accelerated gelation in solutions of low electrolyte content, were not effective in the high salt, high acid solutions. None of the materials tested significantly slowed gelation. In summary, no new procedure was suggested by these studies to more satisfactorily coagulate the silica so that it would be effectively removed by filtration or sedimentation. Detailed results of this work are reported in IN-1270 [5].

2.3 Investigation of Undissolved Uranium-Aluminum Particles Occurring During Dissolution of Fuels Prepared by Powder Metallurgy Techniques (B. E. Paige; V. H. Barnes; Chemistry Section)

In early studies of the continuous dissolution of uranium-aluminum alloys at ICPP, no evidence of preferential dissolution of aluminum was noted. Since these first studies were made, however, fuels containing higher percentages of uranium in the core alloy are being processed because the uranium content has increased in subsequent test reactor fuel plates. Recent dissolution data [2] obtained for uranium-aluminum alloys prepared by wrought alloy techniques and containing 22 to 32 wt% uranium showed that the uranium dissolved more slowly than the aluminum. Newer fuels prepared by powder metallurgical techniques have much larger uranium-aluminide particles in the core [6] than occur in wrought alloy, and the dissolution of uranium may be even slower than for

the alloyed fuel. Solids of unknown origin were encountered during the first reprocessing campaign with powder metallurgy fuel at the ICPP.

Since highly enriched uranium is reprocessed at ICPP, the complete dissolution of uranium must be assured, both from the standpoint of criticality and uranium input accountability. Therefore, extensive studies were undertaken to explore the dissolution of the uranium in the newer fuel. In these studies, actual test reactor fuel plates were dissolved in a small continuous dissolver, and undissolved uranium particles were sought in elutriated solids. When the uranium aluminides were found, the effects of various conditions and chemicals upon their dissolution rate were studied. Data reported here are incomplete, but the evidence of solids elutriation is sufficient to warrant further study. Only unirradiated fuels have been studied to date; possibly, uranium aluminide will be altered sufficiently by irradiation to change the dissolution characteristics. A program to examine highly irradiated ETR fuel is also underway.

Continuous Dissolution of Powder Metallurgical Fuel on a Laboratory Scale. A continuous dissolver having a 3/4-inch ID was fabricated from glass so that the dissolution process could be observed. This dissolver will dissolve about three ETR fuel plates containing about 80 g of U-235 in six hours of continuous operation. Figure 2 is a schematic drawing of the dissolver. As shown in Table VI, the dimensions and operating conditions were selected to correspond to the ICPP continuous dissolver for aluminum fuels in all respects except dissolver height. This particularly affects the residence time which is 13 times longer in the plant dissolver than in the glass dissolver. However, the residence time in the plant dissolver could be less than four minutes if the liquid volume holdup is comparable to the holdup volume measure in the glass dissolver. The velocity of the dissolver solution through the glass dissolver is the same as in the plant dissolver; this is a very important factor in the elutriation of solids.

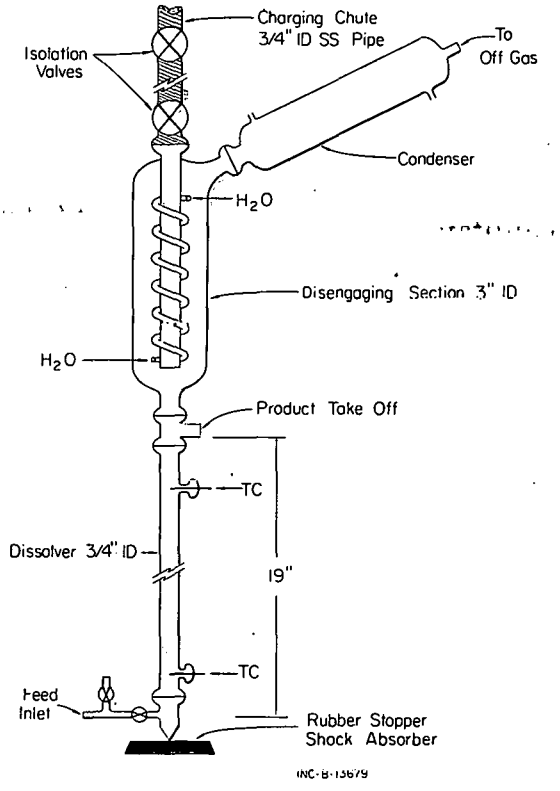

Fig. 2 Laboratory-scale continuous dissolver.

Dissolutions were made in the glass dissolver using ETR fuel plates from elements prepared by Babcock and Wilcox (referred to as ETR-B & W), according to Contract No. C-263 and from elements prepared by Atomics International (referred to as ETR-AI), according to Contract No. C-278A. In addition, plates from the ATR elements prepared by Atomics International (referred to as ATR-AI), according to Contract No. C-264 were dissolved. A continuous centrifuge (Section I-2.12) was operated in conjunction with the dissolver,

TABLE VI

COMPARISON OF DISSOLVERS

	ICCP DISSOLVER (ETR Coprocess Flow sheet)	GLASS LABORATORY DISSOLVER
Height	15 ft	20 in.
Diameter	7 in. ID	0.75 in. ID
Ratio Length/Diameter	26	26
Cross-Sectional Area	44 $in.^2$	0.44 $in.^2$
Velocity (Flowrate/Area)	5.6 $l/hr\text{-}in.^2$	6.0 $l/hr\text{-}in.^2$
Al Dissolution Rate	4.8 $KgAl/in.^2\text{-}day$	4.8 $KgAl/in.^2\text{-}day$
Dissolver Volume	140 l	135 ml
Liquid Holdup Volume	-----	< 10 ml

and crystalline species in the solids collected were determined by X-ray. In preliminary experiments, the ETR-B & W fuel produced solids containing only UAl_4 while the solids from ETR-AI and ATR-AI contained both UAl_3 and UAl_4. Dissolver product concentrations varied considerably during each dissolution and ranged from 1 M acid deficient to 3 M acid. Nevertheless, these data showed that uranium aluminide could be elutriated from a continuous dissolver.

To determine the conditions which would consistently produce a product concentration similar to the plant dissolver product, a series of preliminary dissolutions were made using various feed rates and mercury concentrations with the three types of fuels described above. The unirradiated ETR fuels were very reactive and mercury levels required were considerably lower than those used in ICPP; the ATR fuel required an order of magnitude higher mercury level than the ETR. Based on these studies, the ETR-B & W fuel was dissolved for 15 hours continuously using 6.3 M nitric acid and 0.00045 M mercury. The product was sampled and analyzed approximately every 2-1/2 hours; the average aluminum concentration was 1.39 M with a standard deviation of 0.06; the average acid concentration was 2.06 M with a standard deviation of 0.19; and the specific gravity was 1.299 with a standard deviation of 0.005 at 23°C. The solids collected in the continuous centrifuge contained 7 wt% undissolved metal which was carried from the dissolver by the gases generated on the surface during dissolution. Analysis of the solids showed that a total of 17 wt% of the uranium charged to the dissolver was in the centrifuged solids as UAl_4, together with a small amount of UO_2. High concentrations of dissolved uranium found in the centrifuge supernate, which represent uranium dissolved after leaving the dissolver, accounted for an additional 3 wt% of the

charged uranium. Other materials found in the solids included silicon from the aluminum alloys, boron carbide added to the fuel core as a neutron poison, and α-alumina from the surface of the element.

Dissolution of Uranium Aluminide Particles. The dissolution of uranium aluminide particles was studied using two different solids: (a) the solids collected from the dissolution of ETR-B & W fuel containing 42 wt% uranium as UAl_4, together with other insoluble fuel materials, and (b) pure UAl_3 powder containing 72 wt% uranium, with particle sizes between 44 and 150 mμ. The latter is currently used to fabricate all powder metallurgical fuels. In the dissolution studies, weighed amounts of solids were added to 500 ml of solution so that the solid-to-liquid ratio was the same as existed in the dissolver product; measured aliquots were removed at selected time intervals, filtered to stop the dissolution, and analyzed for dissolved uranium. Dissolutions were made in solutions containing 1.5 M aluminum to simulate dissolver product solutions.

The addition of mercury catalyst at 0.007 M, the usual flowsheet concentration, slightly increases the rate of dissolution, but mercury is not required to dissolve UAl_3 or UAl_4 in nitric acid. The rate of dissolution increases linearly with increasing acid concentration up to 15.6 M nitric acid. In both regards, the dissolution of the uranium aluminide resembles the dissolution of uranium metal rather than the dissolution of aluminum metal. The greatest increase in dissolution rate for uranium aluminide was obtained by increasing the temperature of the solution. Figure 3 shows the dissolution curves obtained in 1.5 M aluminum nitrate, 1.5 M nitric acid, and 0.007 M mercuric nitrate at 30, 60, 80, and 104°C for pure UAl_3 powder; and Figure 4 shows the dissolutions curves for solids obtained from the ETR-B & W fuel. All of the uranium in

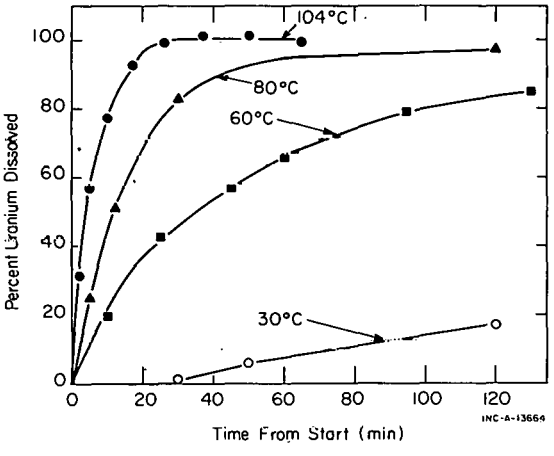

Fig. 3 Dissolution of uranium from UAl_3 powder.

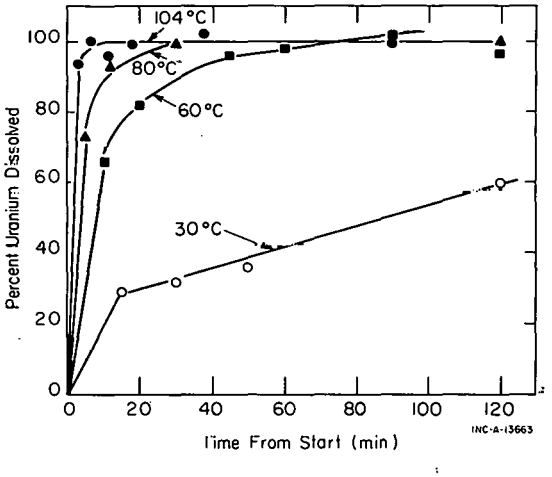

Fig. 4 Dissolution of uranium from ETR dissolution residue.

the ETR-B & W solids dissolved in less than 10 minutes at the boiling point, but about 30 minutes were required to dissolve the pure UAl_3 powder. Experiments showed that the difference in dissolution rates was not due to difference in particle size of the solids; however, the actual size of UAl_4 particles in ETR solids is hard to assess because they are dispersed with other materials which comprise about 25 wt% of the solids. Further work is being performed to determine the relationship between solids collected from the ETR-B & W

fuel, which was the primary fuel processed in 1968, and the ETR-AI fuel which will be the primary fuel processed late in 1969. In addition, an effort is being made to find an additive which will increase the dissolution rate of uranium aluminide.

Conclusions. These studies have shown that uranium aluminide does dissolve more slowly than the aluminum matrix or cladding in unirradiated fuel produced by powder metallurgical methods. It has also shown that uranium aluminide particles as well as small pieces of metal alloy can be elutriated from a continuous dissolver, probably largely because of the gas evolution at the surface which floats the solids up and out of the dissolver. Both mercury and acid increase the dissolution rate somewhat, but increasing the temperature is the most effective way to dissolve uranium aluminide.

Based on the studies thus far, the following steps should be taken to assure complete dissolution of the uranium aluminide particles in the ICPP during processing of aluminum fuel: (a) both of the aluminum dissolvers should be run so that the maximum residence time and minimum upward velocity can be obtained; (b) the dissolvers should be operated at boiling temperature; (c) the cooler in the dissolver product line should not be operated; (d) the dissolver product hold-tanks should be modified so that the solution can be heated to as near boiling as possible, and agitation should be maintained in the tank.

2.4 Description of Test Reactor Fuel Elements and Associated Behavior in Chemical Reprocessing (B. E. Paige; Chemistry Section)

Contracts, specifications, drawings, and other material have been reviewed, and an internal report has been prepared which summarizes the available information regarding composition, identification, and metallurgical history of uranium-aluminum fuel elements used in Test Reactors at the National Reactor Testing Station. Fuel elements from different contracts have been grouped according to types of fuels and to different metallurgical methods of production; data sheets have been prepared using the same format throughout to facilitate easy comparison of the fuels. The contract numbers by which the elements were ordered are identified together with the numbers of the specifications and drawings for the elements, the prefix and suffix used to code the elements, and the number and kind of elements ordered. The materials of fabrication, the dimensions, and the weights of the elements are given, as well as the calculated quantity and proportions of the components and alloys in each fuel element. This information was compiled primarily so that fuel elements can be identified from the ICPP inventory and grouped to reduce the number of problems encountered during the reprocessing and to limit the use of additives such as gelatin to the extraction feed or mercury catalyst to the dissolver. Based on the work reported in "The Effect of Silicon on Fabrication and Reprocessing of Aluminum Alloy Reactor Fuels" [2], the behavior of the fuel during reprocessing has been predicted for dissolution, extraction, and quantities of insoluble residues produced. Only fuels which have not yet been processed at ICPP are included; information about future contracts and additional elements will be added to this data on a continuing basis using the sources of information described in the report.

2.5 Fluoride Concentration in the Concentrated Raffinate from the First Cycle Scrub Stream During Zirconium Fuel Processing (B. J. Newby; Chemistry Section)

During extraction of zirconium fuel dissolver solution, the raffinate from the first cycle scrub stream (IBR) is routed through the headend evaporator and recycled to first cycle feed (IAF). This evaporator is constructed primarily of stainless steel with titanium being used for the heat transfer section. Corrosion becomes significant on titanium in this type solution at a fluoride concentration between 0.01 and 0.05 M. An estimate based on a zirconium decontamination factor of 1.3×10^4 for the first cycle extraction column (IA column) and expected stream composition for the headend evaporator predicted that the evaporator would contain a minimum of 5×10^{-3} M fluoride. Since the estimated fluoride concentration in the headend evaporator was so close to the fluoride concentration where corrosion begins to take place, an experiment was performed to verify the estimation.

A IA column feed (IAF) was prepared having the following composition: 0.54 M Zr, 3.6 M F^-, 2.2 M NO_3^-, 0.62 M Al, 1.3 M H^+, 0.85 g/liter Sn, 0.76 g/liter Cr, 2.2 g/liter B, 0.13 g/liter Hg, and 1.7 g/liter U. One volume of the synthetic IAF was extracted with 0.94 volumes of washed 10% TBP in Amsco as would occur in the extraction column. The average fluoride concentration in the aqueous phase was 3.6 M; the fluoride concentration in the organic phase was $<1 \times 10^{-4}$ M. Thus, if the ratio of IAP volume flow to IBS volume flow is 500 to 65 in the scrubbing column, the fluoride concentration in the IBR stream will be $<7.7 \times 10^{-4}$ M and in the evaporator concentrate will be $<1.5 \times 10^{-3}$ M. This fluoride concentration of $<1.5 \times 10^{-3}$ M is well below the fluoride concentration (0.01 to 0.05 M) where corrosion is expected to begin in the titanium section of the headend evaporator.

Thus fluoride carried into the headend evaporator by an extraction mechanism alone is insufficient to cause corrosion in the evaporator.

2.6 Removal of Dibutyl Phosphoric Acid from Solvent (L. C. Lewis; Chemistry Section)

Because of the excessive losses of uranium to the organic raffinate stream during the last processing campaign an investigation of the solvent recovery system was initiated. The presence of dibutyl phosphoric acid accounts for the majority of the unstrippable uranium; this dibutyl phosphoric acid (HDBP) results from radiolytic and thermal hydrolysis of tri-n-butyl phosphate (TBP).

The chemistry of the existing ICPP solvent recovery or washing system was evaluated along with alternate scrubbing reagents, with emphasis on the breaking of the uranyl-HDBP complexes and removal of HDBP from the solvent. Although a wide range of bases, mixed bases, and complexing agents was tested, no reagent superior to the 0.5 M Na_2CO_3 presently used was discovered.

Summary of Experimental Program. Several types of wash reagents were compared for possible use in the solvent recovery system. Because HDBP is extractable into basic systems, emphasis was placed on evaluating these systems and systems in which a stronger uranium complexant than HDBP is present. The basic systems included mixtures of Na_2CO_3 with NH_4OH or

NaOH. These solvents indeed remove HDBP more effectively than straight Na_2CO_3 but are also very effective as uranium precipitants. Complexants tested were H_2O_2 and the sodium salts of formic, oxalic, citric, tartaric, and hydrofluoric acids in mixtures of NH_4OH and Na_2CO_3. These did not significantly improve either the uranium solubility or the HDBP removal efficiency. An attempt to complex uranium with carbonate ion in the initial HNO_3 wash, by bubbling CO_2 into the aqueous phase, had little effect.

In addition, the effect of HDBP concentration, the presence of zirconium, and the organic-to-aqueous phase ratios were examined. From these experiments and a literature survey, it does not appear that changes in the solvent recovery chemistry will help to prevent HDBP buildup. Some rerouting and early discarding of aqueous wash streams, along with reduced temperature in the headend evaporator, appear to be most promising means for reduction of dibutyl phosphoric acid production.

2.7 Neptunium Decontamination Studies (L. A. Decker, J. P. Clark; Chemistry Section)

Laboratory experiments were conducted on a sample of the contaminated neptunium nitrate solution stored at the ICPP to determine if it could be sufficiently decontaminated in one solvent extraction cycle to permit its shipment to another AEC site for final purification. The concentrated Np-237 solution is contaminated with significant amounts of plutonium, uranium, and fission products (mainly Zr-95 and Nb-95). Extraction of the neptunium in the IV or VI valence state into several concentrations of TBP in kerosene or hexone was evaluated with various concentrations of fluoride as a complexing agent for the fission products. No combination of conditions was discovered which would, in a single, simple solvent extraction cycle, give decontamination of the neptunium from both plutonium and fission products. The attempt to complex the fission products and thus enhance the neptunium/zirconium separation factor was unsuccessful, suggesting that the stability or inextractability of the neptunium IV complexes with fluoride was at least as great as that of the zirconium complexes. Laboratory data did indicate that neptunium IV could be extracted from plutonium III, but significant decontamination from fission products was not obtained simultaneously.

3. FLUIDIZED-BED DENITRATION OF ICPP PRODUCT

In past years the Idaho Chemical Processing Plant has shipped all of its product as liquid uranyl nitrate solution at a concentration of about 350g U/liter. The product has been shipped in stainless steel bottles, contained in "bird cage" type containers to maintain a safe geometry. Because the ICPP liquid shipping containers did not meet all requirements of the new safety regulations for off-site shipments as set forth in AEC Manual Chapter 0529[7], alternative methods of packaging and shipping were investigated. Results of the study indicated that conversion of the liquid product to a solid UO_3 product by fluidized-bed denitration and shipment of the UO_3 in standard Y-12 Model-FD shipping containers were best on several counts: it would (a) satisfy 0529 regulations, (b) reduce shipping costs to a minimum, and (c) circumvent any future regulatory problems that could result with liquid shipments (assuming new satisfactory liquid shipping containers were purchased now). A fluidized-bed process

was chosen over pot or stirred-bed methods of converting uranyl nitrate solution to granular UO_3 because of lower initial investment, better operating characteristics, and experience with fluidized-bed processes at ICPP. Although uranyl nitrate has been successfully denitrated in a fluidized bed [8], the proposed process for ICPP differs sufficiently from previous studies that pilot-plant work was required to define operating parameters. The principal differences in the ICPP process are (a) the uranyl nitrate solution is more dilute than in previous studies and (b) the process will be operated intermittently because of the ICPP activity schedules.

3.1 Pilot-Plant Studies -- Operating Conditions and Results (P. I. Nelson; Development Engineering Section)

The denitration studies were performed in a four-inch diameter pilot-plant calciner (Figure 5). This unit utilizes 12, 1-kW external resistance heaters, and a dry off-gas cleanup system. The off-gas cleanup system consists of sintered metal filters, a condenser, and a high efficiency final filter. The

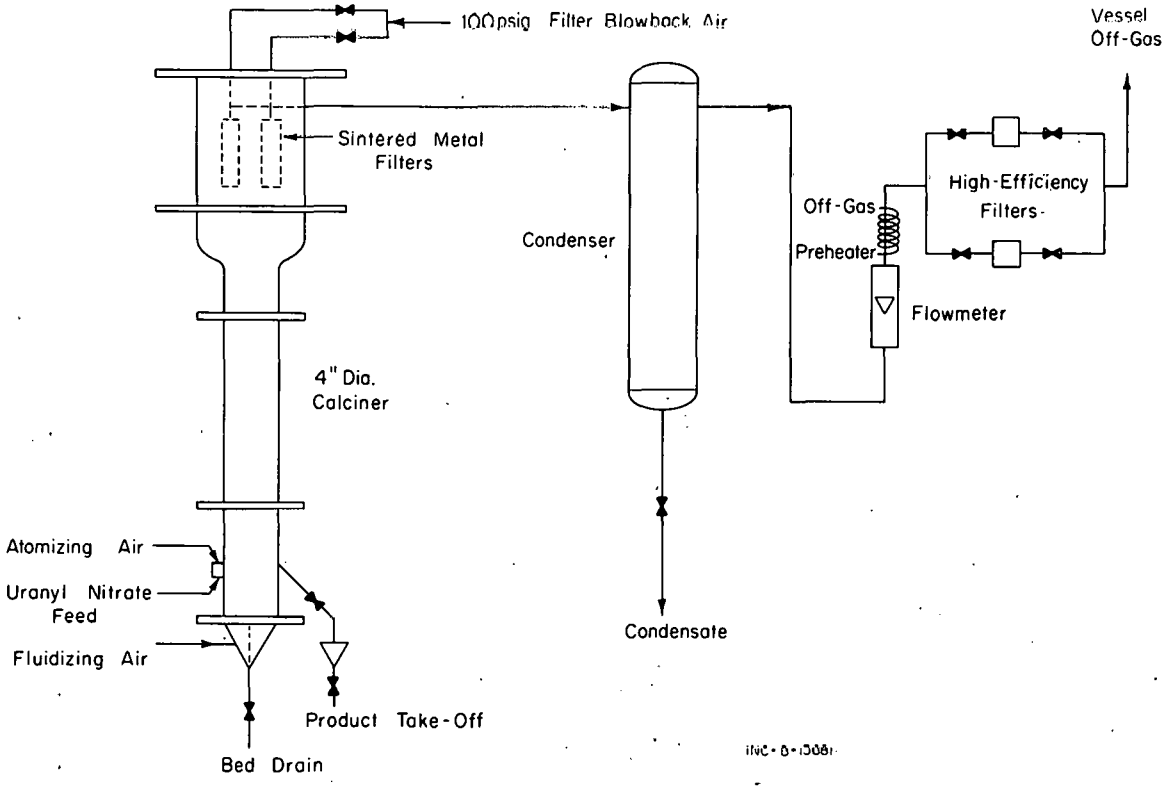

Fig. 5 Flowsheet of pilot-plant fluidized-bed denitration equipment.

two sintered metal filters, equipped with venturi-type blowback nozzles, are blown back alternately with high pressure air (100 psig). The bed level is maintained at approximately 10 inches by the position of the product overflow line. The unit has been operated at bed temperatures of 300 to 350°C, superficial fluidizing velocities of 1.3 to 1.8 ft/sec, nozzle air-to-liquid ratios of 500 to 1000 measured at bed pressure and 70°F, and a maximum feed rate of 3 liters/hr. The feed solution to date has been 1.47 M uranyl nitrate solution (350 g natural uranium/liter) which is the concentration of the present plant product. The

automatic blowback system for the sintered metal filters is being operated at 20 to 30 minute invervals for a duration of 0.2 to 0.3 second; condensate and product are collected continuously.

Granular UO_3 produced in the pilot plant at these operating conditions has an average residual water content of 0.25%, an average residual nitrate content of 0.40%, and a mass mean particle diameter of 0.4 mm. Runs made in the future will be directed toward determining if particle size control will be a problem.

The pressure drop across the sintered metal filters increases slowly to a maximum of 30 inches of water during steady state operation. The reduction of the pressure differential by three to four inches of water after blowback indicates that the calciner off-gas contains only a small amount of fines; this is further supported by the absence of fines in the product.

Analytical results obtained to date indicate that the sintered metal filters satisfactorily remove the UO_3 fines from the denitrator off-gas. An average of about 1 mg of uranium has been detected per liter of condensate. The amount of condensate obtained depends on the feed rate and condenser outlet temperature. In the pilot-plant runs, an average of 0.6 of a liter of condensate per liter of feed has been collected; the condensate contains less than 1.5×10^{-4} percent of the uranium in the feed.

Continuing Studies. Objectives of future runs in the pilot-plant denitrator will be to determine (a) the maximum feed rate consistent with smooth operation of the unit, (b) controllability of particle size, (c) volume and particle size of UO_3 in the condenser off-gas, and (d) the effect of intermittent operation on performance of the unit and on the properties of the UO_3 product.

At the conclusion of these runs, the calciner will be disassembled and checked for possible corrosion or erosion. The amount of uranium retained on the sintered metal filters will be determined by leaching with nitric acid. The mean pore size and pressure drop across the filter will be compared with similar measurements taken on clean filters.

3.2 The ICPP Denitration Installation (W. J. Venable; Process Engineering Section)

The ICPP product denitration facility has been designed and is being installed for use in the next fuel processing campaign. A report covering process and equipment descriptions, including a safety analysis of the process, has been published as IN-1293 [9]. The more important operating aspects and the principal conclusions of the safety analysis report are summarized in the following paragraphs.

Process Description. Figure 6 presents a schematic flowsheet of the ICPP product denitration process with reference keys to the material balance flowsheet shown in Table VII. The denitration process is based on the thermal decomposition of uranyl nitrate solution to uranium trioxide by the reaction

$$UO_2(NO_3)_2 \xrightarrow{\Delta} UO_3(s) + NO_2 + NO + O_2.$$

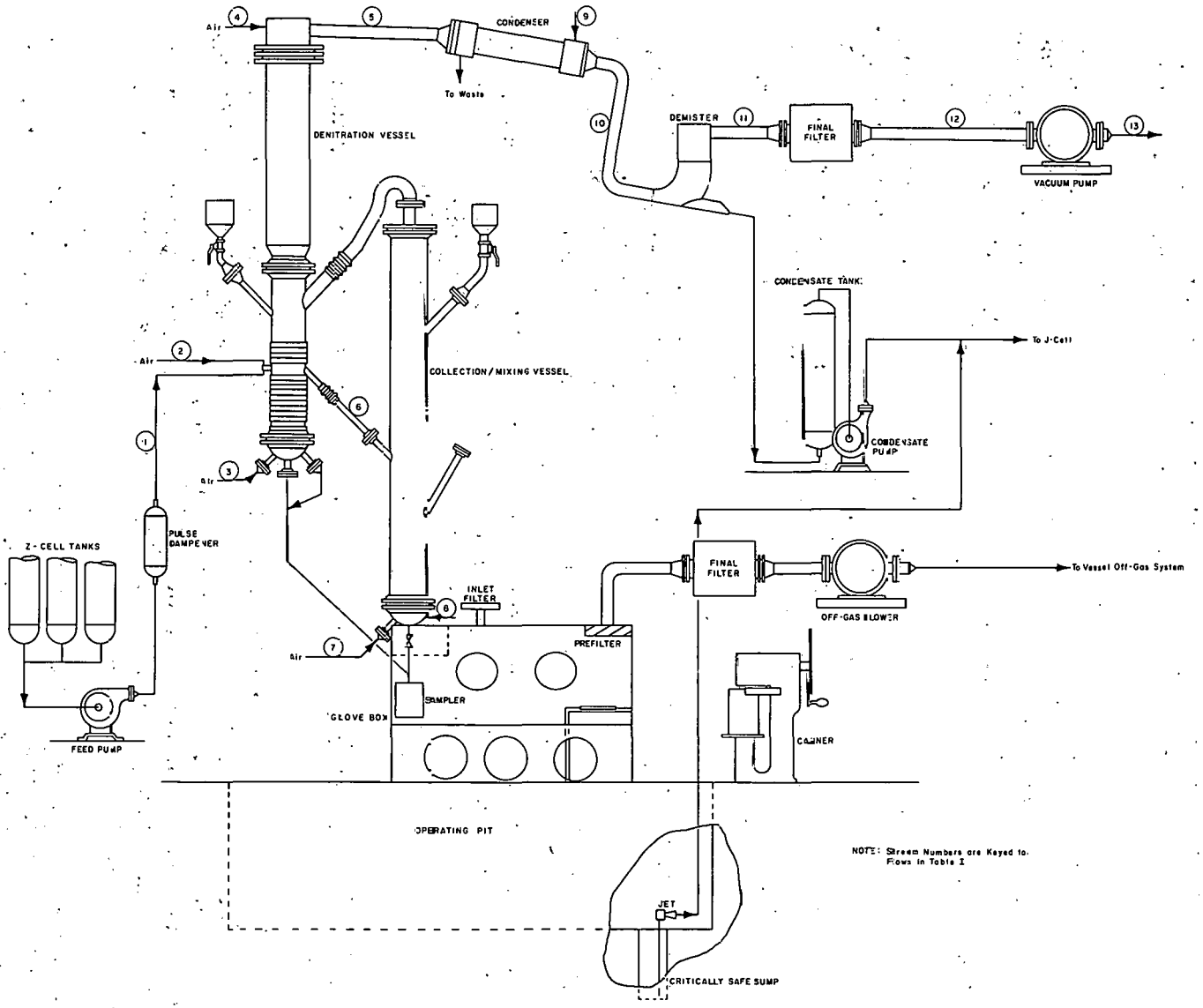

Fig. 6 Schematic flowsheet for denitration of ICPP product.

TABLE VII

MATERIAL BALANCE FOR PRODUCT DENITRATION

Stream	1	2	3	4	5	6	7	8	9	10	11	12	13
Description	Uranyl Nitrate Solution	Air Flow to Nozzle	Fluidizing Air to Denitrator	Blowback Air from Filters	Off-Gas from Denitrator	Product Overflow	Mixing Vessel Fluidizing Air	Mixing Vessel Purge Air	Condenser Cooling Water	Condensate	Off-Gas to Final Filter	Off-Gas to Vacuum Pump	Off-Gas to Vessel Off-Gas System
Flow, l/hr	18								176	5.35			
Flow, SCFH		476	578[c]	70	1897		828[d]	10			1691	1691	1691
Flow, ACFH		667	1372	14.8	7310		720	16			4110	4150	2850
Temperature, °C	21	21	300	21	300	300	21	21	13	55	65	60	112
Pressure, psia		11.3[a]	13.0[b]	88	8.0		18.2[b]	10.5			7.5	7.3	12.3
U, g/liter	353												
HNO_3, M	0.13									4.84			
Sp. grav. @ 25°C	1.48									1.1			
O_2, g-moles/hr		127	153	18.5	315[e]		220	2.65			315	315	315
N_2, g-moles/hr		475	577	69.5	1132		825	10			1132	1132	1132
NO-NO_2 as NO_2, g-moles/hr					56.4[f]					25.9	30.5	30.5	30.5
H_2O, g-moles/hr	896				896					263	633	633	633
UO_3, kg/hr					Trace	7.64				Trace	Trace		

[a] Pressure above the nozzle.

[b] Pressure below the distributor plates.

[c] Assumes superficial velocity of 2 ft/sec (max.) at 300°C and 12.3 psia.

[d] Intermittent flow, not included in off-gas; superficial velocity of 10.0 ft/sec at 21°C and 18.2 psia.

[e] Includes O_2 from the reaction and mixing vessel purge air.

[f] Includes NO_2 from HNO_3 in feed.

The denitrator will be operated on a semi-continuous basis. The uranyl nitrate solution contained in one bank of the ICPP product storage cylinders -- about 140 liters at approximately 350 g U/liter -- will be processed as a batch. The solution will be pumped at a rate of 18 liters/hr to an air atomizing nozzle on the denitrator vessel where it will be sprayed into the heated fluidized bed of UO_3. Here the uranyl nitrate will be converted to UO_3 particles which will overflow continuously to the collection/mixing vessel. During operation, the bed temperature will be 300°C, the pressure immediately above the support plate will be atmospheric, and the pressure above the bed will be less than atmospheric (10.4 psia).

The system will operate under a vacuum, and the off-gas, after leaving the bed, will flow through a filtering section consisting of three sintered metal filters which will remove 98% or more of the entrained UO_3 dust particles. After filtering, the off-gas will be cooled in a condenser to 65°C, and part of the water vapor and NO_2 will be condensed, forming a nitric acid solution. The condensate will flow to a hold tank and will be periodically pumped to salvage tanks from which it can be sampled to determine the amount, if any, of UO_3 escaping the sintered metal filters. The condensate can then be recycled to the solvent extraction system for recovery of uranium (if any significant amount of uranium is detected), but it is not expected that this will be necessary unless a filter breaks.

From the condenser, the remaining off-gas will pass through a demister and a preheater where the temperature will be raised about 10°C before entering a HEPA (high efficiency particulate air) final filter. The final filter will collect any UO_3 in the off-gas and serve as a safety device should one of the sintered metal filters fail. After the final filter, the gases will be pumped by means of a vacuum pump into the ICPP vessel off-gas system.

Each batch of product (the contents of one bank of Z cell storage vessels) will yield about 60 kg of UO_3 containing approximately 50 kg of total uranium. Once all the UO_3 from a batch of product has been collected in the collection/mixing vessel, it will be fluidized to mix it thoroughly and to cool it sufficiently for safe handling.

Sampling and packaging of the product will be performed in a glove box where each 60-kg batch of UO_3 from the collection/mixing vessel will be divided among four plastic bags; only one bag of product will be allowed in the glove box at a time. After thorough mixing, the UO_3 in the collection/mixing vessel will be dropped through a sampler and then into the plastic bag held by a cardboard container. Three additional "grab" samples from each bag of product will be taken as the bag is filled. Hopefully, after the initial operation of the denitration process, enough data can be obtained to reduce the number of required samples to one per can.

After sampling, the product bag will be sealed, and it and the cardboard container will be transferred to a separate compartment in the glove box and placed in a product can. The can will be mechanically sealed, weighed on the existing beam balance, placed in a Y-12 Model-FD foamglass shipping container, or moved to the product vault where it will be stored in a safe array.

Safety Analysis. Since the equipment will handle large quantities of uranium, all vessels have been designed using safe geometry as the primary nuclear criticality safety control. In addition, the equipment will be suitably spaced to avoid nuclear interactions. Details of the safety analysis of equipment and permissible uranium loadings are covered in IN-1293 [9].

Possible emission of radioactive nuclides was considered for two cases. For the first case a realistic approach was taken, ie, one in which expected decontamination factors for the off-gas cleanup equipment would be achieved. The concentrations of radioactive nuclides in the off-gas for this case would not exceed recommended limits at the top of the stack or at ground level for any weather conditions. The second case assumed worst possible conditions, ie, the sintered metal filters in the denitrator vessel failed, and the fines elutriated from the bed (calculated to be about 10% of the production rate) would be lost to the atmosphere via the ICPP stack without any decrease in activity level (or decontamination) occurring in the filters or other off-gas cleanup equipment in the system. Examination of this extreme case shows that for most of the radioactive nuclides in the UO_3 dust in the product off-gas, the maximum permissible limits for personnel exposure would not be exceeded at ground level. For a few nuclides (Pu-238, U-234, and U-235) limits could be slightly exceeded, but only in areas very close to the stack and only during unusual weather conditions (looping and fumigation). Ruthenium and NO_2 release by the denitration process will not exceed the recommended limits at the top of the stack or at ground level for any weather conditions.

4. GRAPHITE FUELS REPROCESSING

Development of a fluidized-bed combustion - nitric acid dissolution headend process for reprocessing graphite fuels at ICPP is continuing. The process for recovering uranium from spent nuclear rocket fuels consists of the following steps: (a) oxidation of the graphite matrix in a bed of fluidized alumina, (b) elutriation of the metal oxide combustion products (U_3O_8 and Nb_2O_5) in the off-gas stream from the burner, (c) removal of the elutriated particles from the off-gas by scrubbing with nitric acid, which also disolves the U_3O_8, and (d) separation of the undissolved solids (mainly Nb_2O_5 with small amounts of alumina and unburned graphite) from the uranyl nitrate solution before feeding to the solvent extraction system for uranium recovery.

The heat transfer and temperature control in the fluidized-bed burner has been significantly improved by the use of a concentric fluidized-bed burner. Pilot-plant studies were made during the past year to determine (a) operability of the concentric fluidized-bed burner, (b) means of eliminating, or reducing to an acceptable level, the uranium oxide coating in the alumina, and (c) the distribution of niobium oxide in the process. In addition, a moderate laboratory development program was conducted in support of the pilot-plant development effort.

4.1 Pilot-Plant Studies of the Fluidized-Bed Combustion - Nitric Acid Dissolution Process (A. P. Roeh, D. C. Kilian, L. C. Borduin; Development Engineering Section)

4.11 Description of the Concentric Two-Stage Fluidized-Bed Burner. A description of the original two-stage fluidized-bed burner was presented in the annual report for FY-1968 [1]. As reported, this unit could be successfully operated within a rather narrow range of the operating variables. However, operation outside this range resulted in severe temperature excursions. Also, hazards inherent in the design of this burner magnified the effects of the operating difficulties. A planned 10-day run for the two-stage burner was terminated after 85 hours when a temperature excursion resulted in a hole being melted in the wall of the first stage.

The two-stage burner was redesigned to improve rates of heat transfer from the first stage. Since burner reliability was of prime importance, the new burner was designed on the principle of double containment. This burner, employing a concentric fluidized bed and shown in Figure 7, consists of a four-inch diameter by 4-1/2-foot-long first stage located concentrically inside a six-inch-diameter second stage that extends 5-1/2 feet above the top of the first stage. Fluidized beds are contained in the four-inch-diameter first stage, in the annular space surrounding the first stage, and in the six-inch-diameter section extending above the first stage.

A fuel charging tube, centered in the second-stage burner and extending from the top of the burner to the top of the four-inch-diameter first stage, allows fuel charging identical to that used in the original two-stage burner. Perforated baffles and deflection baffles are attached to the outer surface of the charging tube to prevent the expulsion of alumina bed particles and the larger unburned graphite particles.

The upper two feet of the four-inch-diameter first stage is perforated to permit particle mixing between the inner and annular fluidized beds. The purpose of the mixing is to (a) improve the transfer of heat between the first stage and annular fluidized beds and (b) permit burning of small graphite particles in the annular fluidized bed, thus reducing the additional second-stage bed height required to achieve a specified graphite combustion efficiency.

4.12 Burner Operability. Fluidization tests were conducted using the four-inch diameter first stage of the burner placed inside a six-inch diameter glass column. These tests demonstrated that the annular bed could be fluidized without severe slugging at superficial velocities up to 2.5 ft/sec (the maximum rate with the installed flowmeters). The four-inch-diameter inner-fluidized bed could also be fluidized without severe slugging at superficial velocities up to 2.0 ft/sec. Similar experiments using a solid wall four-inch-diameter column resulted in severe bed slugging at a superficial fluidizing velocity of 1.0 ft/sec. All of the above tests were conducted with a fluidized bed L/D ratio greater than 10.

Full diameter gas bubbles (severe slugging) do not form in the annular fluidized bed because the inner wall of the annulus prevents a gas slug from forming over the entire annular cross-sectional area. Any gas slugs that

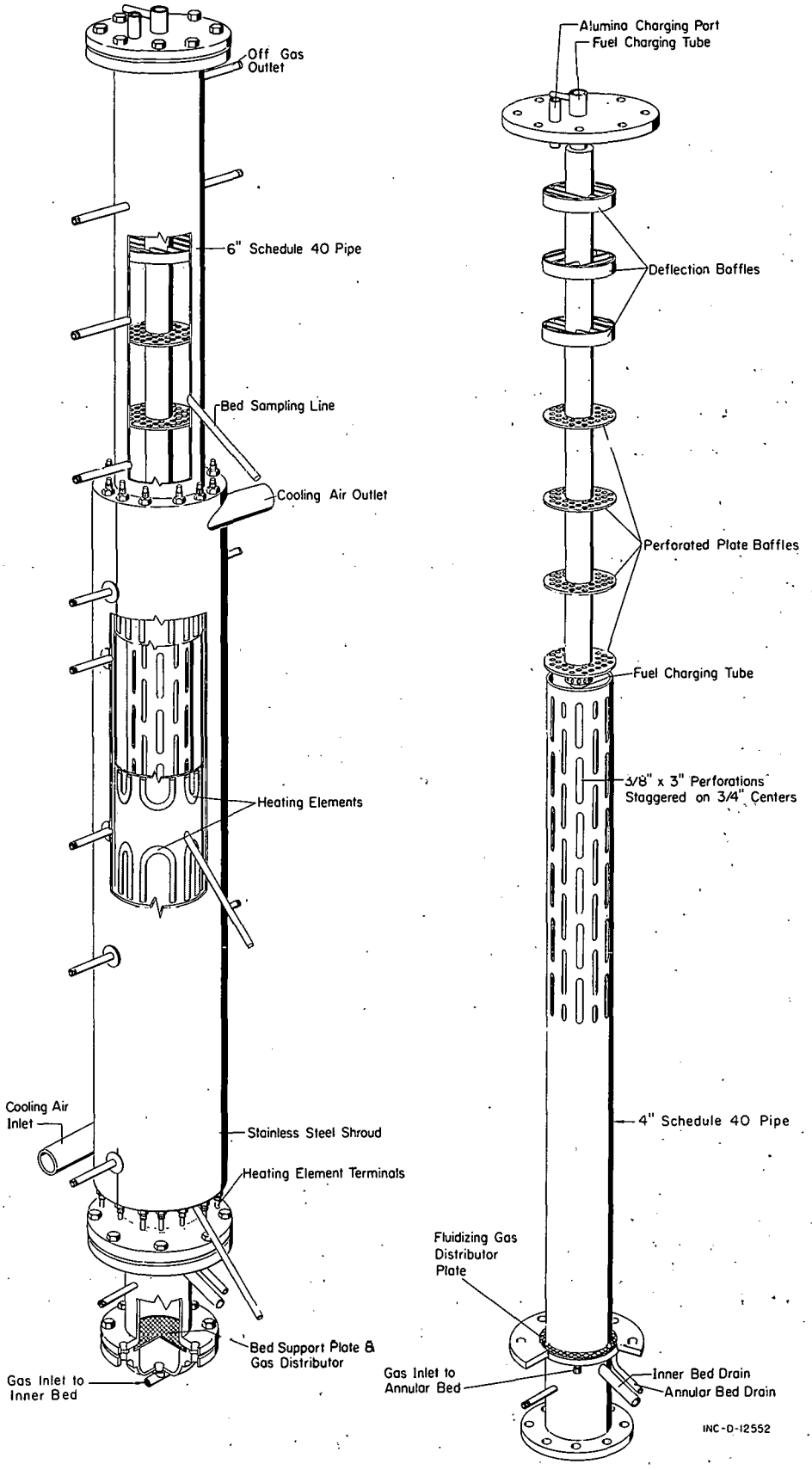

Fig. 7 Two-stage concentric fluidized-bed burner.

form are relatively small and break up readily; thus, severe slugging is prevented even at moderately high fluidizing velocities.

The slotted wall surrounding the upper half of the inner bed allows mixing of both gas and particles between the inner bed and the annular bed. At superficial fluidizing velocities in the annular bed greater than those in the inner bed, slugging is greatly reduced in the inner bed as a result of solids flow through the slots into the inner bed filling any large gas slug tending to form. At inner bed fluidizing velocities greater than those in the annular bed, severe slugging was observed in the region where the wall is slotted.

The two-stage concentric fluidized-bed burner was found to be superior to the original two-stage burner with respect to heat transfer and temperature control; operability over a much wider range of fluidizing velocities and heat generation rates was demonstrated.

The significant improvement in heat transfer and temperature control is a result of both the annular fluidized bed and the slotted wall section between the annular and inner beds. The fluidized, annular bed gives high heat transfer rates from the wall of the inner bed, and the slotted wall permits mixing between the inner and annular beds. Mixing between the beds not only gives improved fluidization in the inner bed as described above but also increases the rate of heat transfer from the inner to the annular bed as a result of a flow of fluidized-bed particles between the two beds.

The improved heat transfer and temperature control in the two-stage concentric fluidized-bed burner compared to the original two-stage burner is evident from the instantaneous temperature differentials observed within the four-inch-diameter first stage of each burner. In the original two-stage burner, a normal temperature spread of 100 to 150°F, and a maximum spread of 300°F, was observed in the first stage during burner operation at high burning rates. In the first stage of the concentric fluidized-bed burner, a normal temperature spread of 25 to 45°F and a maximum spread of 75°F were observed during burner operation at a burning rate approximately 10% higher than the maximum burning rate in the original two-stage burner.

4.13 Combustion Efficiency. Experiments one through nine in the new two-stage concentric burner (Tables VIII and IX) were designed for statistical evaluation of the effects of graphite charging rate (80 to 100% of the stoichiometric equivalent of the oxygen flow rate to the first stage), first-stage fluidizing velocity (1.0 to 1.5 ft/sec), and second-stage fluidizing velocity (1.5 to 2.0 ft/sec), on the graphite combustion efficiency. The effects of changes in these three variables on the graphite combustion efficiency were not statistically signficant. However, combustion in the vapor space above the top of the second-stage fluidized bed was noted in Runs 1 and 3 which were conducted at the highest graphite burning rate. Therefore, the calculated combustion efficiencies for these two runs are higher (by an unknown amount) than the actual combustion efficiencies achieved within the fluidized bed. Omission of these two runs shows that the graphite combustion efficiency increased over a rather narrow range (78 to 88%) as the graphite charging rate is reduced from 100 to 80% of the stoichiometric equivalent of the oxygen flow rate to the first stage. Run 10 was made at a fluidizing velocity of 1.0 ft/sec in each bed, 100% oxygen concentration to the first stage and annular bed, and a fuel charging rate equal to 40%

of the first-stage oxygen stoichiometric equivalent. The graphite combustion efficiency increased to 90% under these conditions. From the results of these tests, it is concluded that increased residence time of graphite particles in the burner is needed to significantly increase the combustion efficiency, since oxygen availability is not a contributing factor.

The maximum combustion efficiency of 90% achieved in the concentric fluidized-bed burner (compared to 98% in the original two-stage burner) can be explained by the effect of the reduced second-stage bed height on the elutriable particle residence time. The maximum possible second-stage fluidized-bed height was 2.5 feet in this equipment adapted from the original two-stage burner with minimum modification in the interest of economy. However, it is anticipated that higher combustion efficiencies can be obtained easily by using a concentric fluidized-bed burner with greater second-stage bed height.

TABLE VIII

SUMMARY OF RUN CONDITIONS IN THE TWO-STAGE CONCENTRIC FLUIDIZING-BED BURNER

Run Number	1	2	3	4	5	6	7	8	9	10
Fluidizing Velocity										
First Stage, ft/sec	1.50	1.00	1.50	1.00	1.25	1.50	1.00	1.50	1.00	1.0
Annular Bed, ft/sec	2.00	2.00	1.50	1.50	1.75	2.00	2.00	1.50	1.50	1.0
Second Stage, ft/sec	1.75	1.50	1.50	1.25	1.50	1.75	1.50	1.50	1.25	1.0
Nominal Graphite Charging Rate, grams/hr	2450	1635	2450	1235	1790	1840	1225	1840	1225	715

TABLE IX

SUMMARY OF RUN RESULTS USING THE TWO-STAGE CONCENTRIC FLUIDIZED-BED BURNER

Run Number	1	2	3	4	5	6	7	8	9	10
Overall Oxygen Utilization[a], percent	35	24	41	32	27	23	15	29	24	18
Graphite Combustion Efficiency, percent	88[c]	82	87[c]	88	81	78	88[d]	83	87.0	90
Throughput Rate, Kg graphite/day/ft^2 (first-stage cross-sectional area)	665	444	665	444	486	500	333	500	333	194
First-Stage Heat[b] Generation Rate, Btu/hour	47,600	31,200	47,000	28,000	32,800	33,800	26,300	37,800	24,600	16,100
Average Instantaneous Temperature Differential										
Within First Stage, °C	30	35	45	30	30	25	40	35	35	-
Within Second Stage, °C	10	15	10	20	15	10	20	10	15	-

[a] Percent of oxygen reacted, based on graphite material balance.

[b] Based on 65% of the charged graphite burning to CO_2 in the first stage of the burner.

[c] Vapor space burning was observed.

[d] Based on the last two hours of the run.

4.14 U_3O_8 Coating on the Alumina. Early development work at ICPP demonstrated that a steady state accumulation of 2 to 4 wt% uranium could be expected to remain in the fluidized bed. A high level of U_3O_8 coating on the alumina particles is undesirable because it increases the required amount of fluidizing gas and, for a plant sized unit, could present a criticality danger which would necessitate frequent removal of the fluidized bed from the burner.

Studies of U_3O_8 coating on the alumina bed particles, conducted both in batch-type, statistically planned programs and in continuous runs of up to several days duration, have established the following general relationships:

(1) Combustion of UO_2 bearing fuel results in much less coating than does combustion of UC_2 bearing fuel.

(2) The U_3O_8 coating rate decreases as the coating on the alumina particles increases.

(3) Increasing temperature increases the coating when UC_2 type fuel is burned as shown in Figure 8. No significant temperature effect on coating occurs during the combustion of UO_2 type fuel.

(4) Combustion of UO_2 type fuel in a bed that is already heavily coated with U_3O_8 leads to a significant reduction in the amount of coating.

(5) The U_3O_8 coating rate is much lower when UC_2 type fuel coated with NbC is burned than when UC_2 type fuel not coated with NbC is burned as shown in Figure 9.

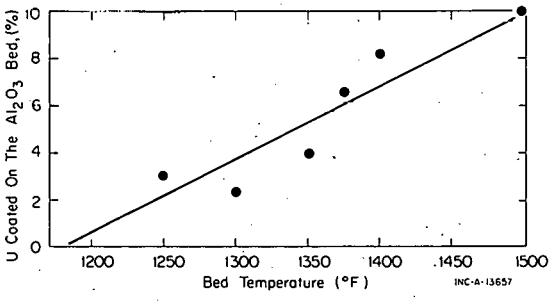

Fig. 8 Uranium coating on alumina bed particles as a function of bed temperature.

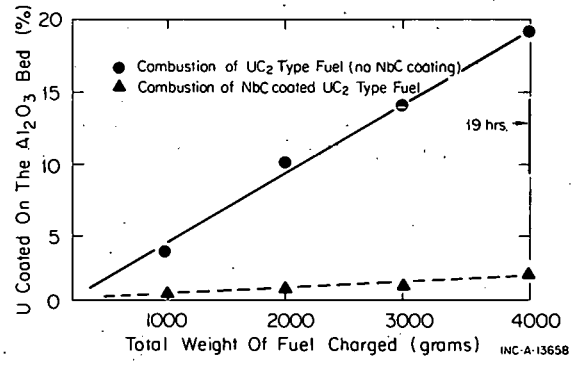

Fig. 9 Effect of niobium carbide on uranium coating rate.

Since the oxidation of UO2 to U_3O_8 does not produce substantial coating (and actually removes a preexisting coating), and the presence of NbC oxidizing to Nb_2O_5 in the system interferes with the coating process, it is conjectured that the coating process is chemical in nature and may be caused by a chemical intermediate in the oxidation of UC_2 to U_3O_8. Even though coating of U_3O_8 on the alumina may not be prevented, the reduction in coating rate with increasing amounts of coating on the alumina indicates that a steady state level of coating on the alumina might be achieved.

Future investigations will be made to determine

(1) The existance and magnitude of the steady state level of uranium oxide coating on the alumina for a given set of operating conditions.

(2) The effect of other bed materials on both coating level and rate.

(3) If the U_3O_8 coating can be removed in situ by a chemical or physical method.

(4) Those operating conditions which minimize both the coating rate and level of U_3O_8 coating.

4.15 Distribution of Nb_2O_5 Within the Process. Niobium carbide, which is present as a coating on some of the exposed surfaces of Rover fuel elements is oxidized to Nb_2O_5 in the burner. The niobium oxide can form small particles that elutriate from the burner or flakes that are too large to elutriate. However, the flakes would probably be reduced in size by the turbulent action of the fluidized bed. A steady state level of niobium oxide in the burner must be established, or, if niobium oxide continues to accumulate in the burner, it must not interfere with the fluidization of the bed. One long-term test has been made with fuel containing niobium carbide. The results of this test showed that 78% of the niobium elutriated from the burner and the final bed contained 3 wt% niobium. A steady state concentration of niobium oxide in the bed was not achieved within the 96 hours of operation but the amount of niobium oxide retained in the fluidized bed was insignificant.

4.16 Aluminum Behavior in the Burner. Aluminum inclusions are present in many of the Rover fuel elements. Removal of these aluminum pieces would be very difficult; therefore, it is proposed to burn them with the fuel. A scoping test was made in the miniburner to determine whether any gross effect, such as sintering bed particles together, resulted from oxidizing aluminum metal in the burner. The weight percent of aluminum in the fuel charged during this test was much greater (by a factor of 10 to 20) than the weight percent of aluminum that would be present in actual Rover fuel elements. Operation of the miniburner was not affected and examination of the system following the run did not reveal any significant effects from the aluminum oxidation.

4.17 Combustion of Graphite Fuel with NO_2. The reaction of UC_2 with NO_2 is reported to form the uranium species UO_3 [10], whereas U_3O_8 is formed by the reaction with oxygen. Therefore, a series of experiments was conducted to determine

(1) If the rate of uranium oxide coating on the alumina particles could be reduced (or eliminated) by burning Rover fuel in the presence of NO_2.

(2) If a coating of U_3O_8 on alumina could be oxidized to UO_3 by exposure to NO_2 at temperatures of 1200 to 1500°F and thus possibly be removed from the alumina.

Experiments were also made to determine the relative reaction rates and ignition temperatures during combustion of Rover fuel in NO_2 and O_2.

The results of these experiments show that

(1) A coating of U_3O_8 on the alumina bed is not reduced by fluidization in an NO_2 atmosphere (50% NO_2 - 50% O_2) at temperatures between 1200 and 1500°F.

(2) U_3O_8 coatings of 2.22 and 9.78 wt% were measured on the alumina bed during combustion of 1000 g of Rover fuel at 1400°F with NO_2 (50% NO_2 - 50% O_2) and pure O_2, respectively. However, the run with NO_2 combustion gas was made with NbC coated fuel which was later demonstrated to reduce the coating rate. Therefore, any effect of burning with NO_2 is confounded with the effect of NbC combustion.

(3) Combustion efficiencies of 64 and 90% were obtained during Rover fuel combustion in NO_2 (50% NO_2 - 50% O_2) and pure O_2, respectively.

(4) The reaction rate of graphite with NO_2 is higher than the reaction rate with O_2 up to 1300°F as shown in Figure 10.

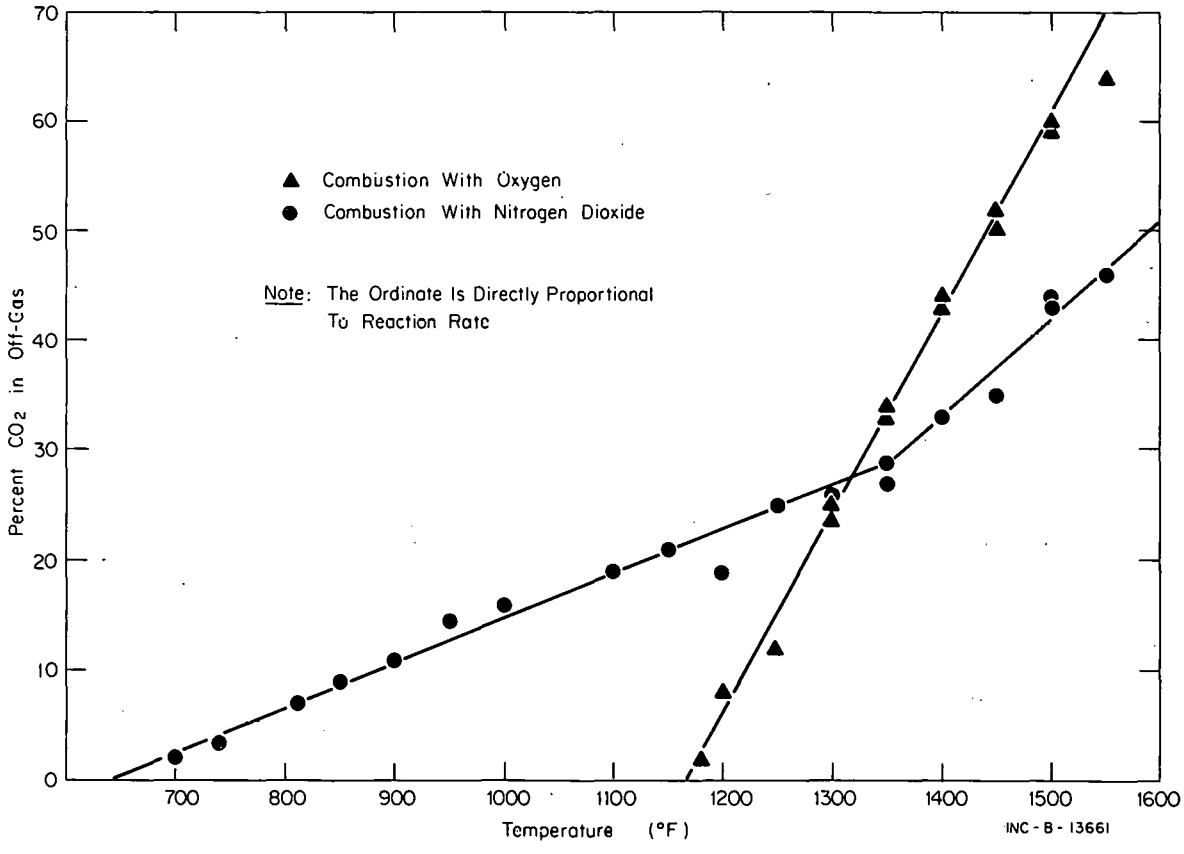

Fig. 10 Combustion rate of graphite in oxygen and in nitrogen dioxide as a function of temperature.

(5) The ignition temperature of graphite is 660°F in an NO_2 atmosphere compared to 1165°F in an O_2 atmosphere as shown in Figure 10.

The reaction of graphite with NO_2 at lower temperatures than the reaction with O_2 is explained by E. Lopez-Menchero et al [11]. The controlling reaction at the lower temperatures is the reaction between carbon and elemental oxygen. At 1150°F, NO_2 is completely dissociated to NO and elemental oxygen, whereas only 1% of molecular oxygen dissociates to elemental oxygen at a temperature of 2730°F. At temperatures above 1300°F, the rate of reaction with molecular oxygen becomes competitive with the rate of reaction with elemental oxygen.

4.2 Calculated Combustion Temperatures for Graphite Combustion (N. J. Kertamus; Chemistry Section)

Calculations were made to define the theoretical maximum combustion temperature that might be encountered in the operation of the graphite burner during a potential process upset, such as the loss of bed fluidization. These calculations suggested that, in the absence of bed fluidization or suitable means of removing the heat of combustion, temperatures far in excess of those required to melt stainless steel could be encountered.

Basis for Calculation. For purposes of calculation, carbon (graphite) was assumed to burn with the stoichiometric amounts of oxygen in combustion gases composed of 100% O_2, 90% O_2 - 10% N_2, and 60% O_2 - 40% N_2. Combustion gas preheat temperatures of 25 and 649°C were also considered. Thermodynamic equilibrium data were assumed for all calculations, except for determining the degree of dissociation of carbon dioxide. For mathematical simplicity, carbon dioxide was assumed to be completely dissociated into carbon monoxide and oxygen such that the overall combustion reaction could be written as $C_{(s)} + 1/2\ O_{2(g)} = CO_{(g)}$. This assumption is basically correct because the high heat of combustion of carbon to carbon dioxide produces sufficient heat to raise combustion gas temperatures to levels where appreciable dissociation occurs, ie, temperatures higher than listed in Table X.

TABLE X

DISSOCIATION OF CO_2 AS A FUNCTION OF TEMPERATURE

Temperature, °C	CO_2 Dissociation, percent
2727	47.3
3227	75.4
3727	89.8

Combustion Temperatures Attainable. With carbon monoxide as the sole combustion product, the values in Table XI illustrate maximum adiabatic combustion temperatures that can be theoretically reached if the total energy

TABLE XI

THEORETICAL COMBUSTION TEMPERATURES OF CARBON IN OXYGEN-NITROGEN MIXTURE

Nitrogen in Oxidizing Gas (Percent)	Oxidizing Gas Preheat Temp. (°C)	Maxium Adiabatic Temperature (°C)
0	25	3543
0	649	4042
10	25	3371
10	649	3882
40	25	2718
40	649	3227

of the combustion reaction is used only to heat the product of combustion, carbon monoxide, and nitrogen when present in the oxidizing gas. No heating of surroundings or fluidizing media are assumed.

While it is apparent that diluting the oxidizing gas with nitrogen lowers the maximum adiabatic combustion temperature, the magnitude of the reduction is not sufficient for nitrogen addition to be of practical benefit in lowering temperatures in the graphite burner. Even the lowest calculated temperature is too high for refractory metals to be of benefit.

4.3 Leaching of Uranium from Elutriated Ash Product (R. G. Butzman and N. J. Kertamus; Chemistry Section)

The combustion process for graphite fuels results in a fuel ash composed largely of U_3O_8, unburned carbon particles, alumina fines, and possibly Nb_2O_5, depending on the composition of the fuel being charged. Laboratory studies performed previously [12] demonstrated, for niobium-containing fuels, a relationship between the proportion of uranium recoverable by nitric acid leaching and the temperature of the fuel during combustion. The goal of the current experimental program is to determine the operating conditions necessary for an acceptable uranium recovery from the ash using a continuous process, preferably a single step process. Preliminary tests have been performed on a batch basis.

The composite ash product used in laboratory batch experiments reported here contained Nb_2O_5. The following ranges of conditions (with the nitric acid solution at its boiling point as the leaching agent in each case) have been investigated: (a) 4 M HNO_3 to 13 M HNO_3; (b) 3 to 100 times the stoichiometric requirement of HNO_3; (c) liquid reagent volume-to-solids weight ratios of

2.2 ml/g to 25 ml/g; and (d) contact times of 7 to 60 minutes. Table XII summarizes the conditions of each experiment and the uranium recovery obtained; results indicate that 99.8 ± 0.1% of the uranium present is "nitric acid leachable" under a wide range of conditions. A single HNO_3 leach test using ash without niobium present resulted in a 99.99% uranium recovery.

TABLE XII

URANIUM RECOVERY BY LEACHING OF GRAPHITE FUEL ASH

HNO_3 Conc.	Stoichiometric Factor[a]	Reagent Vol to Solids Wt Ratio	Contact Time	Uranium Recovered
13 M	100	23 ml/g	60 min	99.78%
13 M	100	23	30	99.75
13 M	100	23	7	99.72
13 M	100[b]	23	60	99.78
13 M	100	23	7	99.99[c]
6 M	5	2.5	7	99.78
6 M	100	25	7	99.75
4 M	3	2.25	7	98.32

[a] Calculated at seven moles HNO_3: one mole U_3O_8 = stoichiometric factor of one.

[b] Also contained 0.05 M HF.

[c] Without niobium in fuel.

Currently, a laboratory continuous leacher is being prepared to study leaching of the product ash. Leachability of the burner bed material will also be studied.

4.4 Conceptual Flowsheet for the Reprocessing of Graphite Fuel (N. J. Kertamus; Chemistry Section)

Conceptual material balance and equipment flowsheets were prepared for the chemical reprocessing of the Rover fuel at ICPP. Figure 11 shows the combustion and leaching of the ash; Figure 12 shows the solvent extraction. The basis for the conceptual chemical material balance (but not necessarily for the plant installation) was a daily throughput of 20 kg of enriched uranium. It was assumed that during the combustion in the fluidized-bed burner that all of the uranium and niobium carbides are burned to the corresponding oxides and are elutriated from the burner. After the uranium is dissolved in 4 M

nitric acid, it is separated from niobium oxide and unburned carbon by centrifugation. This separated dissolver product contains 365 g/liter of uranium and is 0.5 M in nitric acid. This leachate is suitable for routing to the hexone solvent extraction system without an additional feed adjustment step; consequently,

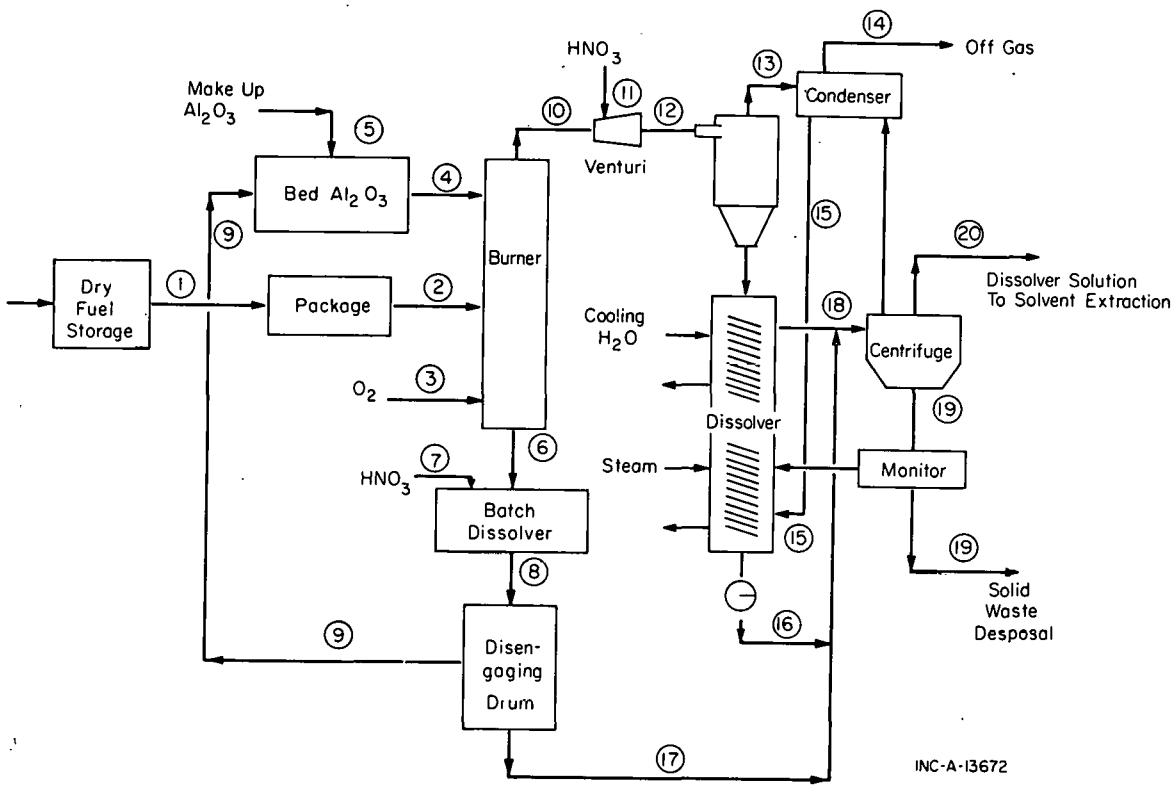

Stream	2	3	10	11	13	18	19	21
	Burner Feed	Fluidizing Oxygen	Elutriated Fines	Dissolvant	Burner Off-Gas	Dissolver Product	Undissolved Solids	Dissolver Product
C, kg/day			2 (a)			2	2	
U, kg/day	20		20			20		20
UO_2^{++}, M						1.51		1.51
H^+, M				4		0.48		0.48
NO_3^-, M				4		3.50		3.50
Liquid Volume, ltr/day				54.7		56.4		56.4
Gases $(CO_2 + O_2)$ (b)								
ft^3/hr (STP)		793			793			

(a) Arbitrarily chosen quantity reflecting the expectation of some unburned carbon to be elutriated with the off-gas.

(b) An excess of oxygen, over that theoretically required for combustion, is included with the fluidizing oxygen to assure efficient combustion.

INC-A-14601

Fig. 11 Conceptual flowsheet for combustion and leaching of Rover fuel.

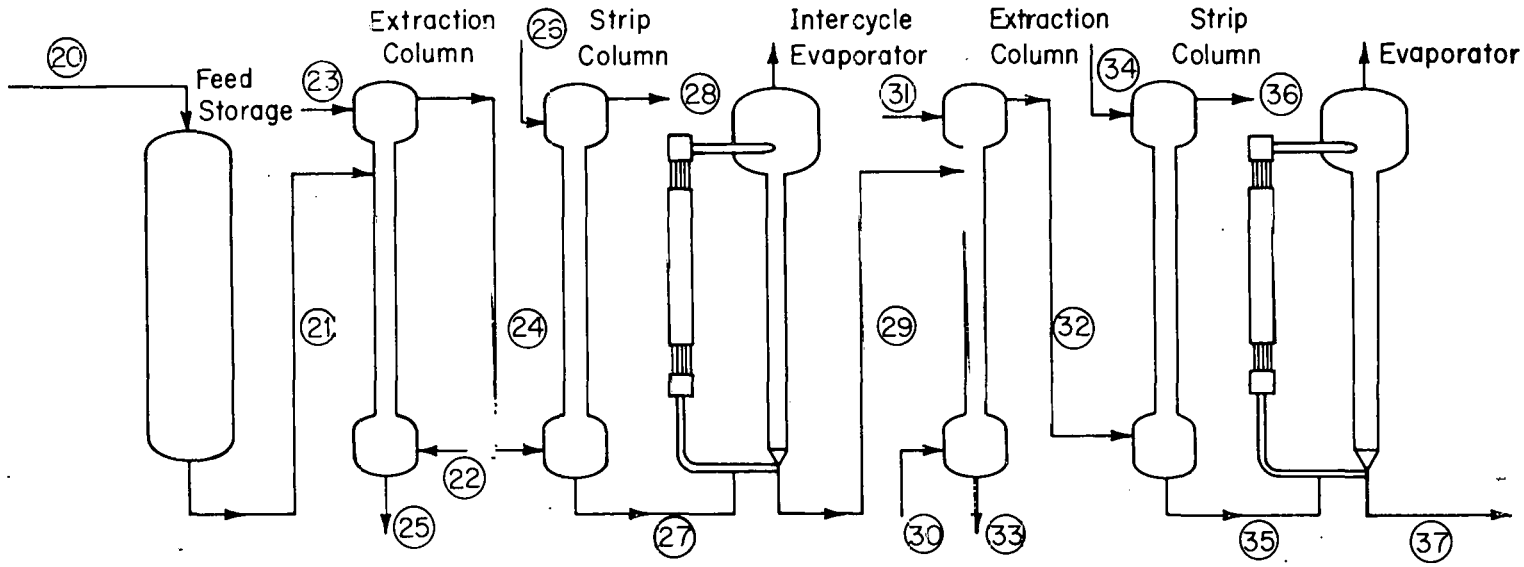

STREAM	20	21	22	23	24	25	26	27	28	29	30	31	32	33	34	35	36	37
	DISSOLVER PRODUCT	IAF	IAX	IAS	IAP	IAR	IBX	IBP	IBR	SECOND CYCLE PRODUCT	IIAX	IIAS	IIAP	IIAR	IIBX	IIBP	IIBR	PRODUCT
U, kg/day	20	85.1			85			85		85			85			85		85
UO_2^{++}, M	1.5*	1.51			0.408			0.656		1.66			0.458			0.755		1.50
H^+, M	0.4E	0.48					0.04	0.04		0.10					0.04	0.04		0.08
NO_3^-, M	3.5	3.5			0.816		0.04	1.35		3.42		6.00	0.916	4.35		1.55		3.08
NH_4OH				0.44		0.19						0.33		0.21	0.04			
NH_4NO_3						0.13								0.03				
Al+++, M				2.0		1.46						2.00		1.45				
$Fe(NH_2SO_3)_2$, M				0.05		0.04												
Solvent			Hexone		Hexone				Hexone		Hexone		Hexone				Hexone	
Liters/Day		240*	888	648	888	888	552	552	888	216	792	576	792	792	480	480	792	242

*Operates 1.65 days/week

Fig. 12 Conceptual flowsheet for solvent extraction of uranium from Rover fuel.

the Rover leachate would not be contacted with TBP-Amsco, and only two solvent extraction cycles would be used. Two solvent extraction cycles should adequately decontaminate uranium from Rover fuel because of the low initial burnup.

These material balances and flowsheets will be updated as the development proceeds.

5. ELECTROLYTIC DISSOLUTION PROCESS FOR EBR-II FUEL

R 2-25-70

5.1 Design of ICPP Electrolytic Dissolution Process (G. F. Offutt; Process Engineering Section)

Design of the electrolytic dissolution system for processing EBR-II and other stainless steel fuels is essentially complete. Construction will begin in the fall of 1969 and will be completed in time for processing fuel in the spring of 1971.

Dissolver Design. The heart of the electrolytic dissolution process is a titanium dissolver (Figure 13) in the form of a V-shaped, horizontal trough, approximately six inches wide at the top, 30 inches deep, and 84 inches long. The dissolving fuel elements will be contained within a niobium basket which is separated from the dissolver vessel by ceramic spacers. The platinum-faced niobium anode is also separated from the cathode (dissolver vessel) and from the niobium fuel basket by ceramic spacers. At the operating voltage of the dissolver, about 15 volts, short-circuiting of direct current from the anode to the cathode is prevented by the "valve metal" characteristics of niobium.

The selected width of the dissolver was based on criticality considerations, and the other dimensions have been selected to give maximum versatility in fuel processing capability. Fuel elements six feet long can be charged to the dissolver, or elements up to three feet long can be charged end to end. A depth of 30 inches will provide a sufficient capacity to permit a reasonable charging frequency of fuel to the dissolver. A remotely operable crane will be used for removal of the dissolvent recirculation pump and the fuel basket as required. Nuclear safety will be guaranteed by (a) limiting the uranium concentration in the dissolvent, (b) using critically safe geometry, and (c) using a soluble neutron poison.

Process Description. The electrolytic dissolution process has the following components: a fuel charging system, an acid (feed addition) system, a dissolver, a dissolvent circulation loop (containing a pump, surge tank, and primary heat exchanger), an off-gas system, a DC rectifier, and associated instrumentation. A schematic flowsheet of the facility is shown in Figure 14.

Fuel elements will be transported in a bottom-opening cask from the fuel storage basin and will be dropped through a charging valve, via a charging chute, into the process cell. An operator, using remotely operated manipulators, will load the elements into the open top of the trough-shaped dissolver. The dissolvent solution, essentially a metal nitrate - nitric acid solution, will be

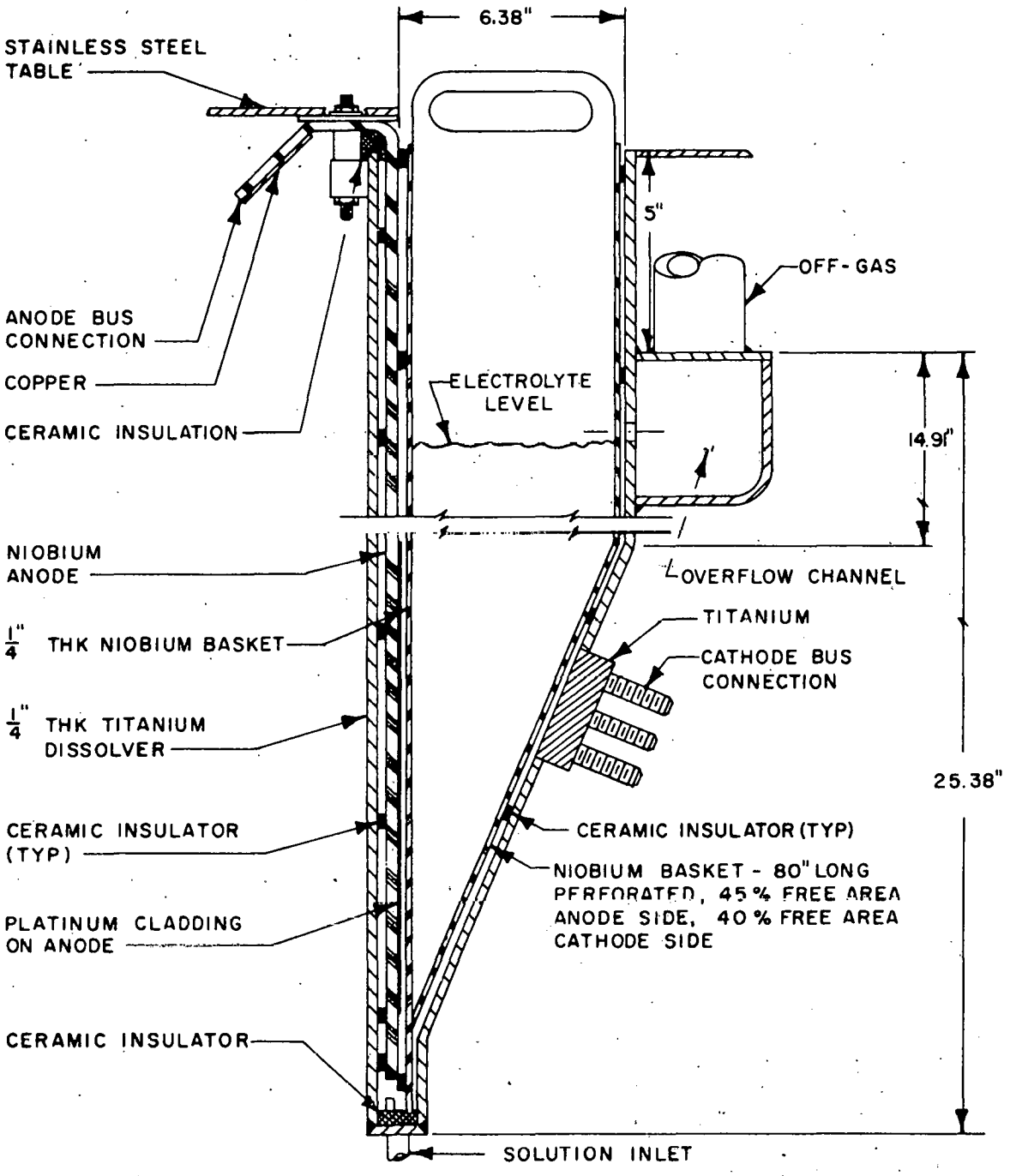

Fig. 13 Sectional drawing of the ICPP electrolytic dissolver.

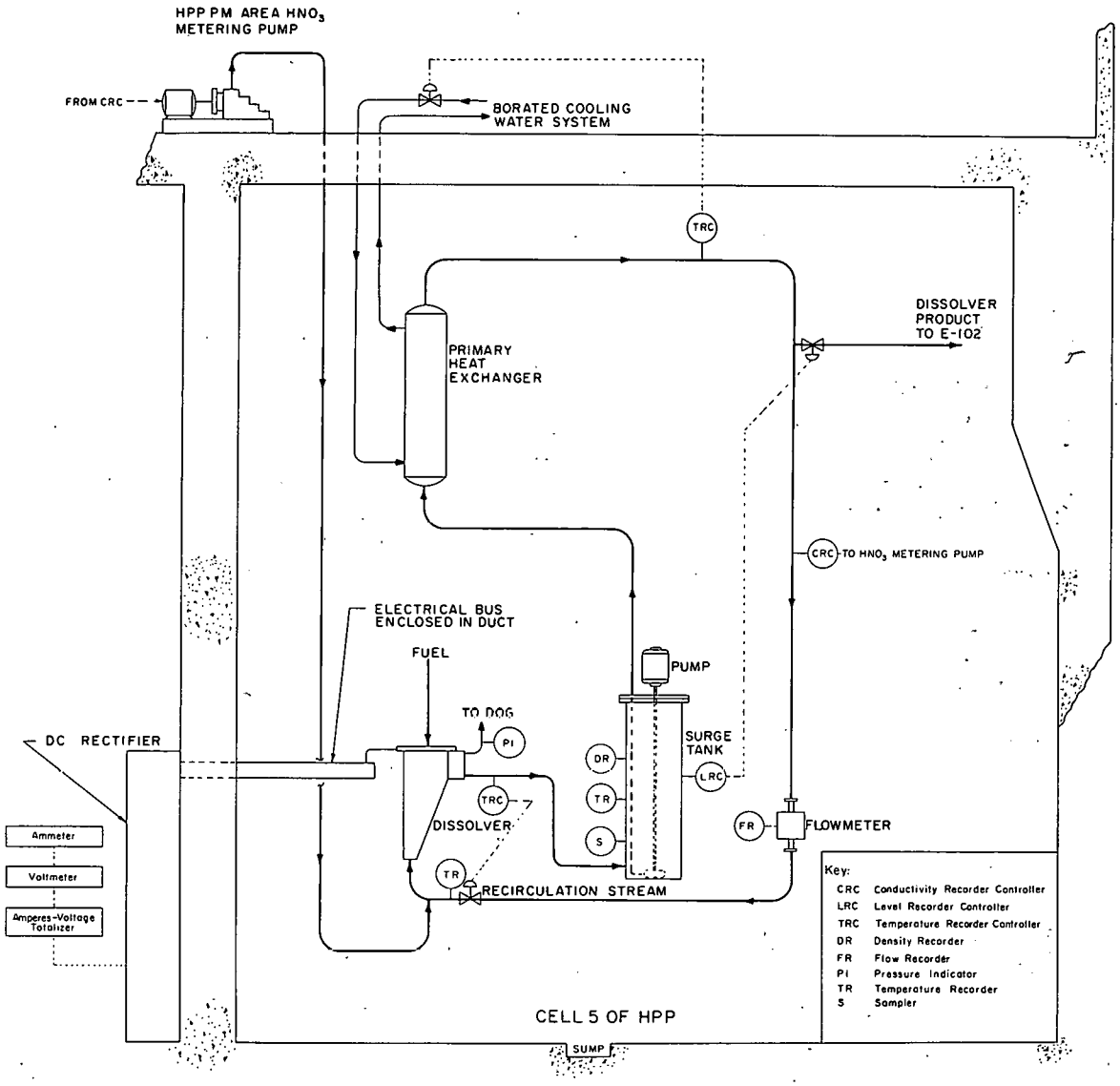

Fig. 14 Schematic flowsheet of the electrolytic dissolution process.

circulated continuously to the bottom of the dissolver. Solution from the dissolver will pass through a surge tank and pump, a cooler, and an electromagnetic flowmeter before being returned to the bottom of the dissolver. Fresh nitric acid and additives, eg, gelatin and a soluble neutron poison, will be added continuously; product solution will be removed continuously and flow to the existing ICPP extraction system for recovery of uranium. A chemical flowsheet for the dissolution and first cycle extraction of EBR-II fuel is shown in Figure 15.

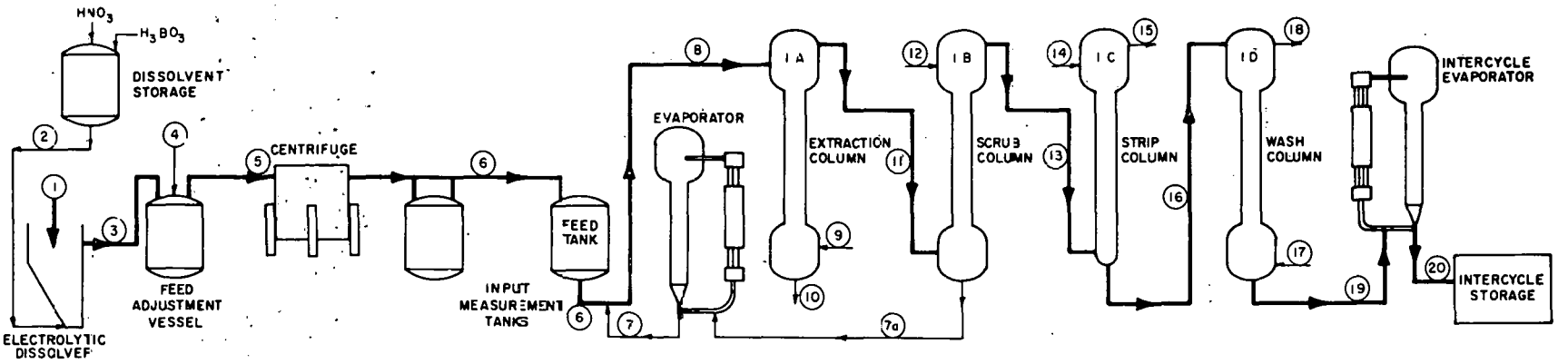

STREAM	1	2	3	4	5	6	7	7a	8	9	10	11	12	13	14	15	16	17 and 18	19	20
DESCRIPTION	FUEL CHARGE [a]	DISSOLVENT	DISSOLVER PRODUCT	FEED ADJUSTMENT SOLUTION [c]	DILUTED DISSOLVER PRODUCT	CENTRIFUGED DISSOLVER PRODUCT	CONCENTRATED	1BR	1BR	1AF	1AX	1AR	1AP	1BS	1BP	1CX	1CR	1CP	1DX	1DR	1DP	FIRST CYCLE PRODUCT
Flow, l/hr		278	278	278	556	555	51	110	587	580	537	580	113	580	300	580	300	15	300		16.6
SS, g/hr	1560																				
U, g/hr	3340																				
Na, g/hr	38																				
Fissium, g/hr	178																				
H, M		8.00	7.40		3.70	3.70	1.60	0.45	3.59		3.41	0.18	-0.50 [d]	0.0	0.005		0.005		0.005		0.09
NO_3, M		8.00	7.80		3.90	3.90	8.68	2.45	4.15		3.97	0.20	1.50	0.05	0.005		0.10		0.10		1.78
Al, M							1.80	0.50	0.09		0.09		0.50								
SS, g/l			5.98		2.99	2.99			2.83		2.83										
U, g/l			12.00		6.00	6.00	0.71	0.20	5.71		5×10^{-4}	5.73		5.74		5×10^{-4}	11.10		11.10		200
Na, g/l			0.14		0.07	0.07			0.06		0.06										
NH_4, M							1.80	0.50	0.09		0.09		0.50								
B, g/l [b]		8.0	2.0		1.0	1.0			1.0		1.0										
Fissium, g/l			0.64 [e]		0.32	0.32			0.09		0.09										
TBP, %										10		10		10		10					
Diluent										Amsco		Amsco		Amsco		Amsco		Amsco			

Basis: 1 Fuel Subassembly Section (EBR-II)
5.620 kg U
0.064 kg Na
0.300 kg Fissium
2.800 kg SS

[a] One fuel section of a subassembly charged each 101 minutes.
[b] Nuclear poison added as H_3BO_3.
[c] Water.
[d] Acid deficient with NH_4OH.
[e] Fifty percent of the fissium will be present as solids.

FORM INC-935 (2-68)

Fig. 15 Flowsheet for dissolution and first cycle extraction of EBR-II fuel.

5.2 Summary of Pilot-Plant Studies on the Electrolytic Dissolver (R. A. Brown; Development Engineering Section)

Pilot-plant study of the electrodissolution of EBR-II type fuel has been completed. The continuous pilot-plant dissolver[12], a 24-inch V-shaped dissolver, was operated for more than 2000 hours. Materials dissolved in the pilot plant were (a) stainless steel pipe, (b) unirradiated EBR-II fuel elements, (c) natural uranium sheathed in stainless steel pipe, and (d) stainless steel rod packaged in aluminum canisters. The dissolver, operating on the solution-contact principle for current distribution, was operated at current densities up to 2.2 A/cm^2.

No significant corrosion was observed on the platinum-clad niobium anode[14]. However, the titanium dissolver vessel, which is the cathode, had numerous small pits, varying in depth from 15 to 20 mils. The niobium basket was pitted and showed the effects of arcing in several places. Estimated operational life was 1.5 years for the vessel. The basket appears to have a long service life.

Dissolution of Stainless Steel Pipe

Since only six EBR-II fuel sections were available, limiting pilot-plant dissolution of this material to approximately 14 hours, the bulk of the experimental program was performed using stainless steel pipe. Extensive designed experimentation led to the following conclusions:

(1) Current utilization increases to 0.65 g/A-hr as current density increases to 1.2 A/cm^2. The apparent effect of larger stainless steel grain size is to decrease dissolution rates.

(2) Acid consumption was 3.4 moles/mole of stainless steel dissolved.

(3) The undissolved solids formation was 2 g/100 g of stainless steel dissolved.

Dissolution of EBR-II Fuel

Six EBR-II elements, containing natural and depleted uranium, were dissolved in the Electrolytic Dissolver Pilot Plant following establishment of desirable operating conditions by the stainless steel dissolution studies. The brief run of 14 hours (approaching steady state) was made at a current density of 1.2 A/cm^2, a temperature of 150°F, a HNO_3 concentration of 8 moles/liter, and an acid rate to maintain 12 g U/liter. The first part of the run was closely monitored and analyzed. A 36-hour heel-out was required for dissolution of residual fuel.

The dissolution of EBR-II fuel proceeded smoothly; stainless-clad fuel elements were opened by electrolytic dissolution and then dissolved by both chemical and electrolytic mechanisms. The sodium bonding material was gradually exposed to the nitric acid and resulted in no explosion hazard.

Closed circuit television equipment was used to monitor the run, and significant parts of the experiment were recorded on TV tape.

Uranium dissolved more rapidly than the stainless cladding after the cladding was opened eletrolytically. No criticality hazard can be expected from an accumulation of undissolved uranium. The uranium and iron concentration - time profiles are shown in Figure 16. Iron concentration rose to a steady state level of 6 g/liter; the uranium concentration profile showed six peak formations, which corresponded to the charging of fuel elements.

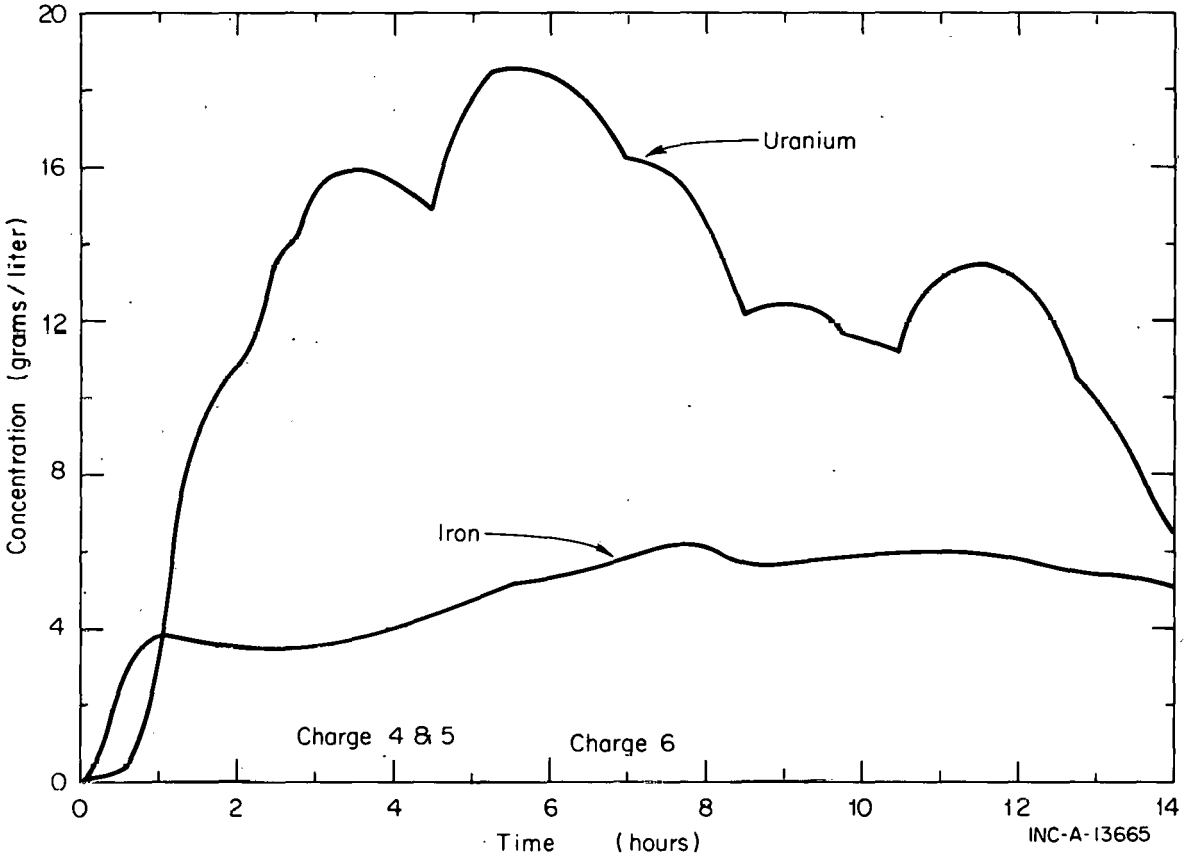

Fig. 16 Solute concentration profiles for the dissolution of EBR-II fuel in the electrolytic dissolver pilot plant.

The overall fuel dissolution rate was 1.35 g/A-hr. Uranium losses in the undissolved solids were less than 0.09% of the total uranium charged. Total undissolved solids represent 3 wt% of fuel charged. Hydrogen concentration in diluted effluent gas products was 0.4 mole % (approximately one-tenth of the explosive limit).

Dissolution of Stainless Steel-Clad Natural Uranium

An experimental pilot-plant run was made with natural uranium rod clad with steel pipe to detect differences due to the form of the uranium in the fuel. The uranium rod did not dissolve as rapidly as was observed with the uranium-fissium alloy in EBR-II fuel. Thus, the chemical dissolution rate would have a significant effect on the overall rate if unalloyed uranium were used.

Dissolution of Stainless Steel Rod in Aluminum Canisters

Since the EBR-II fuel elements are packaged in aluminum cans for storage in the ICPP basin, trial dissolution of simulated fuel packages of stainless steel rods in aluminum canisters was conducted. Both the aluminum canisters and enclosed stainless steel dissolved as predicted. The packaging of EBR-II fuel in aluminum cans should not have any significant effect on dissolver plant operation.

Summary

EBR-II fuel elements and simulated stainless steel fuel elements have been successfully dissolved in the Electrolytic Dissolver Pilot Plant. The system was operated for more than 2000 hours. A dissolution rate of 0.6 g/A-hr was demonstrated, and the sodium-bonded EBR-II elements were dissolved without any safety or criticality hazard. Uranium losses as undissolved solids were less than 0.09%.

5.3 Summary of Chemical Developments for Electrolytic Processing of EBR-II Fuel (B. C. Musgrave, Ed., C. A. Zimmerman, R. G. Butzman, M. W. Wilding, L. C. Lewis, T. L. Evans, M. E. Jacobson; Chemistry Section)

The chemical development of the electrolytic dissolution and the associated solvent extraction processes for EBR-II fuel has been essentially completed and is being reported in a topical report, IN-1285 [14], which will be issued shortly. The major results of this development work are summarized in the following paragraphs.

Fuel Storage. Leach tests conducted over a period of two years on fully irradiated EBR-II fuel elements in storage basin water have demonstrated that these elements, when free of prior cladding failure, can be stored satisfactorily in the basin without failure occurring. Fission products are leached from segments of declad fuel meat at a rate comparable to earlier results with declad aluminum fuels.

Uranium Dissolution. Chemical dissolution of uranium from chopped segments of EBR-II fuel pins in nitric acid occurs at a rate sufficiently rapid to guarantee that undissolved fuel slugs will not fall from the partially dissolved cladding to accumulate in the bottom of the dissolver.

Dissolver Corrosion. Corrosion studies indicate that the dissolver should survive 30,000 hours of operation before corrosion of the cathode, the most vulnerable area, should create any serious difficulty. The commonly used decontamination solutions can be used without excessive loss of metal.

Electrochemical Behavior of Alloys. The electrochemical behavior of stainless steel alloys, both cold and highly irradiated, has been compared. While it is possible to distinguish between the main types of stainless steel alloys by the EMF versus current density curves, and a significant difference occurs with the most highly irradiated material, all of the materials tested can be expected to dissolve in the electrolytic dissolver without difficulty.

Management of Solids. Solid residues resulting from the electrolytic dissolution of EBR-II fuel pins are a mixture of stainless steel grains, silica gel, and insoluble compounds resulting from the fissium alloy. If necessary, these can be solubilized by sodium hydroxide fusion followed by dissolution in nitric acid.

Uranium Extraction. Extraction studies of dissolved EBR-II fuel demonstrated that 99.95% of the uranium would be extracted in three stages. The fine solids which are not removed by the centrifuge will not create any unmanageable difficulty in the extraction column. The first cycle product will be 99.9% free of other metal ions.

5.4 The Electrolytic Behavior of Nuclear Fuel Cladding Alloys (L. C. Lewis and B. C. Musgrave; Chemistry Section)

The electrolytic behavior of several fuel cladding alloys has been examined by means of current-potential measurements. Nichrome and a wide variety of stainless steels have been shown previously to dissolve satisfactorily in the electrolytic dissolver with nitric acid as the electrolyte [15]. Continuing these observations, the effect of neutron irradiation on the dissolution characteristics has now been evaluated for Type 304 stainless steel (the cladding of EBR-II fuel), and the effect of alloy composition on chemical reactivity has been observed for aluminum alloys used as, or considered for, fuel cladding. The results of the latter work could lead to a quick, nondestructive test for alloy activity or passivity under plant dissolution conditions. This work, summarized in the following paragraphs, is the subject of a detailed topical report, IN-1295 [16].

Stainless Steels

Because stainless steels do not give reproducible current-potential curves in nitric acid, their behavior was examined in 5 M sulfuric acid so that some of the effects of mechanical working, thermal sensitization, and neutron irradiation could be compared with untreated material. Readily distinguishable curves were obtained for alloys having significant differences in their major components. Highly irradiated Type 304 stainless steel from EBR-II gave greatly different behavior from that obtained from material which had been irradiated to a much lower integral fast neutron flux. Unirradiated material shows the result of selective dissolution of alloy components as a result of the applied potential. Highly irradiated alloy appears to dissolve uniformly. Type 304 stainless steel which had been exposed to much lower total irradiation behaved essentially as unirradiated material.

Although the difference in behavior is quite marked, it appears that all of the series 300 stainless steels will dissolve in the electrolytic dissolver readily, regardless of metallurgical state or irradiation history.

Aluminum Alloys

The mercury catalyzed dissolution of aluminum and aluminum alloys has been shown previously to be significantly influenced by the alloy composition and the presence of several different cations in solution [17]. The influence of alloy composition and of the presence of mercury catalyst on the galvanostatic

curves was determined for eight aluminum alloys. For some of these alloys, the influence of dissolved cations was determined at concentrations comparable to that to be expected in a continuous dissolver. Although the mechanism of inhibition by dissolved cations has not been established, it was shown that significant increases in the concentration of mercury in the solution did not establish electrode potentials required for satisfactory chemical dissolution rates in the presence of nickel and copper ions. Exploratory investigation showed that satisfactory dissolution rates were achieved in the presence of nickel ion using dimethyl glyoxime to complex the nickel.

For all of the aluminum alloys examined, however, the behavior under applied anodic potential indicated that dissolution of these alloys in the electrolytic dissolver would proceed satisfactorily.

5.5 Evaluation of Hydrocyclones for Clarification of Electrolytic Dissolver Solutions (D. H. Cranney, M. E. Jacobson, B. C. Musgrave; Chemistry Section)

Solid materials as undissolved remnants and insoluble products result from the electrolytic dissolutions of nuclear reactor fuels. Diversion of these solids from the recycle stream of the electrolytic dissolver, with ultimate removal by a centrifuge, will help to reduce fouling of process equipment.

Several hydrocyclones were evaluated for their potential usefulness in clarification of plant process streams. Particular emphasis was placed on the behavior of the solids resulting from dissolutions of stainless steel and EBR-II fuel in the electrolytic dissolver. At the approximate pressure drops that would be practical for a plant installation, 95% of the smaller sized stainless steel solids were removed by the hydrocyclone; at these same conditions, only 10% of the fissium alloy residues from the EBR-II fuel were removed. Interactions between large amounts of solids and high concentrations of added silica gel were also examined. None of the mixtures tested, short of a firm gel, caused any decrease in the effectiveness of the hydrocyclone for particle separation. Details of the investigation are reported fully in IN-1276 [18].

5.6 Corrosion of EBR-II Fuel Elements During Underwater Storage (C. A. Zimmerman and D. W. Rhodes; Chemistry Section)

Fuel Element Leak Tests of Clad EBR-II Fuel Pins

Fuel Element Leak Tests [19] (FELT) were continued using Type 304 stainless steel - clad EBR-II fuel pins that had been stored in the ICPP storage basin for two years. No significant increase was observed in the concentration of radioactive materials in the FELT apparatus during a seven-day test period. Apparently, the five fuel pins, sensitized in a sodium-cooled reactor environment at approximately 516°C, have not suffered cladding penetration or failure during the two-year test period. Results of the first year of testing, with similar results, were reported earlier [1].

Leaching of Unclad EBR-II Fuel Pin Segments

Investigation of the leaching behavior of declad, irradiated, uranium-fissium fuel alloy to determine what would happen if the stainless steel cladding

were penetrated was continued. One pin segment was contacted with storage basin water. A second pin segment was contacted with 6 M NaOH to simulate a failure in which water contacted the sodium bonding between the stainless steel cladding and the uranium-fissium alloy meat.

The fuel pin segments used in these tests had a calculated surface area of 3.1 cm^2 and were initially immersed in 3.1 liters of solution. The results of these two tests, as well as the results of a previous test[1], are presented in Figure 17. In all three tests there is first a rapid increase in the amount of Cs-137 in the leaching solution, which is probably due to loosely adhering surface material on the fuel pin segments, followed by a period of nearly constant or slowly rising total Cs-137 leached and, finally, a rapid increase in the amount of Cs-137 leached.

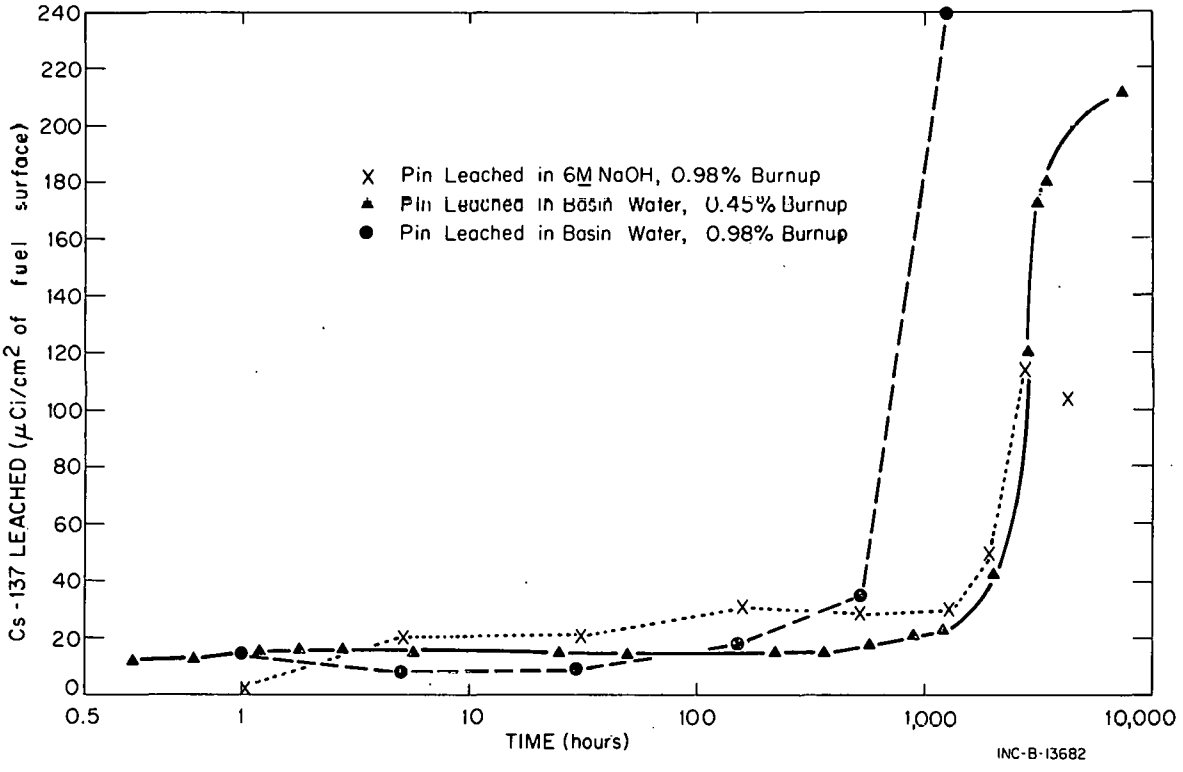

Fig. 17 Curves showing leaching of Cs-137 from unclad EBR-II fuel.

The difference in the time of contact (~500 and 1200 hours) required to initiate the rapid leaching in basin water appears to reflect the difference in at.% burnup of the two specimens. It is probable that the higher burnup results in a more severe deterioration of the alloy, thus requiring a shorter contact time to achieve rapid leaching.

Although the specimen in caustic was from the higher burnup fuel, it behaved in much the same manner as the low-burnup specimen exposed in storage basin water. A different surface reaction may take place in caustic which results in a slower leaching action. This assumption is supported to some extent by studies reported by others[20,21]. These results demonstrate that if the fuel cladding is penetrated, leaching of fission products will occur at a significant but not a catastrophic rate. Further, they substantiate the

conclusion that no penetration of the stainless steel cladding had occurred during two years of storage of EBR-II fuel pins as described in the preceding section.

6. ZIRCONIUM OXIDE FUEL PROCESS

6.1 Aqueous Halide Process -- Ternary Oxide Fuel Dissolution Studies (L. A. Decker, J. P. Clark, T. L. Evans; Chemistry Section)

The Shippingport PWR Core 2, Seed 2 consists of oxide fuel wafers clad in Zircaloy-4. The fuel loading in the core is zoned by varying the composition of the wafers from 26.5 to 54.9% uranium oxide. The other components vary from 67.1 to 39.1% zirconium dioxide, and from 6.4 to 5.2% calcium oxide. These ternary oxide fuel wafers are much more resistant to chemical dissolution than the binary oxide wafers from Seed 1 which were completely dissolved by successive treatments with 20 M hydrofluoric acid and 0.1 M chromic acid solutions [22]. Similar treatment on the ternary oxide fuel left a residue of highly insoluble calcium fluozirconate. However, it has been shown that 90% of the ternary oxide wafer can be dissolved and 99% of the uranium leached from the fuel by contacting with boiling 20 M hydrofluoric acid - 0.1 M chromic acid solution for 24 hours.

II. WASTE MANAGEMENT

1. OPERATING EXPERIENCE IN THE IDAHO WASTE CALCINING FACILITY

At the Idaho Chemical Processing Plant, aqueous wastes resulting from the reprocessing of spent nuclear fuel elements are converted to granular solids in a fluidized-bed calciner, the Waste Calcining Facility (WCF). Since the WCF was first operated with radioactive waste in December 1963, over 1.4 million gallons of aluminum nitrate waste and 0.4 million gallons of zirconium-fluoride waste have been converted to about 25,000 ft^3 of solids. These solids are currently stored in underground stainless steel bins. The third processing campaign in the WCF was completed during FY-1969.

1.1 Brief Description of the WCF (G. E. Lohse, D. P. Wright, C. L. Bendixsen; Process Engineering Section)

The WCF process consists of two main operations, (a) the actual waste calcination step and (b) off-gas decontamination. The primary operation, conversion of the corrosive aqueous radioactive waste to noncorrosive solids, is accomplished in a four-foot-diameter fluidized bed heated by internal heat transfer surfaces. Solutions are injected through pneumatic atomizing nozzles into the heated bed of granular solids which are fluidized with preheated air. The feed, which contains a full range of aged fission products, is sprayed into the bed and decomposes to solids and gaseous products. The solids deposit on the bed particles, some of which are continuously removed, while the gases are carried with the fluidizing and atomizing air to the off-gas decontamination system.

Heat required for the process is supplied through an indirect heat transfer system (bayonet tubes immersed in the bed) which uses a eutectic mixture of sodium and potassium (NaK) as the heat transfer fluid. The fluidized bed is maintained at the proper temperature, usually 400°C, by controlling the temperature of the NaK which is heated to temperatures as high as 760°C in an oil-fired furnace and circulated with an electromagnetic pump. The NaK system of the WCF will be replaced by an in-bed combustion system in the near future to improve process reliability and to increase the throughput capacity at minimal capital cost.

The solid product, continuously removed from the WCF, is transported pneumatically to the storage facility where it is separated from the transport air in a cyclone located above the storage bins. The solids fall by gravity into the bins, and the transport air is returned to the top of the calciner where it is merged with the calciner off-gas.

The second main operation of the WCF process involves the cleanup of the off-gas which contains both radioactive particulate matter and volatile radioactive materials. Cleanup or decontamination is accomplished in a series of devices which include a spray quench tower, a venturi scrubber and associated cyclone-type entrainment separators, heaters, silica gel adsorbers, and high-efficiency filters. The off-gas, after being decontaminated, is discharged to a 250-foot high stack.

1.2 The Third WCF Processing Campaign (G. E. Lohse, D. P. Wright, C. L. Bendixsen; Process Engineering Section)

The third WCF processing campaign was begun in August 1968, and, after a short period of startup on simulated aluminum-type waste, radioactive zirconium-fluoride waste was processed during most of the campaign. The run was terminated in June 1969, after nearly 10 months of operation. Pertinent operating facts are summarized in Table XIII. Significantly, during about 5900 hours of operation, nearly 312,000 gallons of zirconium-fluoride waste were

TABLE XIII

PERTINENT OPERATING FACTS OF THIRD WCF CAMPAIGN

Total Operating Time, hr		7180
Aluminum Waste:	220	
Zirconium Waste:	5856	
Nonradioactive Feed:	308	
Downtime:	796	
Net Volume of Radioactive Waste Calcined, gal		
Aluminum Waste:	17,000	
Zirconium	312,000	
Net Volume Solids to Storage, ft^3		
Aluminum Waste:	250	
Zirconium Waste:	4500	
Nonradioactive Solids:	485	

calcined to about 4500 ft^3 of granular solids. During this time, two unscheduled shutdowns occurred which required about 800 hours of downtime for decontamination, repairs, and restartup.

Typical Zirconium-Fluoride Waste Composition

Waste generated from reprocessing zirconium-uranium alloy fuel contains a substantial concentration (up to 3.0 M) of fluoride which must be complexed with calcium to prevent volatilization during calcination. This raw feed (wastes from the tank farm) is pumped batchwise to a blend tank where calcium nitrate and scrubbing solution recycle are added: the equivalant rates at which these three streams are introduced to the calciner are 55, 18.5, and 22.5 gph, respectively, for an average gross feed rate to the calciner of 96 gph. A typical

analysis of this blended calciner feed solution is zirconium 0.09 M, fluoride 0.95 M, aluminum 0.42 M, nitric acid 1.8 M, calcium 0.68 M, nitrate 4.5 M, and undissolved solids 50 g/liter. Traces of sodium, boron, and fission product ions are also present. After calcination, the solid product has a bulk density near 1.7 g/cc and a mass median particle diameter near 0.9 mm. A typical composition of the solids is 54 wt% calcium fluoride, 21% zirconium oxide, 22% aluminum oxide, and trace amounts of nitrate, water, and other metallic salts.

Off-Gas System Performance

Performance of the off-gas cleanup system was excellent throughout the third campaign. The wet scrubbing system (quench tower and venturi scrubber) removed about 99.9% of the particulate matter and 90% of the ruthenium from the entering off-gas; the silica gel adsorbers removed about 90% of the remaining particulate matter and 99.9% of ruthenium from the off-gas; and the filters removed greater than 99.9% of the remaining particulate matter. Thus, the daily release of Sr-90 to the atmosphere averaged less than 0.1 mCi/day, while that for Ru-106 averaged about 25 mCi/day. The concentrations of these radionuclides in the ICPP stack effluent were less than the radioactivity concentration guide for general population exposure as given in the AEC Manual, Chapter 0524.

Operational Problems

During the campaign, a few problems were encountered which caused two unscheduled shutdowns, both of which were believed to be caused by a high solids carryover to the scrubbing system. During the early part of the campaign, nitric acid was added to the scrubbing solution to dissolve solids (largely calcium fluoride) that had accumulated in the scrubbing solution tank. This released free fluoride which then produced excessive corrosion rates on high-stressed stainless steel components (nuts and bolts in pump flanges) and in turn caused malfunction of the scrubbing system pumps (see Section II-1.3). Recent laboratory tests have indicated that a 5.0 M HNO_3 solution will dissolve about 12.5 g/liter CaF_2 (see Section II-1.4), thereby releasing fluoride ion which corrodes Type 304L stainless steel. By adding $Al(NO_3)_3$ to the scrubbing solution in a ratio of 0.33 moles of aluminum per mole of fluoride, the fluoride released by the dissolution of CaF_2 solids will be complexed and, thus, future scrubbing tank corrosion problems should be minimized.

The high solids carryover is believed to have been caused by an excessive concentration of calcium nitrate in the blended feed. A 10% excess of calcium was routinely added to the raw feed contained in the blend tank to assure adequate fluoride complexing. However, recycle from the scrubbing system was also added to the feed in the blend tank; the recycle contained excess calcium ion as well. The result was a calciner feed stream more highly enriched with calcium than desirable. The excess calcium ion formed calcium nitrate during the calcination process, and continued to build up in the bed until it reached 21% by weight. Corrective action involved dilution of the bed nitrate by briefly calcining aluminum waste; subsequent operation with a lower concentration of calcium ion (5% in excess of the stoichiometric amount) produced satisfactory operation.

Summary of Third WCF Campaign and Proposed Future Operations

In summary, on the third processing campaign, as on previous campaigns, performance of the WCF has been entirely satisfactory. Throughput rates have consistently averaged higher than the original design basis and the on-stream time of 89% exceeded early estimates. The third campaign, which ended June 4, FY-1969, marks the last time the NaK heating system will be used. The WCF is now being decontaminated; following this, it will be carefully inspected in preparation for installation of an in-bed combustion heating system (see Section II-3). With the new heating system, reliability of the process is expected to be even better, and throughput rates are expected to be significantly greater than those experienced to date.

1.3 Corrosion Experience in the WCF While Calcining Zirconium-Fluoride Containing Wastes (T. L. Hoffman; Chemistry Section)

During operation with radioactive zirconium-fluoride containing feed solution, failures due to corrosion were encountered on a flow control valve and two pumps in the scrubbing system. The component parts involved in these failures were corrosion evaluated as follows:

Bellows on Flow Control Valve. The weld points on the seal bellows of a flow control valve were pitted, resulting in leakage of the scrubbing solution through the pitted areas. The main body of the bellows was etched but not corroded severely. Normally, erosion occurs where the valve seats, but in this particular valve erosion occurred above the seat point. High velocity eddy currents are presumed to have been present during operation, and the impaction of entrained solids may have caused erosion of the metal.

Scrubbing Solution Pumps. Loss of discharge pressure from the scrubbing solution pumps (referred to in Section II-1.2) indicated probable corrosion. Visual examination of the first pump indicated that the impeller had loosened, because the locking nut had dropped from the shaft and the shaft key had vibrated loose, freeing the impeller. On the second pump, bolts securing the discharge flange beneath the solution level inside the tank had corroded, loosened, and had fallen to the bottom of the tank. Solution was then being recirculated inside the tank instead of to other parts of the scrubbing system.

Examination indicated that pump parts made of Types 347 and 304 stainless steel were attacked significantly by the scrubbing solution, while parts made of Type 304L showed little corrosion other than etching. Castings were attacked severely -- some pitting was as deep as 1/4 inch. Wherever there was evidence of millsand in the castings, the area was extensively corroded.

Bench tests previously performed indicated that at 50°C a corrosion rate of 0.1 mil/month could be expected for Types 347 (Cb and Ta) and 304L stainless steel in the normal scrubbing solution. At 65°C, a rate near 1.0 mil/month may be expected, and at 102°C, a rate near 12 mil/month may be encountered. The scrubbing solution temperature for the last three months of operation was about 65°C; the presence of unusual quantities of fluoride (see Section 1.2) would lead to more rapid corrosion under these conditions. In general, the corrosion rates experienced in the scrubbing system are about the same

as was anticipated from development work for the exposure conditions and, as originally anticipated, periodic replacement of some parts of the system will be required.

Complexing of Fluoride-Containing Solutions. When calcining zirconium process raffinate in the WCF, potentially corrosive mixtures of hydrofluoric and nitric acids are created in the scrubbing solution, the fluoride being carried into the scrubbing solution principally in solids elutriated from the fluidized bed. Since complexing ions for fluoride are normally present, and to a certain extent their concentrations can be adjusted, data on the effect of aluminum, calcium, and zirconium on corrosion were obtained.

The corrosion rate of Type 304L stainless steel in a 1.0 M hydrofluoric - 4.8 M nitric acid mixture at 75°C was 220 mil/month. Rates were reduced to 120 mil/month by the addition of 0.55 M calcium nitrate to the original hydrofluoric - nitric acid mixture, primarily because some of the fluoride was removed from solution by the precipitation of CaF_2. The corrosion rate was further reduced to 29 mil/month by the addition of 0.36 M aluminum nitrate, and to 3 mil/month when 0.27 M zirconium nitrate was added to the original acid mixture. Significantly, the inhibition of corrosion of Type 304L stainless steel in hydrofluoric - nitric acid mixtures by calcium ion is much less than that by aluminum or zirconium ions.

1.4 Apparent Solubility Isotherms for Calcium Fluoride in Nitric Acid Solution (M. W. Wilding; Chemistry Section)

Calcium fluoride, which is produced during the calcination of fluoride-containing radioactive wastes in the Waste Calcining Facility, must be dissolved in decontaminating solutions containing nitric acid during cleanup of the scrubbing system. Inasmuch as solubility values for calcium fluoride in nitric acid at various temperatures did not appear to be available in the literature, apparent solubility values were obtained experimentally at four different temperatures and various concentrations of nitric acid.

Reagent grade anhydrous calcium fluoride (CaF_2) was used, after heating 48 hours at 105°C, to obtain constant weight. Weighed samples (1 g) of the dried CaF_2 were then contacted with 50 ml of nitric acid in the range 0.1 to 10 M HNO_3 and maintained for 170 hours at 24, 35, 50, and 70°C. The test samples, which were contained in polyethylene bottles, were agitated periodically. All samples were filtered, before cooling, through filters having 0.45 μ diameter pores. The residues (undissolved solids) were oven dried at 105°C for 48 hours and weighed. The amount in solution was then determined by weight difference. As an analytical check, samples of the supernatant solutions were diluted ten-fold to prevent re-precipitation of the undissolved solids, and were then analyzed for calcium.

The solubility isotherms for CaF_2 as a function of nitric acid concentration, with temperature as a parameter, are shown in Figure 18. These curves were drawn using average values obtained from triplicate samples. The deviations in the measurements are shown graphically. The check results obtained by determining the concentration of calcium in solution agreed with the values obtained by weighing within ± 5%.

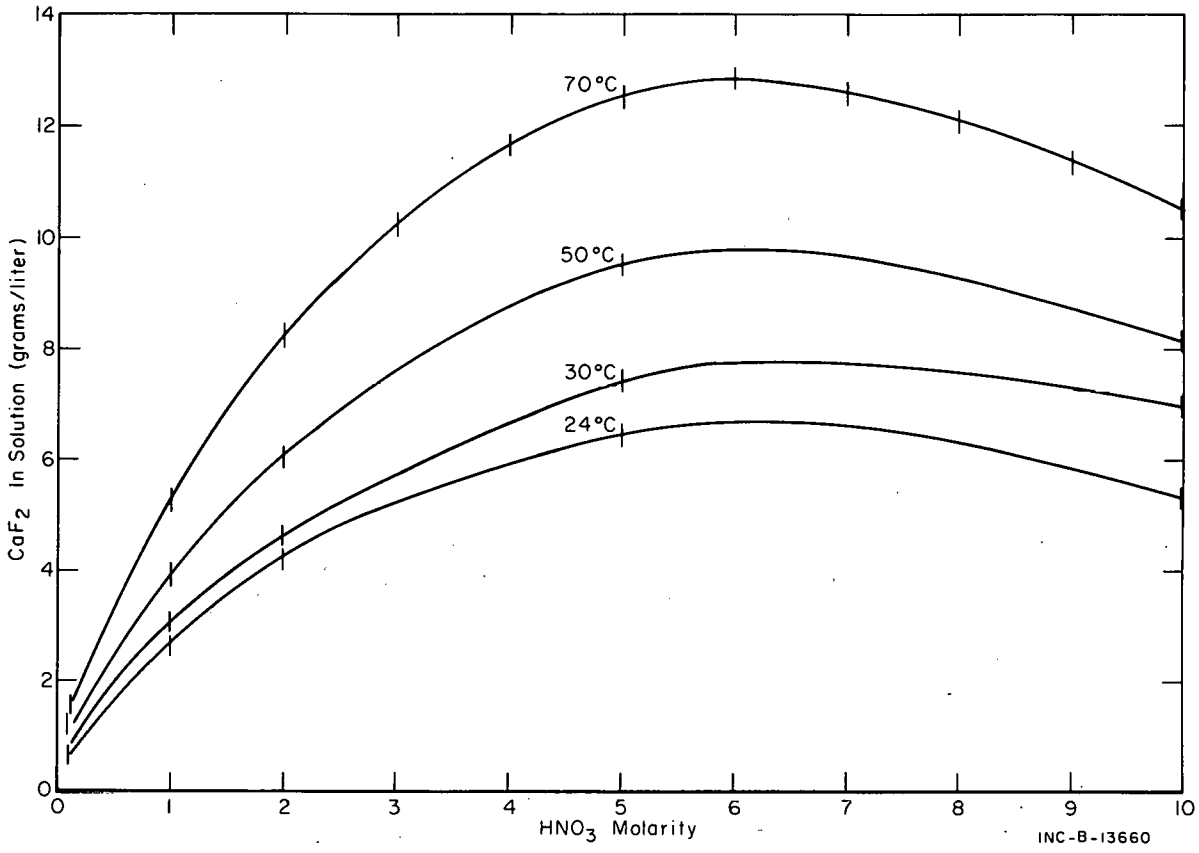

Fig. 18 Solubility isotherms for CaF_2 in nitric acid.

Tests also were run at 70°C using 3, 4, 6, 7, 8, and 9 M HNO_3 to better define the maximum in the curve. A maximum occurs at 6 M HNO_3. The reasons for the decreasing solubility with increasing acid concentration above 6 M HNO_3 were not readily apparent; no additional studies were made to investigate this phenomenon.

2. STORAGE OF SOLID WASTE AT THE WCF

2.1 Review of Safety Aspects of ICPP WCF Solids Storage (G. E. Lohse; Process Engineering Section)

High-level radioactive aqueous wastes resulting from the solvent extraction of uranium from nuclear fuel elements are calcined to granular solids in the Waste Calcining Facility at the Idaho Chemical Processing Plant (ICPP). The granular solids are stored in stainless steel bins which in turn are contained inside buried concrete vaults. This arrangement thereby provides double containment and means for detecting failure of the primary containers or seepage of surface or ground water through a fissure in the concrete vault. Provisions for retrieval of the solids are included.

A critical review of the safety aspects of the ICPP solids storage facilities has been completed and an internal company report has been prepared. Conclusions of the study indicate that these facilities are capable of withstanding

natural phenomena such as earthquakes and flooding, and, with proper design elsewhere, that the concept of storing granular solids in bins inside secondary containment is a completely acceptable approach to permanent disposal of highly radioactive waste.

The pertinent findings of this study indicate

(1) The occurrence of an earthquake of magnitude seven with an epicenter 20 miles north of the ICPP would produce a maximum credible ground acceleration at the storage area of 32% of gravity. This acceleration would not damage the concrete vault structure, nor do direct damage to the bins. The bin anchor bolts possibly might shear. With anchor bolt failure some damage may be inflicted on bin vent piping above the bins. However, release of radioactive solids into the vault or to the environment should not occur. If the ground acceleration is 18% of gravity, the maximum probable value, then no damage to the bins, anchor bolts, or piping is anticipated.

(2) Climatology and hydrology of the area precludes any major flooding circumstances in the current geological era. If, through some currently inconceivable phenomena, the storage area were to be totally flooded, the stainless steel bins have sufficient corrosion allowance that their integrity should be maintained for at least 500 years. If such a phenomenon were to occur after the integrity of the bins was expended, fission products will have decayed to stable nuclei and only transuranic nuclides would be of concern. The water leach rate of transuranics from calcined solids has been shown to be very low. Adsorption of transuranics by soil materials from the ground and/or surface water would prevent any serious biological hazard to mankind.

(3) Mass movement of the regolith is impossible even at sustained wind velocities of 100 mph.

(4) Explosion hazards do not appear credible.

Summary

A critical review of the safety aspects of the ICPP solids storage facility indicates that these facilities are capable of withstanding natural phenomena such as earthquakes and flooding, and that this concept is a completely acceptable approach to permanent disposal of highly radioactive waste.

2.2 The Third WCF Solids Storage Facility (D. P. Wright; Process Engineering Section)

The stainless steel bins of the second solids storage facility for the WCF currently contain approximately 18,000 ft^3 of solids and, at a projected solids waste generation rate of 6400 ft^3/year, the bins should be filled during late FY-1971. Thus, a third solids storage facility will be required at ICPP and

must be ready to receive radioactive solids waste at that time. A design criteria document was completed and detailed design work is underway. Excavation for the installation of a concrete storage vault to contain the new storage bins was started during FY-1969. Completion of the facility is scheduled for the second quarter of FY-1971.

Design features of the third solids storage facility are similar to those of the second storage facility (Figure 19) [23] and include

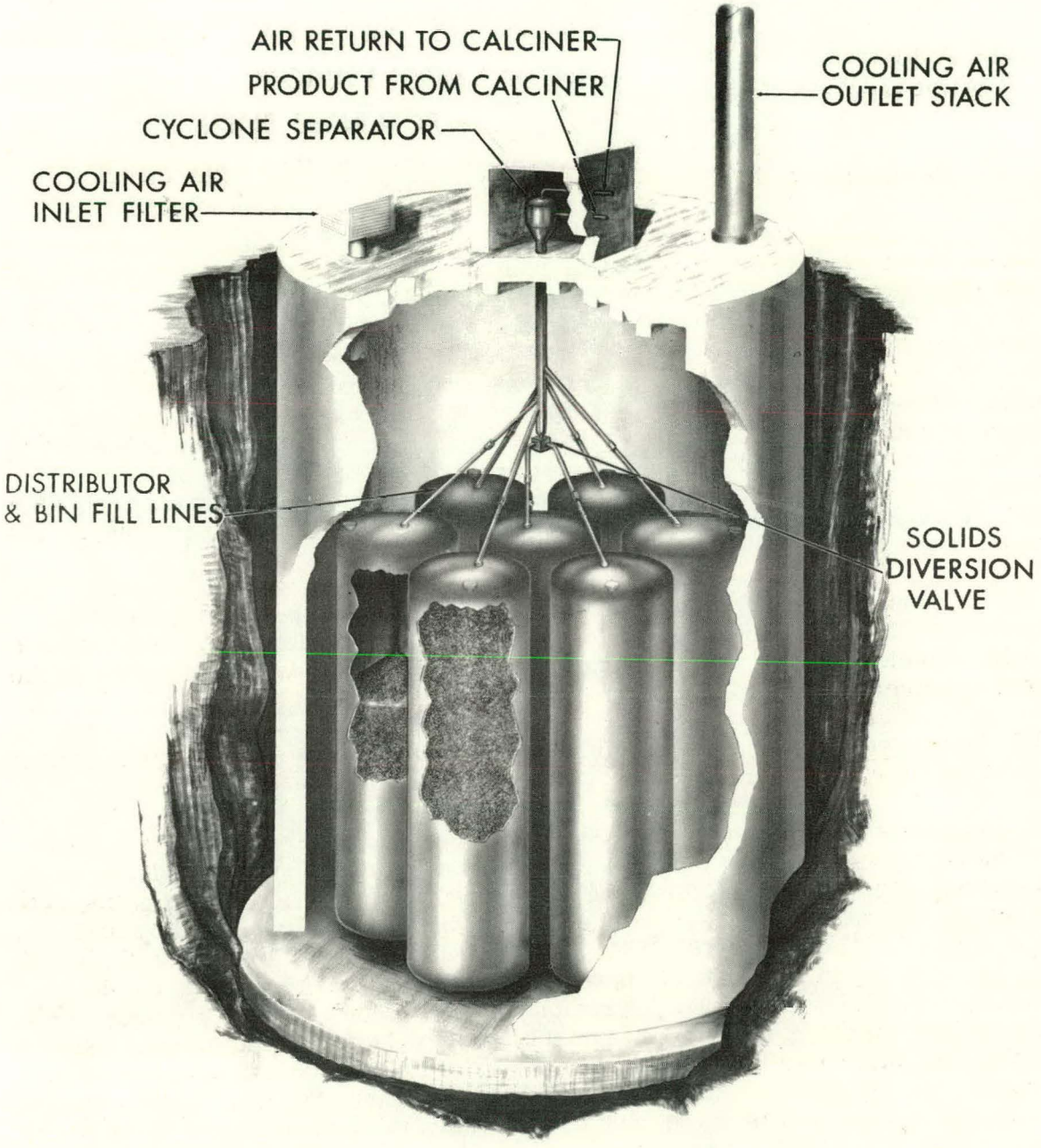

Fig. 19 Second facility for storage of granular calcined solids.

(1) A design limit of 290°C on vessel-wall temperature to ensure structural integrity.

(2) Bins made of ASTM A240 Type 304 stainless steel plate with wall thickness incorporating a 1/8-inch corrosion allowance.

(3) A pressure tolerance for the bins of ± 3.75 psig pneumatic pressure plus the hydrostatic load of calcined solids.

(4) Bins designed to withstand earthquake-induced lateral forces of 30% of the vertical load.

(5) Cooling of the bins by natural convection of atmospheric air over the bin surfaces.

(6) Provisions for installing a solids removal system.

Minor changes will be incorporated into the design for the new storage facility. While the diameter of the bins will remain at 12 feet, the overall height of the six peripheral bins will be increased from 42 to 53 feet, and overall height of the seventh and center bin will be increased to 61 feet. This will give the third facility a nominal capacity of 40,000 ft^3 as compared to 30,000 ft^3 for the second storage facility; the concrete containment vault remains the same size. The bins will be filled randomly, rather than one at a time, thus allowing more complete utilization of the vault space by simplification of the filling system. One special-purpose bin will contain a solids diverter valve which may be used to selectively collect high heat-generation-rate waste. This bin will contain corrosion coupons and an extensive system of thermocouples to measure temperature gradients.

The primary solids level indication will be by temperature measurement as sensed by bin - center line and wall thermocouples. However, one ultrasonic level detector device and one capacitance probe also will be installed on the vertical risers of separate bins to indicate solids level.

2.3 Corrosive Effects of Zirconia Calcine in Storage (C. A. Zimmerman; Chemistry Section)

Measurements to detect corrosion have been made after a two-year exposure of metal specimens to nonradioactive calcine from zirconium process waste solutions. The results of this long-term test show average weight gains up to 1 mg on the welded 2-$in.^2$ specimens of carbon steel, aluminum alloy 6061-T6, and Types 304, 304L, 316 ELC, 347, and 405 stainless steel after two years exposure at a temperature of approximately 200°C. The conditions and detailed description of this long-term corrosion test have been reported previously [13]. The slight weight gains are presumably due to the formation of oxide surface films. On the basis of these tests, the existing Type 304 stainless steel bins appear to be suitable for storage of this calcine. The tests are continuing at higher temperatures (up to ~300°C) to investigate the possibility of corrosion due to higher bin wall temperatures.

2.4 Leachability of Zirconia Calcine Produced in the WCF (M. W. Wilding, T. L. Evans, and D. W. Rhodes; Chemistry Section)

Granular calcined solids produced in the WCF by fluidized-bed calcination of highly radioactive zirconium fluoride-type waste solution were leached with distilled water at 25°C. The results, which are reported in IN-1298 [24], indicated that approximately 60% of the Cs-137 and 40% of the Sr-90 were leached from the zirconia-type calcine by continuous leaching for 2000 hours. Only a fraction of a percent of the Pu-239, Ce-144, and Ru-106 was leached under the same conditions. Less than 1% of the aluminum and zirconium, about 3% of the calcium, and approximately 50% of the residual nitrate were dissolved in the distilled water. Apparently, the plutonium, cerium, and ruthenium are tightly bound in the matrix, possibly by the formation of insoluble compounds, while the cesium, strontium, and nitrate are, in general, only retained by physical occlusion.

These results suggest that although the calcine matrix is relatively insoluble, the relatively high leaching rates of the long-lived radionuclides Cs-137 and Sr-90 require that the dry solid be prevented from being contacted by water during long-term storage. This is currently done at the ICPP by storing the solid underground in stainless steel bins contained within a concrete vault.

Studies have been initiated recently to study the leachability of both the alumina- and zirconia-type calcine after these calcines have been converted to crystalline compounds by heating to a high temperature. This study is intended to establish the characteristics of calcine that has been in long-term storage at temperatures sufficiently high to effect the formation of crystalline species.

2.5 Migration of Cesium-137 in Granular Calcined Radioactive Waste (M. W. Wilding, Chemistry Section; L. T. Lakey, Reactor Safety Studies Section)

Studies of the migration of Cs-137 in the Idaho Chemical Processing Plant calcine product at temperatures of 900 to 1200°C were continued using the experimental and mathematical techniques described in the annual report for 1968 [1]. The migration, induced by placing a small quantity of solids containing Cs-137 in contact with similar solids containing no Cs-137, was observed over a temperature range of 900 to 1200°C, with and without gas flow, and in both air and argon atmospheres. The movement of Cs-137 in granular alumina solids was detected using a gamma-ray spectrometer scanning system. As shown in Figure 20, significant migration was first noted at 900°C and was rapid at 1200°C. Gas flowing at 36 fph through the granular solids increased the migration rate 15-fold over that measured at no flow. Substitution of argon for air had little effect on the migration rate. Temperature gradients up to 100°C/in. also had little effect, indicating the Soret effect is small.

Effective diffusivities ranging from 10^{-7} cm^2/sec at 900°C to 10^{-3} cm^2/sec at 1200°C were calculated from a mathematical model simulating the experiment and derived for a constant diffusivity. However, the diffusivity was found to be a function of time and concentration, and both a transformation of the alumina crystalline structure and a change in the cesium species may be possible causes of the changing diffusivity. Because of the variable diffusivity, no quantitative relationship between diffusivity and temperature could be

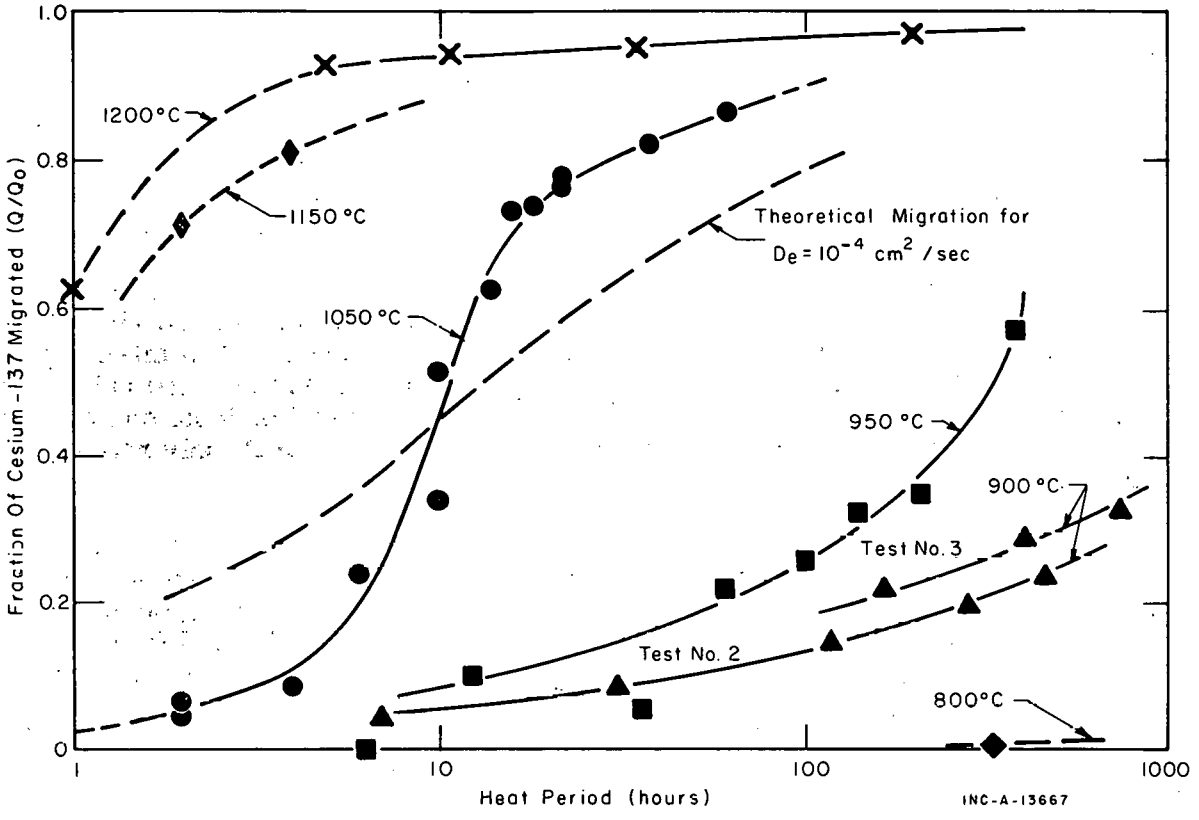

Fig. 20 Curves for migration of Cs-137 as a function of time and temperature.

established. Though qualified by the changes in alumina structure or cesium species, the calculated diffusivities show that the movement of Cs-137 is controlled by transport through the intra- or interparticle voids, rather than by diffusion in the alumina crystals.

3. STUDY OF CALCINATION USING IN-BED COMBUSTION OF FUEL FOR HEATING

3.1 Pilot-Plant Waste Calcination Studies (T. K. Thompson; Chemical Engineering Development Section)

In-bed combustion, the burning of a hydrocarbon fuel directly in a fluidized bed, is being investigated as a method of supplying process heat for fluidized-bed calcination of radioactive liquid wastes in the Waste Calcining Facility. Pilot-plant studies on the calcination of simulated aluminum and zirconium wastes in a 12-inch diameter calciner have been reported in detail[25] and have demonstrated the feasibility of in-bed combustion heating. Additional development work reported here includes safety studies to determine the effect of perturbations in waste feed and oxygen flows, and scoping studies concerning the in-bed combustion calcination of simulated high sodium wastes.

3.11 In-Bed Combustion Safety Studies. A series of tests were made in

the 12-inch diameter pilot-plant calciner to study the effects of waste feed and oxygen interruptions and above-bed burning on the in-bed combustion calcination process. This work was done using simulated complexed zirconium fluoride waste and kerosene fuel. These tests were designed to simulate operation during startup, ie, where a large amount of excess oxygen is used to control above-bed burning.

Feed Interruption Tests

Several tests were conducted where the waste feed flow was completely stopped while operating at ~450°C. The feed interruption resulted in an increase in the bed temperature at a rate of 14 to 16°C/min, with very little or no above-bed burning (indicated by the vapor-space temperature being greater than the bed temperature). The bed temperature excursion can be controlled easily by either reducing the fuel rate or resuming the waste feed flow to the process. Bed and vapor space temperature responses to a typical waste feed interruption are shown in Figure 21.

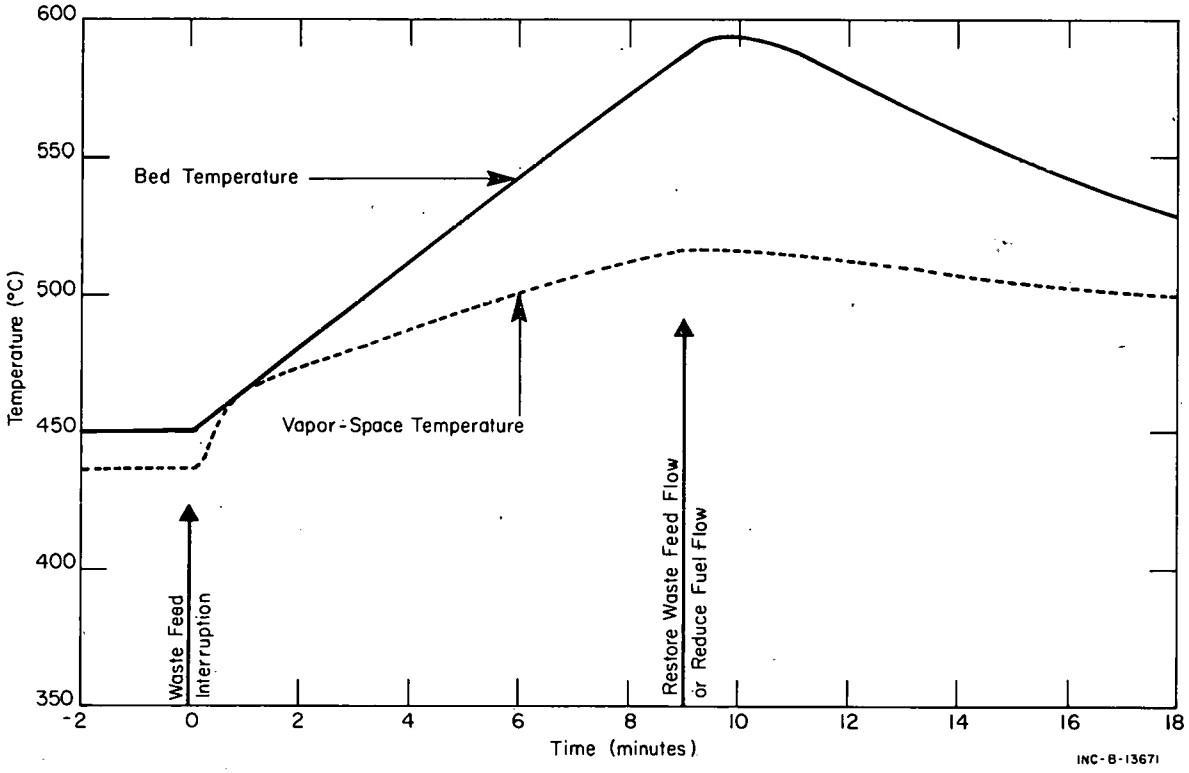

Fig. 21 Temperature effects during a typical interruption of waste feed flow.

Oxygen Interruptions

Tests were conducted to study the effect of interruption of fluidizing and fuel atomizing oxygen, both singly and together, on the bed and vapor space temperature response. Two distinct types of system response resulted after an oxygen interruption. One type of response -- designated Type I and shown in Figure 22 -- resulted in a decrease in bed temperature and an increase in the vapor-space temperature. The other type -- designated Type II and shown in Figure 23 -- resulted in decreasing bed and vapor space temperatures.

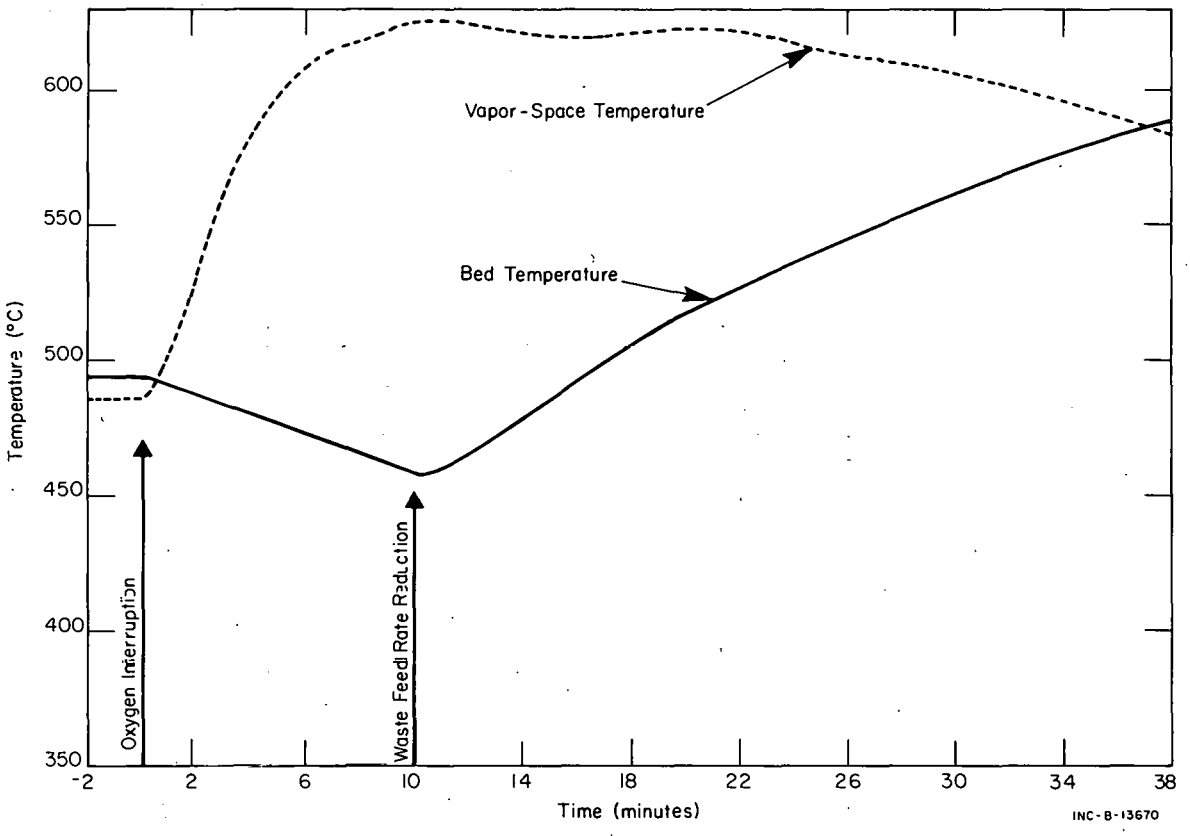

Fig. 22 Typical Type I temperature curve for interruption of oxygen flow.

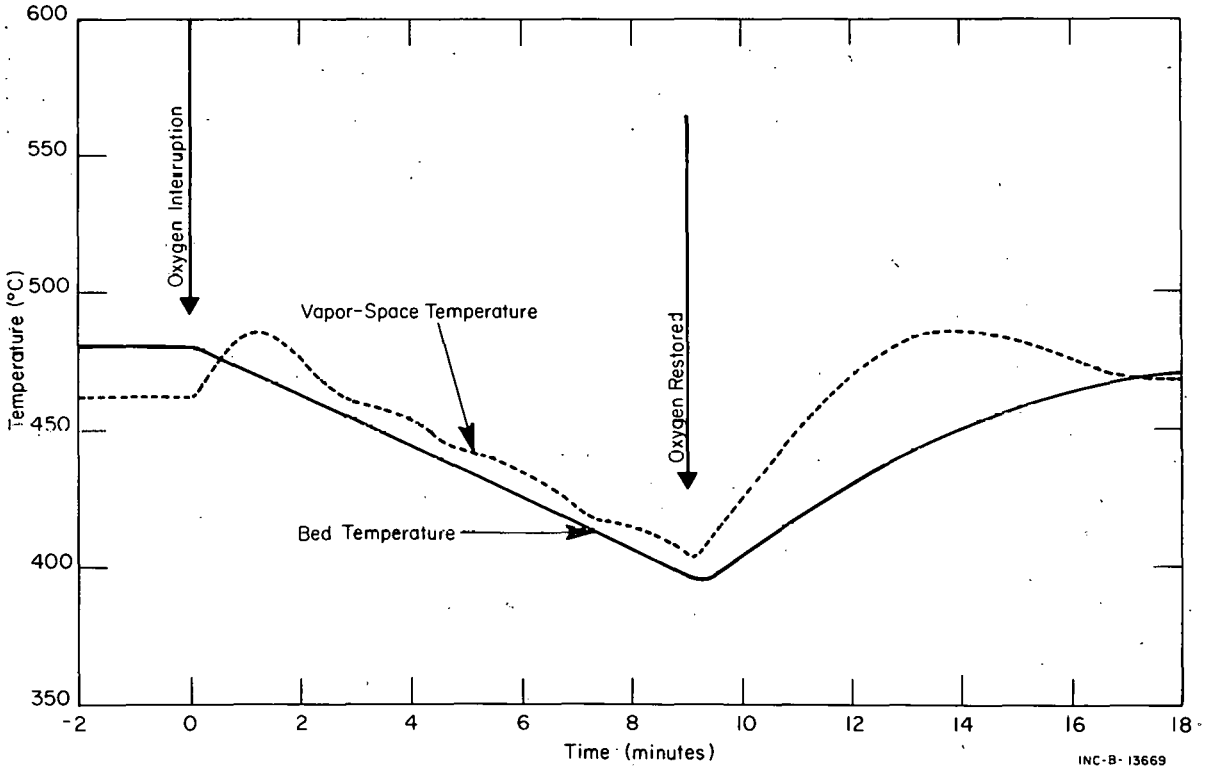

Fig. 23 Typical Type II temperature curve for interruption of oxygen flow.

Above-bed burning, indicated by the vapor-space temperature being higher than the bed temperature, occurred in each case.

Interrupting the flow of fuel atomizing oxygen resulted in a Type I system response as shown in Figure 22. Steady state operation can be established by restoration of the oxygen flow or by atomizing the fuel with air and reducing the waste feed rate (as shown in Figure 22) to reduce the thermal load on the system and allow the bed temperature to increase until in-bed combustion is resumed.

Fluidizing oxygen interruptions resulted in both Types I and II system responses as shown in Figures 22 and 23. Operation can be continued by restoring the oxygen flow or by increasing the fluidizing air and decreasing the waste feed rates in order to increase the bed temperature.

Total oxygen interruptions (fluidizing and atomizing) may result in either Type I or Type II system responses as shown in Figures 22 and 23. Steady state can be restored by either increasing the oxygen flow or fluidizing air; using air to atomize the fuel, or reducing the waste feed rate.

Above-Bed Burning Studies

Above-bed burning is defined as the condition where the vapor-space temperature is greater than the bed temperature in the fluidized-bed calciner vessel. Two distinct types of above-bed burning are possible: Type I, shown in Figure 22, where the slope of the vapor-space temperature plot is positive; and Type II where the vapor-space temperature plot slope is negative, as shown in Figure 23. The Type I above-bed burning condition occurs when greater than 100% of the stoichiometric oxygen required for combustion is still present in the system following a perturbation such as an oxygen interruption. Combustion still occurs as evidenced by the amounts of CO_2 and CO present in the off-gas; however, a large part of the combustion occurs in the vapor-space above the fluidized bed. A Type II condition results when there is less than 100% of the stoichiometric oxygen present in the system following a perturbation. The combustion reaction is "smothered" by lack of sufficient oxygen as evidenced by the low amounts of CO_2 and CO in the off-gas. Typical off-gas compositions for Types I and II above-bed burning are shown in Table XIV.

In-bed combustion safety studies have shown that (a) the response of the calciner to drastic process upsets allows adequate time to both indicate the occurrence of the upset and to take corrective action, and (b) the effects of such drastic upsets can be moderated by adjusting other process parameters to permit additional time to correct a major process upset.

3.12 In-Bed Combustion Calcination of Purex 1 WW Waste. A synthetic waste similar to Purex 1 WW was successfully calcined at 500°C in the 12-inch diameter fluidized-bed calciner using in-bed combustion heating. The reactions occurring in the calcination process were postulated, and good agreement was obtained between calculated and experimental compositions of the off-gas and calcined solids. Sodium was mainly confined in the calcined solids as $Na_3Al(SO_4)_3$ and $NaFe(SO_4)_2$; the friable product resulted in high fines elutriation rates.

TABLE XIV

TYPICAL OFF-GAS COMPOSITION FOR ABOVE-BED BURNING
(MOLE %)

Component	Type I	Type II
H_2	0.04	0.22
N_2	67.9	77.5
CO	2.4	1.3
CO_2	16.3	5.3
O_2	12.2	14.3
Aliphatic Hydrocarbon	0.06	0.08
Aromatic Hydrocarbon	0.003 Max	0.004 Max
Percent Stoichiometric O_2 Fed to Calciner		
In Fluidizing and Atomizing Gases	124%[a]	61.9%[b]
In Feed as NO_3^-	33.4%	33.4%
Total	157.4%	95.3%

[a] Oxygen added to fluidizing air, but fuel atomized with air.

[b] No extra oxygen with fluidizing air; fuel atomized with air.

Experimental Conditions

A scoping study was conducted in the 12-inch diameter pilot-plant calciner, using in-bed combustion heating[25], to determine the feasibility of fluidized-bed calcination of acid Purex-type wastes. The feedstock used was a simulated 1WW (1960) Purex waste with no UO_2 or fission products. Some NH_4^+ was present from $Fe(SO_4)_2$ $(NH_4)_2 \cdot 6H_2O$ used as the source of iron and sulfate. The compositions of 1WW waste and the simulated waste, as well as the chemicals used in preparation of the simulated waste, are given in Table XV.

TABLE XV

COMPARISON OF 1WW WASTE AND EXPERIMENTAL FEEDSTOCK

Component	1WW Waste (1960)	Experimental Feedstock	Chemical Source of Experimental Component
H^+	5.60 M	4.420 M	HNO_3
Fe^{+3}	0.50 M	0.509 M	$Fe(SO_4)_2(NH_4)_2 \cdot 6H_2O$
Cr^{+3}	0.01 M	0.009 M	CrO_3
Ni^{+2}	0.01 M	0.011 M	$Ni(NO_3)_2 \cdot 6H_2O$
Na^+	0.60 M	0.3 and 0.6 M	$NaNO_3$
Al^{+3}	0.10 M	0.171 M	$Al(NO_3)_3 \cdot xH_2O$
NO_3^-	6.10 M	6.040 M	HNO_3
SO_4^{-2}	1.00 M	1.130 M	$Fe(SO_4)_2(NH_4)_2 \cdot 6H_2O$
PO_4^{-3}	0.01 M	0.029 M	H_3PO_4
NH_4^+	----	0.865 M	$Fe(SO_4)_2(NH_4)_2 \cdot 6H_2O$
Sr	0.002 M	----	
Zr	0.007 M	----	
Mo	0.005 M	----	
UO_2^{++}	0.010 M	----	

Sodium concentrations of 0.3 and 0.6 M were used in the simulated feed; no bed caking was evident at either concentration, nor was there any evidence of undecomposed $NaNO_3$ in the calcined solids. Operating conditions and some product properties are shown in Table XVI.

TABLE XVI

CALCINATION OF SIMULATED PUREX WASTE --
OPERATING CONDITIONS AND PRODUCT PROPERTIES

Feedstock	Simulated 1WW 1960 Purex Waste
Fuel	Kerosene ($C_{11.6}H_{23.2}$)
Starting Bed	Alumina Calcine
Waste Feed Rate	25 liters/hr (8.5 gal/hr-ft^2)
Fuel Rate	1.5 gal/hr
Bed Temperature	500°C
Calciner Pressure	14.7 psia
Waste Nozzle Air Ratio	325 to 500 @ bed temperature and pressure
Fuel Nozzle Gas Ratio	∿700 @ bed temperature and pressure
Fluidizing Velocity	1.4 to 2.2 ft/sec
Oxygen Consumption Rate	140 to 250% of theoretical
Product Rate	∿1.4 lb/hr
Fines Rate	∿2.6 lb/hr
Product Bulk Density	∿1.2 g/cc
Fines Bulk Density	∿0.7 g/cc
Product MMPD	∿0.5 to 0.7 mm
Bed Height	∿28 in.
Bed Weight	∿130 lbs
Fluidized-Bed Density	∿0.92 g/cc
Total Operating Time	64.6 hr

Comparison of Calculated and Experimental Values

Theoretical solids product and off-gas compositions were calculated based on the assumption that the following reactions occur:

Combustion Reaction:

$$C_{11.6}H_{23.2} + 17.4\ O_2 \longrightarrow 11.6\ CO_2 + 11.6\ H_2O$$

Calcination Reactions:

$$Al^{+3} + 3\ Na^{+} + 3\ SO_4^{-2} \xrightarrow{\Delta} Na_3Al(SO_4)_3$$

$$Cr^{+3} + PO_4^{-3} \xrightarrow{\Delta} CrPO_4$$

$$3\ Ni^{+2} + 2\ PO_4^{-3} \xrightarrow{\Delta} Ni_3(PO_4)_2$$

$$Fe^{+3} + PO_4^{-3} \xrightarrow{\Delta} FePO_4$$

$$Fe^{+3} + Na^{+} + 2\ SO_4^{-2} \xrightarrow{\Delta} NaFe(SO_4)_2$$

$$4\ Fe^{+3} + 3\ O_2 \xrightarrow{\Delta} 2\ Fe_2O_3$$

$$SO_4^{-2} \xrightarrow{\Delta} SO_2 + 2\ O_2$$

$$2\ NO_3^{-} \xrightarrow{\Delta} N_2 + 3\ O_2$$

$$2\ NH_4^{+} + 2\ O_2 \xrightarrow{\Delta} N_2 + 4H_2O$$

It was assumed that the preferential reaction involving sodium in the calcination was the formation of $Na_3Al(SO_4)_3$, which is limited by the amount of aluminum in the system. The remaining sodium reacts to form $NaFe(SO_4)_2$, and the remaining sulfate is reduced to SO_2. The theoretical solids production rate was 2920 g/hr based on the above reactions. The theoretical and experimentally determined compositions of the calcined solids and of the off-gas are compared in Tables XVII and XVIII. Agreements are generally good. Typical scrubbing solution compositions are given in Table XIX.

Conclusions

The signficance of this run was (a) the formation of thermally stable sodium compounds [$Na_3Al(SO_4)_3$ and $NaFe(SO_4)_2$] instead of unstable compounds which will fuse at operating temperature and cause caking of the fluidized bed, and (b) the demonstration that Purex-type wastes can be successfully calcined using the in-bed combustion fluidized-bed calcination process.

TABLE XVII

PROPERTIES OF CALCINED SOLIDS

Component	Experimental Values		Theoretical Values
Chemical Composition	Product	Fines	
NO^{-3}	[b]	[b]	0
Al^{+3}	13.3	4.85	3.9
PO_4^{-3}	1.43	2.79	2.4
SO_4^{-2}	41.01	61.96	48.5
Fe^{+3}	16.8	23.7	24.4
Na^{+}	7.5	10.5	10.8
NH_4^{+}	[b]	[b]	0
Total Volatiles[a]			
Percent Weight Loss	5.9	15.4	--
Densities (g/cc)			
Absolute	3.20	3.17	--
Particle	2.21	--	--
Intraparticle Porosity	0.31	--	--
Attrition Index	12.2	--	--

X-Ray Analysis: Both product and fines show α-Fe_2O_3 and $Na_3Al(SO_4)_3$ as major components. A possible minor constituent is $NaFe(SO_4)_2$. No evidence of crystalline $NaNO_3$, Na_2O_2, or Na_2O was observed.

[a] The total volatiles determination was run at 700°C with no evidence of fusion.

[b] Less than the 1.24 wt% lower limit of the analytical method used.

TABLE XVIII

TYPICAL OFF-GAS COMPOSITION
(Dry Basis -- Volume Percent)

Component	Experimental	Theoretical
N_2	54.67	57.27
O_2	25.03	26.83
CO_2	11.96	15.28
Co	6.93	0
H_2	0.89	0.0003
SO_2	0.006	0.62
NO_2	0.284	0
N_2O	0.220	0
P_2O_5	[a]	0

[a] Less than the 6×10^{-5} volume percent lower limit of the analytical method used.

TABLE XIX

TYPICAL SCRUBBING SOLUTION COMPOSITIONS

Component		To Scrubber	From Cyclone	From Condenser
Al^{+3}	(g/liter)	0.031	0.079	0.056
SO_4^{-2}	(M)	0.052	0.059	0.040
PO_4^{-3}	(g/liter)	0.046	0.085	0.052
H^+	(M)	7.34	6.04	2.22
NO_3^-	(M)	7.60	6.10	1.97
Fe^{+3}	(g/liter)	0.257	0.472	0.408
Na^+	(g/liter)	0.210	0.350	0.210
TS[a]	(g/liter)	2.44	5.55	1.47
UDS[b]	(g/liter)	0.21	0.27	0.10
NH_4^+	(M)	[c]	[c]	[c]

[a] Total solids at 500°C.

[b] Undissolved solids.

[c] Less than the 0.04 M lower limit of the analytical method used.

3.2 Corrosion in the In-Bed Combustion Process (C. A. Zimmerman, D. W. Rhodes; Chemistry Section)

The possibility of corrosion occurring as metal dusting during the in-bed combustion of hydrocarbons in the Waste Calcining Facility (WCF) had been recognized. Laboratory tests of Type 347 stainless steel exposed to synthetic in-bed combustion gas for 1200 hours at 500 and 600°C, reported previously [1], indicated that metal dusting corrosion might be associated with the in-bed combustion process at these temperatures.

A second test was conducted using the same synthetic gas composition (N_2-75, O_2-15, CO_2-7.5, and CO-2.5 mole %) to confirm the results of the previous test and to determine the extent of metal dusting at 450°C, the anticipated operating temperature of the WCF. Type 347 stainless steel specimens used were 3/4 inch wide, 5-1/2 inches long, and 0.05 inch thick. Welded and non-welded specimens were machined to size to provide equivalent surface finishes. This test was run for 2170 hours with specimens exposed at average temperatures of 450, 500, and 535°C.

Photomicrographs of cross sections (two segments per photomicrograph) of the non-welded specimens are shown in Figures 24, 25, and 26. Examination of these photomicrographs indicates that some material penetrated the surface and moved into the metal (presumably carburization) at 500 and 535°C. The specimen exposed at 535°C showed some pitting attack, grain growth, and precipitation at the grain boundaries. The specimen exposed at 500°C showed precipitation; grain growth, however, is not nearly as pronounced as in the

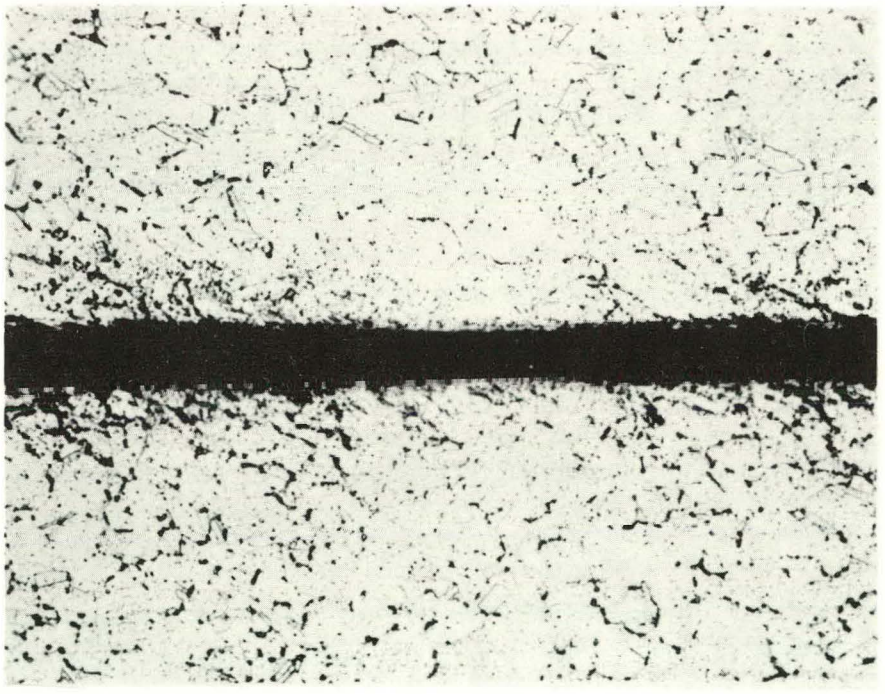

Fig. 24 Photo. Non-welded specimen exposed at 535°C showing pitting attack, grain growth, and precipitation at the grain boundaries.

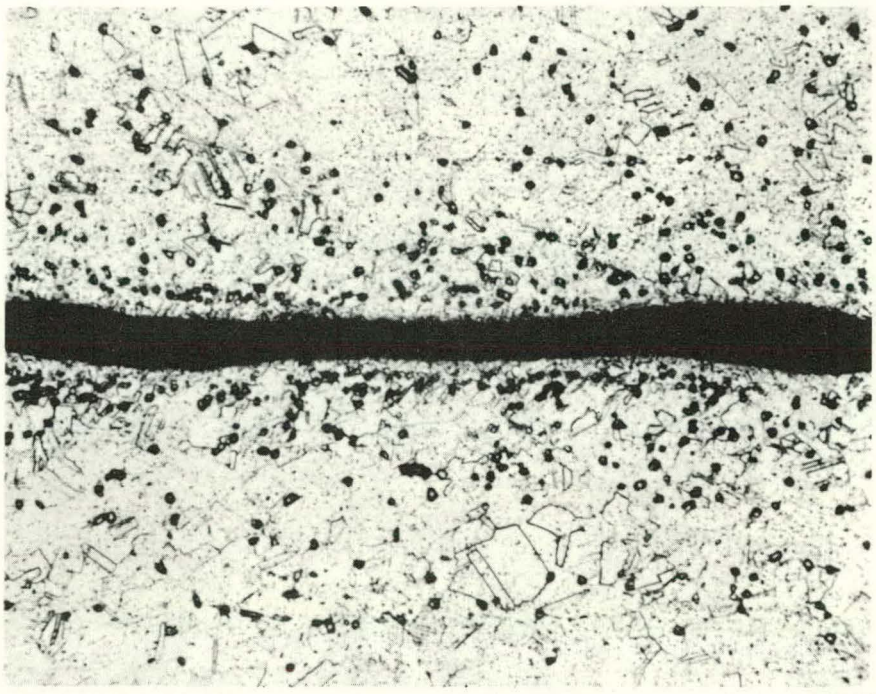

OXALIC ACID ETCH 500X

Fig. 25 Photo. Non-welded specimen exposed at 535°C showing precipitation and mild grain growth.

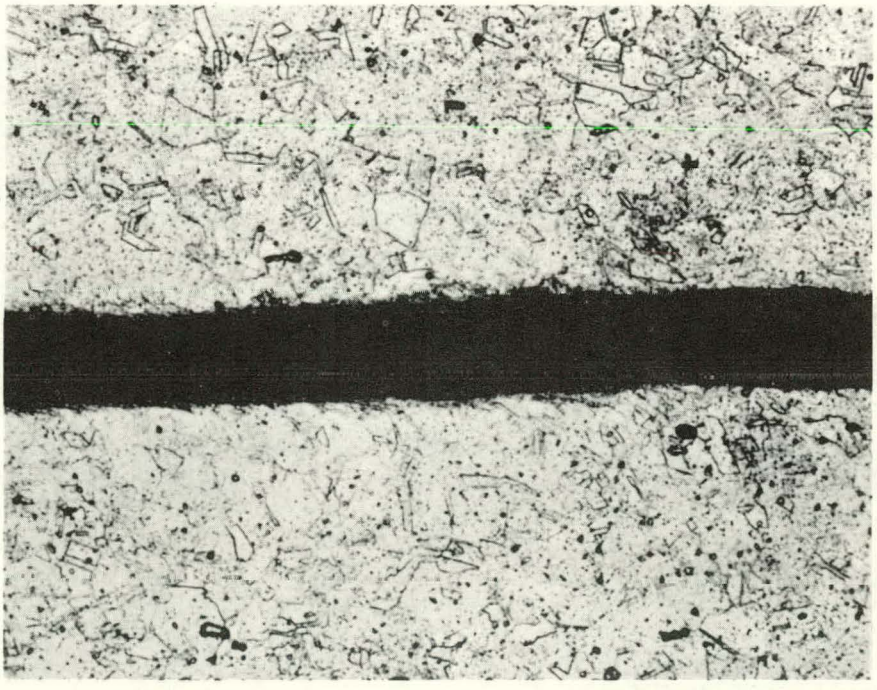

OXALIC ACID ETCH 500X

Fig. 26 Photo. Non-welded specimen exposed at 450°C showing only slight precipitation or grain growth.

specimen exposed at 535°C. The specimens exposed at 450°C (the anticipated calciner bed operating temperature) showed precipitation or grain growth to be very slight. Welded specimens showed the same results as noted for the non-welded specimens.

This series of tests indicate, as did the previous series [1], that low operating temperatures and complete combustion to exclude the formation of carbon monoxide are desirable. The specimens exposed to the combustion gas for over 2170 hours indicate that corrosion of Type 347 stainless steel by metal dusting or other mechanisms is negligible at 450°C under the conditions of this test. However, since the present Type 347 stainless steel plant calciner has experienced about 40,000 hours of operation in NaK-heated waste calcination, the condition of the metal in this vessel will also be a factor in determining the useful life of the calciner.

4. ADDITIONAL WASTE MANAGEMENT STUDIES

4.1 Decontamination of Waste Evaporator Condensate (M. W. Wilding, D. W. Rhodes; Chemistry Section)

For several years, condensate from the waste evaporator at the ICPP has been mixed routinely with other waste effluents and then released to the ground water. Although the concentration of radionuclides in the effluent at the discharge point has been well below drinking water tolerances, laboratory studies indicated that additional decontamination of the condensate could be achieved using ion exchange resins.

Organic cation exchange resins (Amberlite IR-120 and -200) were used in laboratory experiments to remove radionuclides from waste evaporator condensate. One hundred milliliters of condensate solution at both pH 1.0 and 4.0 was equilibrated with 1 g of resin by agitating continuously for 24 hours. The results indicated that slightly higher distribution coefficients for Sr-90 and Cs-137 were obtained with the IR-200 resin. The distribution coefficients with both resins were in the range of 2000 to 10,000 for Sr-90 and 100 to 300 for Cs-137, indicating that significant decontamination of the condensate waste can be obtained with an ion exchange system. Since the condensate used was that resulting from the operation and decontamination of the WCF, additional tests will be run at a later date with condensate produced during operation of the CPP to assure general usefulness of the process for all ICPP waste evaporator condensates.

4.2 Activity of Rhodium-Alumina Catalyst Used for Decomposition of Nitrous Oxide in the ICPP Rare Gas Plant (N. J. Kertamus; Chemistry Section)

Tests were made to compare the activity of rhodium-alumina catalyst which apparently had lost effectiveness in the rare gas plant with new rhodium-alumina catalyst. The catalyst removed from the rare gas plant showed sufficient activity to provide the needed conversion of N_2O if the proper contact were obtained. It was concluded that the loss of effectiveness was due to sintering of the bed which in turn caused channeling of the gas, rather than being due to

degradation of the catalyst. More reliable operating conditions for future operation of the plant are suggested.

Observations on the Catalytic Decomposition of Nitrous Oxide

Plugging in the cryogenic portions of the rare gas plant indicated that nitrous oxide originally present in the dissolver off-gas was not being removed by the rhodium catalyst. Table XX gives the major components present in the dried dissolver off-gas along with reaction conditions and results of processing the gas in the plant converters. The data indicate very incomplete decomposition

TABLE XX

DECOMPOSITION OF NITROUS OXIDE OVER RHODIUM-ALUMINA CATALYST IN GAS PLANT CONVERTERS

Off-Gas Composition (Volume Percent)				
Gas	Before Converters	After Converters[a]	GHSV[b]	Volume Percent N_2O Decomposed
N_2	71.7			
O_2	14.3			
A	0.9			
N_2O	11.2	2.5	790	77
H_2O	2.0			
N_2	76.5			
O_2	15.6			
A	0.9			
N_2O	7.0	1.2	620	83
N_2	78.5			
O_2	6.3			
A	0.9			
N_2O	11.8	1.0	460	91
H_2	2.4			

[a] Converter temperature, ~815°C.

[b] Gaseous hourly space velocity = scf(gas) per cf(bed) per hour.

of the N_2O. Data previously obtained with nitrous oxide gas compositions in the same range indicated that the rhodium-alumina catalyst decomposed greater than 99% of the nitrous oxide originally present in the gas, and that the product gas contained less than 0.05 volume percent of nitrous oxide.

Because of the apparent loss of catalyst activity for nitrous oxide decomposition, the rhodium-alumina converters were opened and unpacked. The condition of the catalyst removed from the top several inches of both converters appeared to be normal with no evidence of sintering or fines; the lower portion was more difficult to remove because of sintering between the catalyst particles. It is significant to note that the middle and bottom portions of the catalyst beds had been heated to >1090°C.

These observations suggested two possible reasons for the loss of catalyst activity for nitrous oxide decomposition. First, the excessive temperatures might have destroyed the micro-surface area of the alumina support or caused sintering of the active rhodium sites on the catalyst; and second, fusion of the catalyst particles may have caused appreciable channeling of the gas through the bed. This second explanation suggests that instead of utilizing the whole bed, the gas contacted only a small portion of the bed with a space velocity higher than was calculated for the bed assuming the total catalyst volume was available for reaction.

Experimental Program

In a laboratory scale reactor, portions of the sintered catalyst, unsintered catalyst, a laboratory prepared catalyst, and a new commercial catalyst were tested for activity. All gave comparable and satisfactory results. As nitrous oxide was catalytically decomposed, the exothermic decomposition reaction produced a characteristic temperature profile in the bed. This temperature profile is illustrated in Figure 27 below. In every test where nitrous oxide was decomposed catalytically, the temperature profile described in Figure 27 occurred, although the position and magnitude of the inflection varied depending on conditions of the test. Similar temperature profiles were noted in literature [27] studies on catalytic decomposition of nitrous oxide.

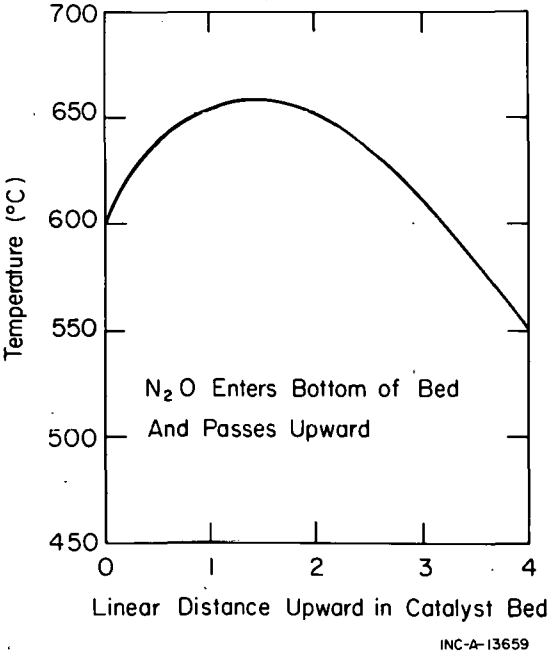

Fig. 27 Temperature profile of catalyst bed.

Differences in activity between catalyst samples removed from the top and bottom of the converters had been expected because of the high temperatures recorded at the bottom of the beds. However, results showed that both portions were still highly active for nitrous oxide decomposition, although the top portion may be slightly more active.

Thermodynamic calculations showed that, although a wide range of conditions

were highly favorable, in the temperature range 425 to 925°C the equilibrium constants ranged from 1×10^{10} to 3×10^{7}; thus, equilibrium is favored by operation at lower temperatures. A new batch of rhodium-alumina catalyst was tested at conditions comparable to those used for the rhodium catalyst that had been removed from the converters; this catalyst gave excellent removal of nitrous oxide in the range 460 to 600°C.

Conclusions

Laboratory tests of the rhodium-alumina catalyst removed from the nitrous oxide decomposition units led to the following conclusions:

(1) Excessive temperatures caused sintering (or fusion) of catalyst particles and particulate matter (from the catalyst surface) to plug the bed. This combination probably caused gas channeling in the catalyst bed such that the entire bed was not available or accessible to the dissolver off-gas; consequently, complete catalytic decomposition of nitrous oxide was not possible.

(2) Catalyst activity per se was not destroyed by heating the catalyst to temperatures in excess of 1090°C.

(3) Operating conditions should be maintained below 650°C, and preferably 550°C, for greatest catalyst lifetime.

III. REACTOR TECHNOLOGY SUPPORT

1. LOFT ASSISTANCE PROGRAM

The Chemical Technology Branch is conducting several development studies in support of the Loss-of-Fluid Test (LOFT) which will be conducted at the National Reactor Testing Station. The LOFT project is the field simulation of a loss-of-coolant accident for a pressurized water-cooled reactor. Originally, the program consisted of releasing the coolant deliberately from a 50-MW pressurized water reactor, thus permitting the fuel core to melt and release fission products into the reactor shell and containment building. Subsequently, the LOFT program has been changed to tests of emergency core cooling systems.

The specific development studies undertaken by this Branch include (a) the evaluation of surface coatings and sealants for the interior of the containment shell; (b) the development of procedures for decontamination of the facility; (c) the development of a continuous fission product sampler for the containment atmosphere; and (d) the operation of a fission product generation and containment unit -- the Contamination-Decontamination Experiment (CDE) -- for conducting these studies, as well as to provide general support for the LOFT program. Progress in these areas is reported in the following sections. Additional LOFT support studies in the areas of sampling and sample analysis are being performed by the Analytical Chemistry Branch at the ICPP[28] in close cooperation with the studies being performed by the Chemical Technology Branch.

1.1 The Contamination-Decontamination Experiment (L. T. Lakey, D. E. Black, R. L. Nebeker, W. P. Palica, and R. L. Ring; Reactor Safety Studies Section)

The CDE was installed to augment the LOFT support studies being conducted at the ICPP. In the CDE, high-level or tracer-level fission product aerosols are produced under conditions simulating those anticipated in the LOFT. The high-level fission product aerosol is generated by melting a small, highly irradiated, short-cooled fuel capsule in the presence of steam, using a radio-frequency induction furnace. The fission products released are transported by the steam to an 86-ft^3 containment vessel. The low-level tests are conducted by injecting tracer quantities of a single fission product, predominantly as one species (eg, methyl iodide) into the CDE vessel. In both high- and tracer-level tests, the containment conditions are controlled to simulate anticipated LOFT conditions. These fission product aerosols are used in studies on the contamination and decontamination of various protective coatings and equipment, in the testing of various LOFT sampling devices, and for the development of analytical methods for analysis of LOFT samples.

During the current fiscal year, three methyl iodide and two elemental iodine tracer runs were conducted in the CDE. The major objective of these tests was to determine the sampling accuracy of the Continuous Sampler-Monitor (CSM) for these species. In addition, coated sample surfaces were contaminated for subsequent study of decontamination methods. Results are reported in the appropriate sections, following, which deal with the particular areas of interest.

R 2-25-70

1.2 Development of a Continuous Sampler-Monitor (R. E. Schindler and R. R. Hammer; Reactor Safety Studies Section)

A Continuous Sampler-Monitor (CSM) is being developed to determine the airborne noble gas, total iodine, organic iodide, and total fission product concentrations in the containment building atmosphere during the Loss-of-Fluid Test (LOFT). The CSM now being tested for the LOFT consists of a scrubber, located in the containment building, which continuously samples the airborne fission products and separates them into liquid and gas streams. The scrubber is located in the containment building to minimize fission product plate-out in the long sampling lines which would be necessary, otherwise, for the LOFT. The CSM is designed to wash most of the inorganic iodine and particulate fission products from the sample of containment atmosphere into a liquid stream, leaving essentially only xenon, krypton, and organic iodides in the gas stream. After leaving the containment building, the liquid and gas streams are separated, monitored individually for the gross activity levels, and then sampled to determine the concentrations of individual isotopes. A detailed description of the CSM is documented in IN-1309 [29].

Previous testing has demonstrated that samples from the CSM gas stream will provide accurate noble gas concentrations [1], and that the scrubber will wash particles larger than 0.2 μ diameter into the liquid stream [13]. Evaluation of the CSM was continued during the current reporting period with traced elemental iodine and methyl iodide. Detailed results have been reported in the LOFT Quarterly project reports [30] and are summarized in the following paragraphs.

Experiments in the CDE with tracer levels of elemental iodine indicate that the total iodine concentrations determined by the CSM will agree to within 10% of the values determined by particulate-iodine (Maypack) samplers under simulated LOFT conditions. In the case of airborne methyl iodide, the CSM gas stream samples gave values which were approximately one-half the actual concentrations in the containment atmosphere; the balance of the methyl iodide was absorbed in the basic thiosulfate scrubbing reagent. As the temperature of the scrubbing solution was increased, absorption of the methyl iodide increased. Ethyl iodide was less soluble in the scrubbing solutions and should be more accurately determined in the gas phase.

The CSM gross activity monitors on both the gaseous and liquid streams were found to respond satisfactorily to iodine injections in the CDE and to be capable of rapid response to changes in containment atmosphere activity.

1.3 Applicability of Chemically Removable Coatings to Reactor Containment Buildings (B. J. Newby, T. L. Evans, and K. L. Rohde; Chemistry Section)

Studies were performed to select commercially available coating systems that would protect surfaces from contamination by volatile fission products and that could be remotely decontaminated effectively from these fission products. These coatings were to be suitable for application on the interior surfaces of a reactor containment building with special emphasis on the conditions present during an unperturbed loss-of-coolant accident. A summary of the principal results, reported here, is taken from a detailed description of the studies as reported in IN-1170 [31]. Although most conditions for testing

coatings in these studies were selected with respect to an unperturbed nuclear accident, the results of these studies will be helpful in selecting coatings for any surface where contamination with volatile fission products is possible.

Two very promising methods of remotely decontaminating the coated inside surfaces of reactor containment buildings contaminated with volatile fission products were developed; these methods depended upon the use of chemically removable coating systems. Such systems consisted of a permanent undercoat to protect the substrate and a temporary outer coating which could be removed, along with sorbed fission products, by chemical reagents. In the strippable coating system, the outer coating was rapidly dissolved; in the corrodible coating system, the outer coating was gradually removed by prolonged chemical attack.

The most promising strippable coating system evaluated used Amercoat 66 as the permanent undercoat, Turco 5302 as the temporary outer coating, and isophorone at 70°C as the chemical stripping reagent. Gross gamma decontamination factors of 400 were obtained with this system using stripping reagent contact times of less than 15 minutes. Turco 5302 has certain limitations which might influence its actual application; it is not suitable for prolonged exposures in high radiation fields, in pressurized steam, or to alkaline and oxidizing reagents. In a more ideal strippable coating system, an aqueous stripping reagent would be preferred over an organic one since special problems in safety and waste handling are always present with large-scale use of organics.

The most promising corrodible coating system evaluated used Phenoline 368, both as the permanent undercoat and temporary outer coating, and alternate treatments with Turco 4502 and oxalic acid (corroding reagents) to remove the temporary outer layer. The Phenoline 368 corrodible coating system is suitable for use in containment buildings or other nuclear installations where there may be repeated steam releases or a release of long duration. This system has good resistance to pressurized steam and radiation. Gross gamma decontamination factors of greater than 1000 can be obtained from this system by spraying with the appropriate corroding reagents for about 40 hours. Surfaces protected from contact with direct spray are also decontaminated. The disadvantage of such a system is the disposal problem created by coating solids generated during decontamination. The individual coating particles generated were quite small and could be slurried from containment buildings. However, there is always the possibility of pipe line plugging during transportation to permanent waste storage.

1.4 Effect of Decontamination Reagent Temperatures on Iodine Decontamination Efficiency (B. J. Newby and K. L. Rohde; Chemistry Section)

It may not be possible to contact all contaminated surfaces inside the LOFT containment building during Emergency Core Cooling System (ECCS) tests with decontaminating reagents at the same high reagent temperature -- 80°C -- that has been used in most previous decontamination studies. The current tests were performed to determine how the decontamination of coated and steel surfaces from iodine is affected by varying the decontamination reagent temperature.

Carbon steel (ASTM Designation A-212, grade B), Type 304 stainless steel (RMS No. 64), and carbon steel coupons painted with the Amercoat 66 and Phenoline 368 coating systems were contaminated with molecular iodine in CDE Tracer Run 6. The stainless steel and coated coupons were decontaminated by first deluging them with water at 24°C for five minutes and then spraying them at various temperatures (20, 40, and 80°C) for 15 minutes at 30 psig with 2 lb/gal Turco 4502 and then with 0.5 lb/gal oxalic acid; water deluges were used after each reagent treatment. In addition to the above treatment, carbon steel coupons were sprayed at various temperatures (20, 40, and 80°C) for 15 minutes at 30 psig with 1 lb/gal Turco Alkaline Rust Remover. During decontamination, the spray nozzle was 15-1/2 inches from the coupon, the decontamination reagents were recirculated at a rate of 1.1 gal/min, and a Spraying System Nozzle 1/4 GG SS 6.5 was used; the spray density was 1 gal/min-ft^2.

The results, summarized in Table XXI, show that

(1) Iodine contamination (plate-out) on the carbon steel and coated surfaces is greater than on stainless steel surfaces.

(2) A water deluge prior to a decontamination procedure will not remove nonparticulate-iodine from coated and carbon steel surfaces, but will remove about 50% of this activity from stainless steel surfaces.

(3) Efficient nonparticulate-iodine removal can be obtained from stainless steel surfaces at reagent temperatures ranging from 20 to 80°C.

(4) Very little nonparticulate-iodine is removed from Amercoat 66 and Phenoline 368 coatings at reagent temperatures of less than 40°C; increasing reagent temperature from 40 to 80°C increased the iodine decontamination factors by a factor greater than four.

(5) The decontamination of carbon steel is a function of oxide removal; when these coupons were sprayed at 80°C with Turco 4502, oxalic acid, and Turco Alkaline Rust Remover, much of the oxide was visibly removed and moderately effective decontamination was obtained.

1.5 Iodine Decontamination Behavior of Stainless Steel (T. L. Evans, B. J. Newby, and K. L. Rohde; Chemistry Section)

Stainless steel was one of the materials considered as a lining for the LOFT test chamber (containment structure) during the LOFT-ECCS tests. In anticipation of such an application, studies were carried out to develop a procedure for the rapid decontamination of stainless steel surfaces. Aspects studied included effects of spraying pressure, spraying time, and stability of the decontaminating reagents.

TABLE XXI

MOLECULAR IODINE DECONTAMINATION AS A FUNCTION OF REAGENT TEMPERATURE

Surfaces Contaminated in a CDE Tracer Run and Decontaminated by Spraying with Each Reagent for 15 Minutes at 30 psig.

Surface	Temperature of All Decontaminating Reagents (°C)	Initial Activity on Surfaces cpm/coupon (10^6)	Decontamination Factor (D.F.) Obtained by Deluging with Water at 24°C	D.F. Obtained by Treatment with Turco 4502 and Oxalic Acid	D.F. Obtained by Treatment with Turco 4502, Oxalic Acid, and Turco Alkaline Rust Remover
Amerccat 66	20	1.12	1.02	1.0	
	40			1.6	
	80			6.6	
Phenoline 368	20	1.44	1.01	1.5	
	40			2.8	
	80			12	
Stainless Steel	20	0.079	2.15	180	
	40			480	
	80			1300	
Carbon Steel	20	1.02	1.04	1.8	4.4
	40			1.7	7.1
	80			3.5	57

Equipment and Test Procedure

Type 304 stainless steel coupons having a No. 64 RMS finish were contaminated in a laboratory contaminator with molecular iodine in the presence of pressurized steam. The coupons were held in the contaminated steam atmosphere for 24 hours; the pressure was allowed to decay from 22 to 3 psig over the 24-hour period. Contaminated coupons were washed with water, counted for iodine contamination, decontaminated, and counted for residual iodine activity. All coupons were decontaminated by spraying with a Spraying System Nozzle 1/4 GG SS 6.5. The distance between spraying nozzle and coupons was 15-1/2 inches.

Pressure Versus Deluge Spraying

After an ECCS test, the LOFT test chamber could be decontaminated with a deluge system followed by a high pressure spraying system. It would be convenient and much more economical if all surfaces could be decontaminated with a deluge decontamination system alone without having to install and use the high pressure spraying system for that purpose. To test this possibility, coupons were decontaminated at two different spraying pressures while spraying them with about the same volumes of decontaminating solutions. This study showed that decontamination efficiency is independent of spraying pressure, and that a deluge system should be satisfactory for decontaminating the stainless steel surfaces of the LOFT test chamber.

In the tests, part of the stainless steel coupons were sprayed with 2 lb/gal Turco 4502 for 25 minutes at 40°C and 15 psig (pumping rate of 0.78 gal/min) and then with 0.5 lb/gal Turco 4521 for 25 minutes at 40°C and 15 psig. Other stainless steel coupons were sprayed with 2 lb/gal Turco 4502 for 10 minutes at 40°C and 90 psig (pumping rate of 1.8 gal/min) and then with 0.5 lb/gal Turco 4521 for 10 minutes at 40°C and 90 psig. Under both decontamination conditions, surfaces were sprayed with about 19 gallons of solution during the spraying time period. In comparing results obtained using the two different spraying pressures (see Table XXII), it is evident that pressure made very little difference in decontamination efficiency.

TABLE XXII

EFFECT OF SPRAYING PRESSURE ON IODINE REMOVAL FROM STAINLESS STEEL

Decontamination Factors Obtained by Spraying with 2 lb/gal Turco 4502 and 0.5 lb/gal Turco 4521 at 40°C	
10 minutes at 90 psig (with each reagent)[a]	25 minutes at 15 psig (with each reagent)[a]
325 ± 136[b]	360 ± 154[b]

[a] Coupon surfaces were sprayed with about 19 gallons of solution during this time period.

[b] Standard deviation for eight replicates.

Effect of Spraying Time on Decontamination Efficiency

Studies were carried out to measure iodine decontamination from stainless steel (using low spraying pressures) for different spraying times. Contaminated stainless steel surfaces were sprayed for either 10 or 100 minutes with 2 lb/gal Turco 4502 at 40°C and 15 psig and then with 0.5 lb/gal Turco 4521 under the same conditions. Spraying time had a significant effect on decontamination achieved. The average decontamination factors were 414 and 749 for spraying times of 10 and 100 minutes, respectively. The scatter from five replicate tests was such that the difference was significant at the 93% confidence level.

Effect of Decontamination Solution Stability on Decontamination Efficiency

It is important that the decontamination efficiency of potential decontaminating reagents for the LOFT test chamber not be markedly decreased due to reagent instability caused by conditions existing during a decontamination cycle. During a typical decontamination cycle, a reagent solution might be heated, sparged, sprayed on various surfaces, recycled, reheated, and sparged again for a number of hours. In a series of tests, potential decontamination reagents for the LOFT test chamber were treated to simulate a decontamination cycle (ie, were aged) and then used to decontaminate iodine from stainless steel surfaces; decontamination behavior of the aged solutions was compared with the behavior of freshly prepared solutions to determine the effects of aging.

Decontaminating solutions were aged by sparging five gallons of solution at 80°C for 48 hours with 2 cfh of air in a stainless steel vessel in the presence of 1 ft^2 of Phenoline 368 surface, 1 ft^2 of Amercoat 66 surface, and 1 ft^2 of carbon steel surface. Then, in a typical decontamination cycle, contaminated coupons were sprayed with aged, 2 lb/gal, Turco 4502 for 100 minutes at 40°C and 15 psig and then with aged Turco 4521, Turco 4521A[a], or oxalic acid for 100 minutes at 40°C and 15 psig. Table XXIII summarizes the iodine decontamination factors obtained for the different reagent combinations. Comparison with the decontamination effectiveness of a fresh Turco 4502 - 4521 treatment shows that aging decontaminating reagents does decrease decontamination efficiency. The results also show that of the aged solutions, (a) aged Turco 4502-oxalic acid gave the best decontamination efficiency, (b) aged Turco 4502-4512A gave slightly less, and (c) aged Turco 4502-4521 gave the poorest decontamination efficiency. The differences between the average decontamination factors for (a) and (b), and for (a) and (c), were significant in a test at the 75 and 98% confidence levels, respectively. Thus, 2 lb/gal Turco 4502 - 0.5 lb/gal oxalic acid is recommended for the LOFT test chamber, and this combination will be used in future decontamination studies unless it is found that oxalic acid is too corrosive to materials it may contact during the decontamination cycle or in transportation to or storage in the waste tanks.

[a] Turco 4521A is identical to Turco 4521 with the exception that it contains inhibitors to make it more stable in contact with carbon steel.

TABLE XXIII

EFFECT OF DECONTAMINATION SOLUTION STABILITY ON IODINE REMOVAL FROM STAINLESS STEEL

Coupon No.	Decontamination Factors Obtained by Spraying Each Reagent of the Following Combinations for 100 minutes at 40°C and 15 psig			
	Fresh Turco 4502-4521	Aged Turco 4502-4521	Aged Turco 4502-4521A	Aged Turco 4502-Oxalic Acid
1	>900	150	458	241
2	869	228	440	>625
3	>646	218	220	880
4	>1000	169	535	632
5	---	150	199	310
Average	>850	180	370	>540

1.6 Methyl Iodide Contamination-Decontamination Behavior of Coatings (B. J. Newby and K. L. Rohde; Chemistry Section)

Coated coupons were contaminated with methyl iodide in CDE Tracer Run 7 and the contamination-decontamination and penetration behaviors of the coatings were studied and compared with those of coatings contaminated with molecular iodine in earlier runs. The coatings used for these studies were Amercoat 66 and Phenoline 302.

Contamination-Decontamination Behavior

Contaminated coupons were decontaminated in quadruplicate by first deluging them with water at 24°C for five minutes and then spraying them at 80°C for 15 minutes at 30 psig with 2 lb/gal Turco 4502 and then with 0.5 lb/gal oxalic acid, with water deluges after each reagent treatment. During decontamination, the spray nozzle was 15-1/2 inches from the coupon, the decontamination reagents were recirculated at a rate of 1.1 gal/min, and a Spraying System Nozzle 1/4 GG SS 6.5 was used; the spray density was 1 gal/min-ft^2. Two days elapsed between contamination and decontamination of the coupons.

The average methyl iodide decontamination factors obtained from Amercoat 66 and Phenoline 302 by deluging them with water prior to any other decontamination treatment were 1.01 and 1.03, respectively. Thus as is true with molecular iodine, a water deluge prior to any other decontamination treatment will not remove methyl iodide from coated surfaces.

Table XXIV shows the average contamination-decontamination behaviors of Amercoat 66 and Phenoline 302 using Turco 4502 and oxalic acid as the

TABLE XXIV

CONTAMINATION-DECONTAMINATION BEHAVIOR OF COATINGS AS A FUNCTION OF IODINE SPECIES

Decontamination Procedure: Treatment with Turco 4502 and Oxalic Acid for 15 minutes at 80°C and 30 psig.

		Amercoat 66	Phenoline 302
Iodine Species	Plate-out (cpm/coupon)	D.F.	D.F.
Molecular	1.13×10^6	6.6	16
Methyl Iodide	1.20×10^5	8.2	7.9

decontaminating reagents and either methyl iodide or molecular iodine as the contaminating species. The plate-out of molecular iodine on coated surfaces was more than that of methyl iodide under roughly the same contaminating conditions. However, there is little if any difference between methyl iodide and molecular iodine decontamination factors obtained from the same coating system using the same decontamination procedure.

Penetration Behavior

The penetration of methyl iodide was obtained both in coatings that had been subjected to decontamination and in undecontaminated coatings. The activity at increasing coating depths was determined by removing thin layers of the coating with fine sandpaper and counting after each layer removal.

The experimental technique involves initial removal of paint from all surfaces of the coupon except for the one perpendicular to the detection device to reduce background. Only about one-half of the surface of the coupon is counted. This is accomplished by two close fitting lead shields which surround the coupons: one shield has an opening exposing the central portion of the surface; the other has no opening and serves to establish a background count. The difference in the two readings is then taken as the observed radioactivity. The coating thickness is always taken with a micrometer at the midpoint of the portion of the coupon being counted.

Methyl iodide and molecular iodine penetration curves for undecontaminated Phenoline 302 and Amercoat 66 are shown in Figure 28; all data have been normalized to an arbitrarily selected initial activity of 50,000 cpm. The molecular iodine data were obtained from earlier CDE runs in which the source of iodine was irradiated molten reactor fuel. The curves show that, like molecular iodine, methyl iodide penetrates deeply into coatings under the CDE contaminating conditions, and that methyl iodide penetration may be different for different coatings. There is little difference between the methyl iodide and molecular iodine penetration curves for Phenoline 302. The diffusivity for molecular iodine in Amercoat 66 appears to be greater than that for methyl iodide.

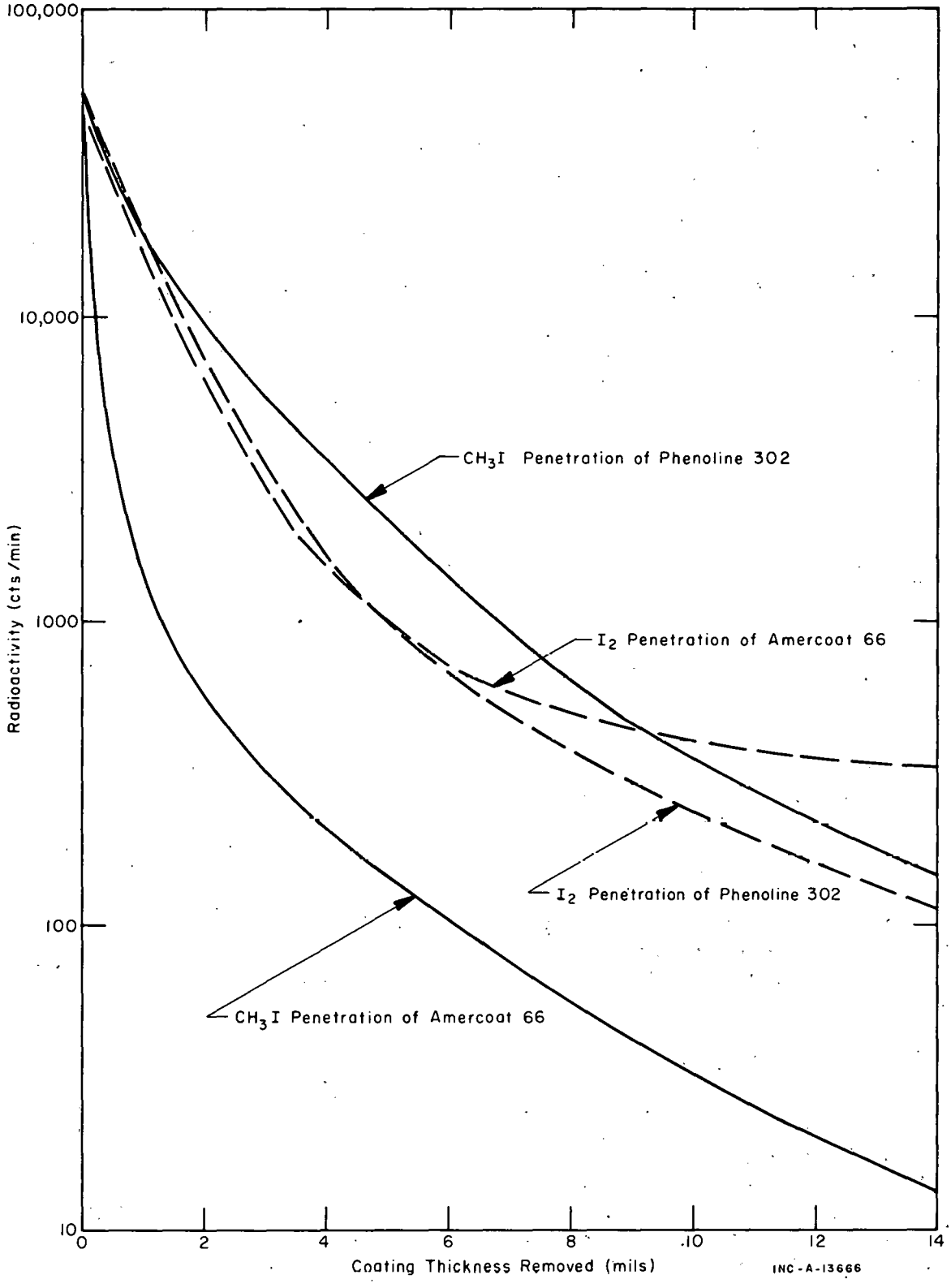

Fig. 28 Penetration of molecular iodine and of methyl iodide into undecontaminated coatings.

Penetration curves for decontaminated coatings are not shown but they essentially duplicate the curves for the undecontaminated coatings when allowance is made for surface layers that may have been removed by the decontamination process. Decontamination by short-term spraying does not leach methyl iodide that has penetrated into coatings.

1.7 Proposed LOFT Waste Management Program (R. L. Nebeker, Reactor Safety Studies Section; D. W. Rhodes, Chemistry Section; G. E. Lohse, Process Engineering Section)

Large volumes of liquid wastes, contaminated with both chemicals and radioactivity, must be disposed of safely following each of four scheduled Loss-of-Fluid Tests (LOFT). In support of these tests, the Idaho Nuclear Chemical Technology Branch was requested to evaluate the LOFT liquid waste management problems and recommend changes or additions to the system proposed for the original LOFT test. The results of this evaluation are summarized in the following paragraphs.

Anticipated Quantity and Composition of LOFT Waste

The radioactivity of the waste generated at the LOFT site will vary over a wide range, depending on the source of the waste. High-activity wastes will also be generated in the Test Area North (TAN) Hot Shop during decontamination of the LOFT reactor vessel following each test. The activity contents of the different waste streams for both the normally expected cases and those representing the result of a maximum credible accident were estimated and are shown in Table XXV. The "normal" values are based on estimated fission product releases of 0.03% of the halogens and 0.0012% of the particulate fission products present in the core at the time of meltdown, assuming normal functioning of the ECCS in accord with the design criteria. Maximum values [32] are based on releases of 50% of the halogens and 1% of the particulate fission products present in the core at the time of meltdown. The maximum and minimum volumes of waste generated -- also shown in Table XXV -- represent the extreme limits of waste production expected in a test.

A portion of the LOFT wastes will also be contaminated with chemicals from cooling water additives, sprays, and decontamination solutions. Because the presence of certain chemicals restricts the disposal methods used -- in some cases more severely than radioactive contaminants -- the chemical compositions of the LOFT wastes were also estimated. The results are listed in Table XXVI together with the standards for drinking water where available.

Proposed LOFT Waste Management Program

As a result of the study, it was concluded that final disposition of LOFT wastes should include a combination of three different disposal methods: (a) reprocessing and conversion to a granular solid, (b) disposal to an on-site well, and (c) disposal to an impervious surface pond -- depending on the type and source of the individual waste streams. The guidelines governing these methods have been documented previously [33,34]. In addition to meeting the disposal guidelines, the disposal program proposed by Idaho Nuclear was integrated with the system proposed for the original LOFT in an effort to

TABLE XXV

ANTICIPATED LIQUID WASTE FROM EACH LOFT-ECCS TEST

Type of Waste	Typical Sources	Volume (1000 Gallons)	Total Activities (μCi/ml)	
			Normal	MCA[a]
High Activity	Reactor and ECCS water, containment decontamination and pressure suppression spray solutions	76 to 198	10 to 27	1.5×10^4 to 4×10^4
Intermediate Activity	Reactor water (before blowdown) and control rod seal water	54 to 147	10^{-5} to 10^{-1}	10^{-5} to 10^{-1}
Low Activity	Pump seal water, secondary water, and cooling water to primary and secondary equipment	2856 to 5483	0 to 10^{-4}	0 to 10^{-3}
Nonradioactive	Heating and ventilating equipment, diesel and compressor coolant	10,000 to 15,000	0	0
From TAN Hot Shop	Decontamination solutions, reactor water	35 to 60	10^{-5} to 2.6	10^{-3} to 4×10^3

[a] Possible activity in case of maximum credible accident.

TABLE XXVI

CHEMICAL ADDITIVES ANTICIPATED IN LOFT WASTE

Source	Chemical Additive	Maximum Anticipated Concentration[a] (mg/liter)	Drinking Water Guideline (mg/liter)
All Water	Cl_2	<5	250 (Cl^-)
	Total Dissolved Solids	?	500
Primary Water	NH_4OH	10	
	H_3BO_3	1200	
	Hydrazine	<100	
	LiOH	<10	
Secondary Water	Na_2HPO_4	<300	
	Na_3PO_4	<300	
Water Softening Waste	NaCl	5000	
Decontamination Solution	NaOH	60,000	
	$C_2H_2O_4$	60,000	
	K_2CrO_4	7200	0.05 (Cr^{+6})
	KOH	170,000	
	$KMnO_4$	50,000	0.05 (Mn)
Pressure Reduction Sprays	NaOH	100,000	
	$Na_2S_2O_3$	10,000	
CSM	NaOH	4000	
	$Na_2S_2O_3$	160	
Demineralizers and Regeneration	NaOH	5000	
	H_2SO_4	5000	250 ($SO_4^=$)

[a] Assumes no dilution, decomposition, neutralization, etc.

minimize required modifications. The new system proposed for the LOFT wastes is shown schematically in Figure 29.

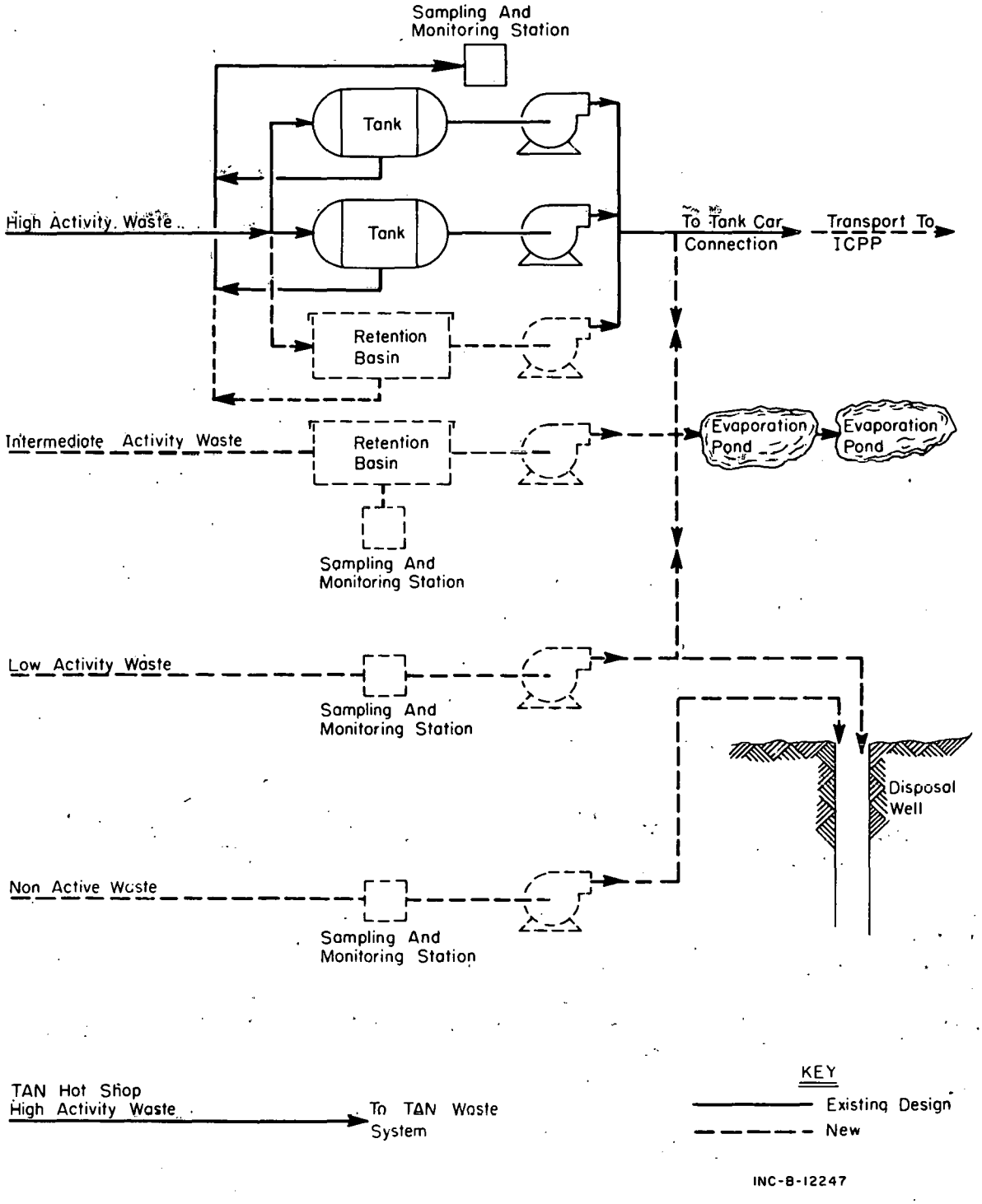

Fig. 29 Proposed LOFT liquid waste disposal system.

With this system, high-activity wastes would be stored temporarily in two 50,000-gallon tanks and then would be transferred to the ICPP for processing and conversion to a granular solid for storage, or evaporated in existing TAN facilities. Economic studies show that processing at the ICPP would be the more economical and flexible method. Intermediate-level wastes would be stored in impervious covered basins until the activity decayed to acceptable discharge levels; the basins would be covered to prevent release of volatile fission products (particularly iodine) to the atmosphere. Low-activity or nonradioactive wastes which contain high concentrations of chemicals could be disposed of by discharging to impervious evaporation ponds. Most of the waste generated in each LOFT-ECCS test could be disposed of by the latter method if the waste were stored for 10 to 20 days in covered retention basins to allow the radioiodine to decay to acceptable levels. The nonradioactive wastes with chemical compositions below those for drinking water limits could be disposed of by discharging to the existing TAN disposal well.

The proposed program is flexible enough to allow disposal of any type waste by the most economical means commensurate with the disposal guidelines. For example, sampling may show that the wastes presumed to be high in activity could actually be discharged safely to evaporation ponds rather than transferred to the ICPP for processing. Conversely, if a system malfunction occurred which would release large amounts of activity to wastes anticipated to be low in activity, these wastes could be stored and transferred to the ICPP for processing.

These recommendations are predicated on the presently available LOFT operating criteria. Future changes in the LOFT program could alter materially the results of this study. In addition, more stringent pollution control guidelines could be placed in effect, which could require changes in the recommended program.

2. OTHER REACTOR TECHNOLOGY SUPPORT PROGRAMS

2.1 HTGR Reference Fuel Reprocessing Plant Study (W. A. Freeby, R. D. Modrow, and B. R. Wheeler, Process Engineering Section; L. C. Borduin, Development Engineering Section; N. J. Kertamus, Chemistry Section)

The Conceptual Plant Policy[35] announced in the Federal Register of March 12, 1955, allows a commercial reactor operator to deliver spent fuel elements to the AEC for financial settlement if reasonably priced private reprocessing services are not available. The financial settlement involves charges for reprocessing (based on cost data for a conceptual plant), charges for conversion of the uranium to UF_6, and credits for the contained nuclear material in the spent metallic-clad fuel. This policy makes it possible to identify the reprocessing cost for spent commercial fuels from light-water reactors. Analogous to this, a need now exists for similar cost data applicable to a conceptual plant capable of handling fuel from High-Temperature Gas-Cooled Reactors (HTGR) since there are no commercial processors for the graphite matrix fuels. As a result of this need, the AEC Division of Production requested Idaho Nuclear Corporation to prepare an HTGR Reference Plant Study as part of the development of processing costs.

The conceptual reference plant is a single purpose, self-contained facility with a capacity of 260 metric tons per year of heavy metals from HTGR fuels. The design criteria, determined during the study, are being used by an Architect-Engineer (A-E) to prepare a conceptual design and capital cost estimate for the plant. Idaho Nuclear Corporation will use the capital costs generated by the A-E to calculate a unit reprocessing charge and the effect of a number of variables, such as throughput rate, on the charge.

Fuel Description

The conceptual plant arrived at in the current design studies is capable of processing various types of HTGR fuel, but the HTGR reference and Fort St. Vrain fuels, with a small amount of Peach Bottom fuel, now appear to be the most likely fuels requiring financial settlement. The reference fuel is assumed to contain a SiC-coated, two-particle fuel system. Each fuel particle consists of an inner uranium and/or thorium fuel particle with successive coatings of buffer carbon, SiC, and pyrolytic carbon. Before burnup, fertile particles contain thorium, and fissile particles contain U-235. The latter fuel particles, however, can also contain thorium and U-233. Thus, after burnup, both types of particles may contain mixtures of thorium and U-233; the fissile particles will contain U-235, as well.

Process Description

Proven processes, and those that appear to be the most highly developed and promising, are specified for the conceptual plant and are depicted schematically in Figure 30. A crush-burn-grind-leach process is assumed for use in reclaiming the heavy metals from the fuel. Bulk graphite is burned from the crushed fuel blocks in a fluidized-bed burner, freeing the fuel particles which are removed continuously from the bed and are screened to separate the two types of particles from each other and from the inert bed material. The fissile particles are placed in storage; the fertile particles are crushed, the inner buffer carbon burned in a fixed bed burner, and the heavy metals leached from the particles. A conventional solvent extraction system using a modified Acid-Thorex process is used to separate and purify the uranium and thorium. The U-233 is denitrated to UO_3 in a fluidized-bed denitrator, and the thorium is stored as a second-cycle-raffinate solution indefinitely, pending a decision on further treatment. Fissile particles are placed in suitable containers for long-term storage since there appears to be very little incentive for reprocessing them. Alternatively, however, these particles could be processed in the same facilities as those employed for the fertile particles.

2.2 Testing of Protective Coatings for the Inside of Nuclear Reactor Containment Vessels (W. T. Jordan, B. J. Newby, and K. L. Rohde; Chemistry Section)

The use of commercially available protective coatings for finishing the inside of nuclear reactor containment vessels with the expectation that they will effectively survive a loss-of-coolant accident and will in no way interfere with the proper operation of the reactor safety systems during and after the accident represents a very severe service for these materials. Studies were carried out to design test procedures for the evaluation of coatings for the above application, to determine what levels of performance are possible for currently commercially available coatings, and to determine whether

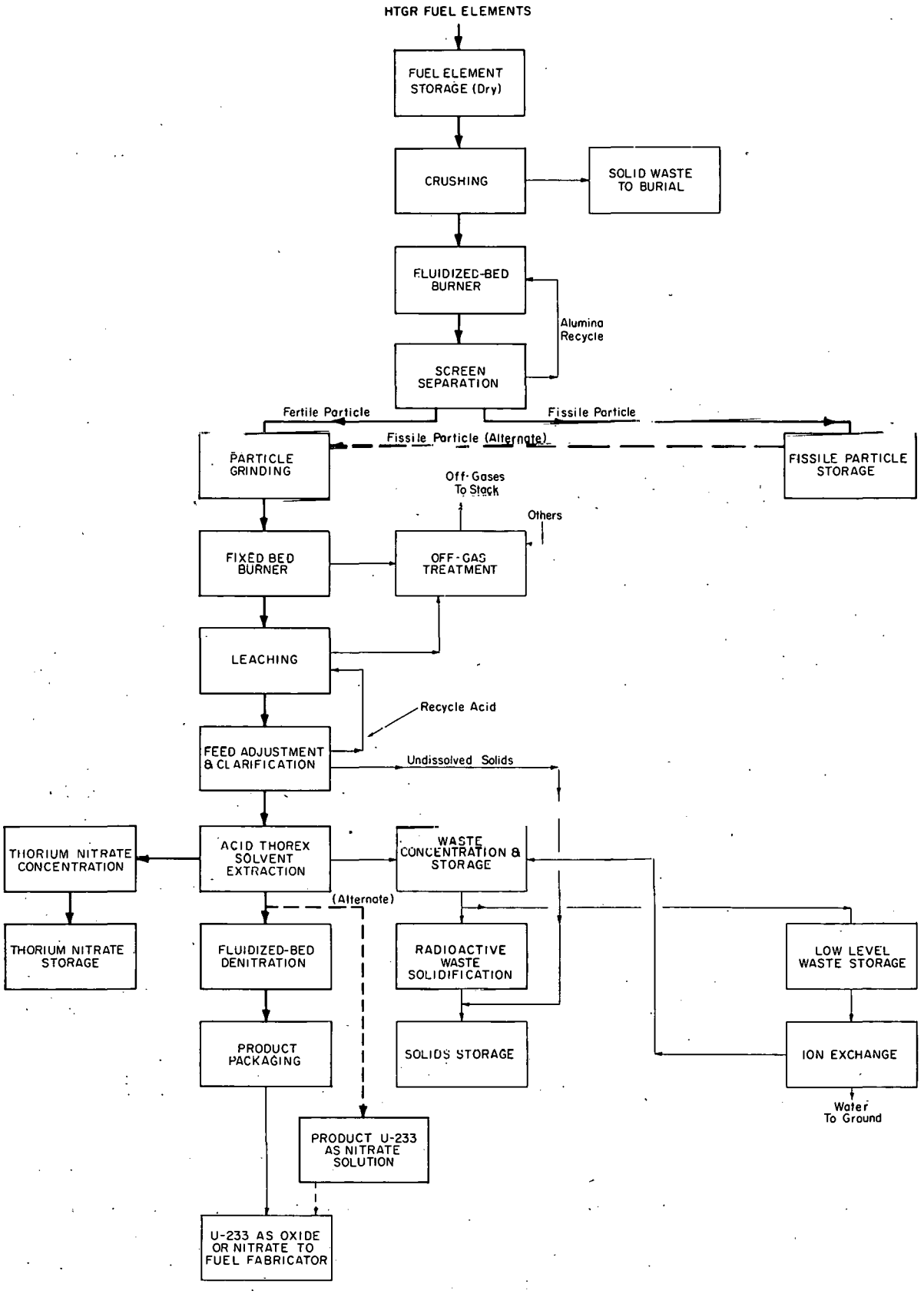

Fig. 30 Block flow diagram of HTGR reference plant process.

or not the tests and performance levels measured were meaningful in terms of the desired application. A detailed description of the studies and results has been published in report IN-1253 [36]; a summary of the principal areas of study and the findings is reported here.

Tests were designed to examine coatings for the following characteristics:

(1) Ease and reliability of application

(2) Repairability

(3) Resistance to gamma irradiation and steam

(4) Resistance to steam at elevated temperature and pressure

(5) Resistance to dilute bases used in containment structure pressure reduction spray systems

(6) Nonsorption of sodium borate (nuclear poison) from emergency core cooling systems

(7) Ability to seal small imperfections in a containment structure surface

(8) Resistance to high pressure steam jets.

The tests were verified by applying them to five coating systems shown earlier to have excellent resistance to radiation, chemicals, and pressurized steam. Except for the steam jet test, the tests studied were successful in determining whether or not the coating systems had the desired characteristics. The steam jet test was not initially done on a large enough scale to produce meaningful results, and scale-up of the test, in the current program, was not feasible. The results obtained with the specific coatings tested clearly indicate that there are products available which can give the performance required in nuclear reactor containment structures under accident conditions. The test conditions and the levels of performance sought, except for the steam jet test, all appear to be significant in terms of the projected application and the capabilities of commercially available coatings.

2.3 Chemical Treatment of Test Reactor Fuel Elements to Minimize Formation of Boehmite Film (C. A. Zimmerman; Chemistry Section)

A corrosion product film, identified as boehmite (α-Al_2O_3-H_2O), forms on aluminum alloy 6061-0 fuel plate cladding when it is exposed under conditions similar to those anticipated in the Advanced Test Reactor. The accumulation of this oxide of low thermal conductivity could shorten the service life of the fuel elements. Both a mid-cycle cleaning treatment, which removes the oxide film and permits further use of the fuel, and a preirradiation conditioning, which slows the rate of film growth, are being developed. The latter appears more practical since it would be done on the unirradiated fuel element.

Mid-Cycle Cleaning Treatment

A special mid-cycle cleaning treatment for removal of the boehmite was proposed after literature review and preliminary laboratory investigation[13]. This cleaning treatment involved the immersion of the coated aluminum in a boiling 1 M phosphoric acid - 0.4 M chromium trioxide solution for one hour followed by a water wash and immersion of the aluminum in a boiling 3 M nitric acid solution for three minutes. This last step is done to remove a phosphorous containing surface film remaining after the boehmite removal step. Metal loss from the two-step cleaning procedure is not expected to exceed about 0.2 mils of aluminum as general corrosion. Further investigation of this procedure has demonstrated that it is effective in cleaning of aluminum alloy 1100- and 6061-clad fuel plates that have been exposed in reactor core environments.

Preirradiation Conditioning

During the investigation of the proposed mid-cycle cleaning procedure, it was observed that cleaned aluminum upon which a coating of bayerite (β-Al_2O_3-$3H_2O$) was developed (during exposure in distilled water at 60°C) did not form the boehmite coating as fast as the "as-received" aluminum with an air-formed oxide film. An attempt to confirm this observation has been made using specially prepared aluminum alloy 6061-0 coupons.

These coupons were first exposed in aerated distilled water at 60°C for varying lengths of time to determine the rate of growth of the bayerite film. It was apparent that this film undergoes its maximum thickness growth during the first 168 hours of exposure and that, at 168 hours, the thickness of the bayerite film formed was less on the chemically cleaned specimens (0.13 mil) than on the "as-received" specimens (0.31 mil). Film thickness measurements were made using an eddy-current apparatus (Permascope). X-ray diffraction analysis verified that the film formed in the aerated distilled water at 60°C was bayerite.

To determine the response of treated and untreated surfaces in a reactor environment, four coupons representing the aluminum alloy in (a) the "as-received", (b) the "as-received and water treated", (c) the "chemically cleaned", and (d) the "chemically cleaned and water treated" condition were exposed in the Reactor Engineering Corrosion Loop[37] for a total of 292 hours at 350°F (177°C) and pH of 5.0 to 5.3 with a flow rate of 45 fps. Film thickness measurements are shown in Figure 31. Each value presented represents the average of a minimum of five measurements of film thickness. The specimen in the "as-received" condition has the greatest film growth while the "chemically cleaned and water conditioned" specimen undergoes the least amount of boehmite growth.

"Chemically cleaned and conditioned" aluminum specimens and specimens in the "as-received" condition have also been tested in distilled water in an autoclave. Preliminary data on film growth in an autoclave under simulated reactor conditions are shown in Figure 32. At 210°C, a relatively high temperature for the water in the reactor, film growth begins immediately and proceeds for about 10 days at a relatively high rate on the "as-received" specimens. The specimens which were conditioned started with a thin coating of bayerite;

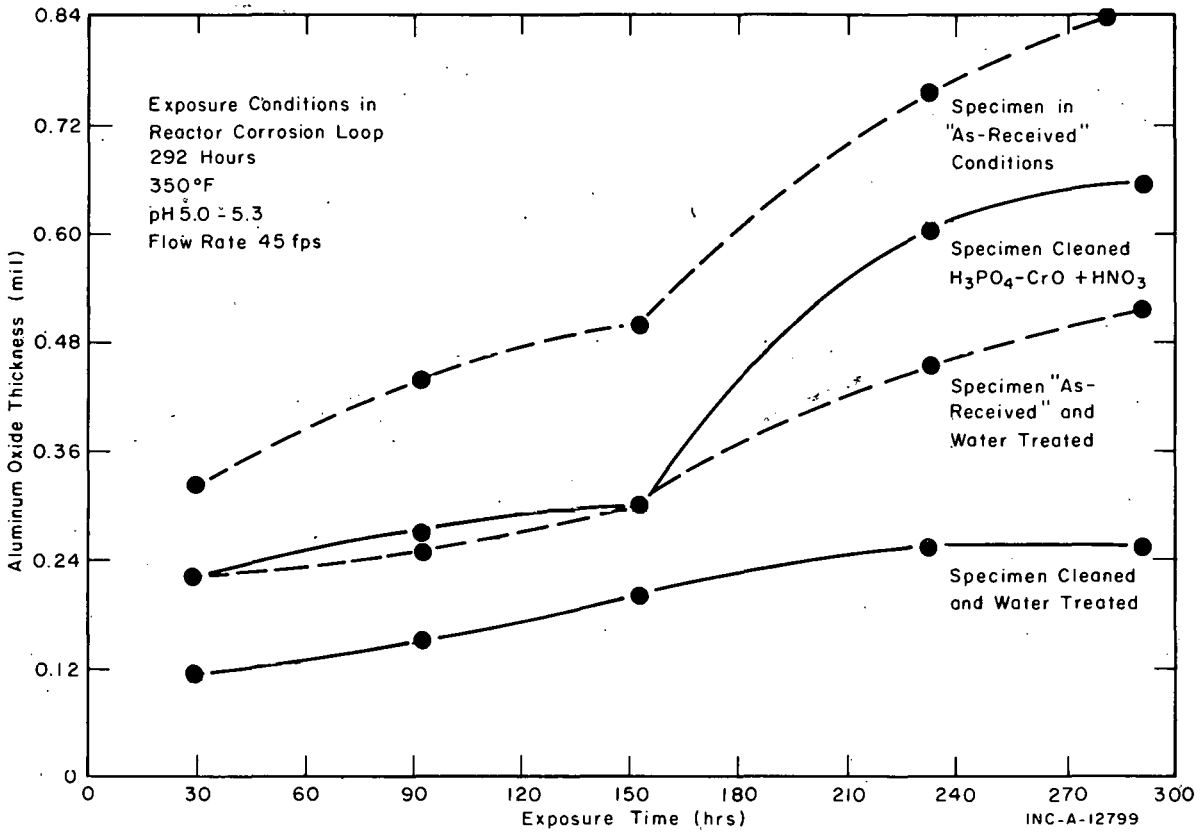

Fig. 31 Oxide film buildup on Type 6061 aluminum.

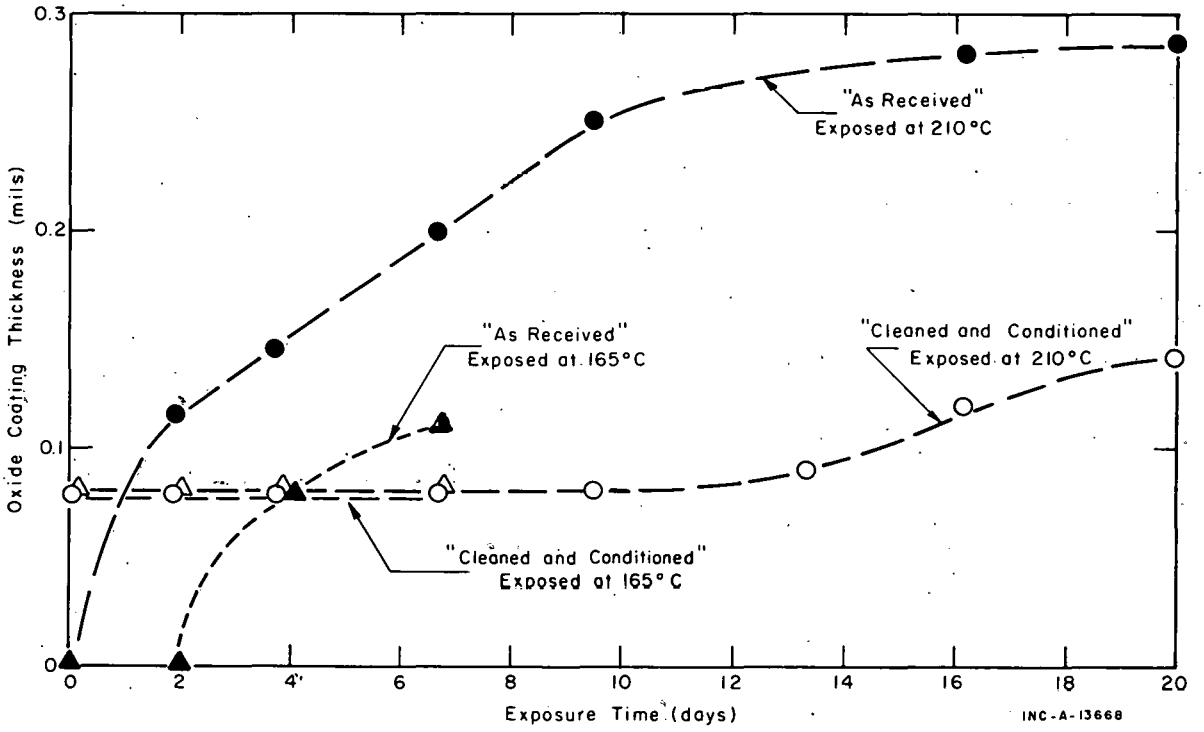

Fig. 32 Film growth under simulated reactor conditions.

at 210°C this film converted slowly to boehmite over a period of about 14 days without any significant increase in thickness; then a slow growth of boehmite started. At 17 operating days, the design life of the fuel element, the film thickness on the conditioned specimens was significantly less than on the specimens in the "as-received" condition. At 165°C, there is a brief induction period before rapid film growth starts; but even at this lower temperature and film growth rate, the film thickness on "as-received" specimens at six days exceeds that on the conditioned specimens exposed at the higher temperature. Previous experience has indicated that film growth rates in a reactor are generally greater than those experienced in autoclave tests; therefore, the film thicknesses shown in Figure 32 are representative of significant films under reactor conditions.

Examination of this conditioning procedure is currently being undertaken to determine whether the reduction in film growth observed can be obtained under reactor conditions of radiation and high thermal flux. Investigation of methods of application of the chemical cleaning and water conditioning as well as other variations in the procedure will also be continued.

An aluminum specimen fabricated to have narrow channels simulating a reactor fuel element has been cleaned and conditioned in the laboratory. The aluminum was evenly cleaned and the bayerite coating formed was uniform when checked using an eddy current film thickness gauge. No signs of pitting or accelerated attack were observed on this test specimen.

2.4 Manufacture of Uranium Aluminide Employing Fluidized-Bed Techniques (E. S. Grimmett and G. W. Hogg; Development Engineering)

Uranium aluminide compounds have desirable properties for use as fuel in test reactors and possibly power reactors. A potentially efficient process is under development for producing nuclear-fuel-quality uranium aluminide using fluidized-bed technology; the process reactions and theory have been discussed in detail in earlier reports [13, 1]. In this process, uranium aluminide is produced from uranyl nitrate and aluminum powder without the costly intermediate production of uranium metal. Uranium aluminide samples of increasing purity have been produced by the process, and no apparent insurmountable obstacles have thus far been uncovered.

The fluidized-bed process is based on four consecutive reactions:

(1) $UO_2(NO_3)_2 \xrightarrow{350°C} UO_3$ (on an aluminum powder base)

(2) $UO_3 \xrightarrow[370°C]{CH_3OH} UO_2$

(3) $UO_2 \xrightarrow[400°C]{CCl_4} UCl_3$

(4) $UCl_3 + Al \xrightarrow{700°C} UAl_3$.

Air is used as the fluidizing gas in the first reaction and argon in the subsequent reactions.

Description of Experimental Equipment

Recent efforts have concentrated on the development of satisfactory experimental equipment for small-scale production of UAl_3 in a two-inch diameter fluidized bed. The design and operation of the equipment requires special attention due to the high operating temperatures, the difficulties of fluidizing the aluminum particles while simultaneously atomizing the uranyl nitrate feed in the fluidized bed, and the prevention of alpha contamination in the laboratory.

Heat has been supplied to the fluidized bed by external resistance heaters, supplemented in some cases with internal calrod heaters. A slit-plate-type grid to support the fluidized bed results in reasonably good fluidization over the required range of fluidizing velocity and temperature.

The diameter of the fluidizing vessel is purposely small to reduce criticality problems when processing U-235 compounds and to allow small-scale testing. The two-inch diameter fluidized bed is very sensitive to atomizing air velocities and fluidizing conditions. If the atomizing velocity is too high, the uranyl nitrate is spray dryed (never contacts aluminum particles as a liquid) or the UO_3 coating is removed from the aluminum particles by abrasive action. If the fluidizing velocity is too high, the fluidized bed becomes transparent to the uranyl nitrate spray. If the atomizing or fluidizing velocities are too low, bed caking results from the poor heat transfer within the bed. Hence, current effort has been to firmly establish the effects of these variables on particle coating and fragmentation.

Alpha-particle contamination is minimized by operating the equipment in a controlled-atmosphere glovebox and filtering the off-gas. When performing experiments which employ enriched uranium, the process equipment is operated through sealed glove ports.

Experimental Results to Date

Testing to date indicates that the smallest particle-size range that can be readily coated in the present equipment using current methods is approximately 200 to 250 mesh. However, with further development or improved equipment it appears practical to coat particles as small as 300 mesh. The desired final-product particle size range is 170 to 350 mesh; to obtain this size, an original minimum particle size of the aluminum of approximately 190 mesh would be required, followed by plasma are densification of the resulting hollow spheres of uranium aluminide to less than 10% voids.

Contamination of product samples with UO_2, UCl_3, Al_2O_3, carbon, and aluminum has been a major problem recently. Also, the uranium aluminide compounds have ranged from UAl_2 to UAl_3 or UAl_4. A recent 200-g sample submitted for metallurgical testing contained approximately 82% UAl_3 (87% enriched), 17% Al_2O_3, 0.06% chloride, and 1% UO_2. It is believed that the Al_2O_3 was formed due to the reaction of UO_2 and Al and that more complete chlorination might remove the Al_2O_3.

The results of the experimental runs indicate the solution to the problem of producing quality uranium aluminide compounds involves accurately determining (a) the initial uranium to aluminum ratio, (b) the reaction end points, (c) the optimum operating temperatures, and (d) the optimum amount of aluminum nitrate additive.

In determining the correct initial uranium to aluminum ratio, allowances must be made for aluminum losses due to attrition and side reactions and for uranium losses due to spray drying, formation of volatile side products, and pulverization due to the abrasive action of the fluidized particles.

The determination of the reaction end point is particularly important in the chlorination step. If chlorination is not complete, UO_2 is present in the final product, and if the material is excessively chlorinated the aluminum to uranium ratio in the final product is reduced and excessive UCl_3 remains in the product. The usual end point indicators such as sudden temperature deviations or visible changes in the off-gas are not useful because of the gradual depletion of reactant.

Operating temperature is very important in the chlorination and high-temperature conversion reactions due to the possible formation of an impermeable crust on the particles that alters the extent of the reactions by occluding the reactant.

Aluminum nitrate is added to the uranyl nitrate solution to produce reactive UO_3. Excessive aluminum nitrate reacts to form Al_2O_3, and insufficient aluminum nitrate requires high temperatures and results in undesirable side reactions during the reduction step.

Theoretical and Experimental Studies in Progress

Theoretical studies have been developed and experimental studies are in progress to help provide the information necessary to produce quality uranium aluminide compounds. The theoretical studies include the development of mathematical models for the reaction steps which involve diffusion with chemical reaction. The purpose of the models, which are basically the fixed-particle-size, unreacted-core type, is to allow prediction of the extent of the reaction and to provide insight into the effect of the many variables (particle size, concentration of reactants, diffusion rates, temperature of reaction, etc) on product quality. Theoretical studies are expected to contribute to the determination of the reaction end points, optimum operating temperatures, and optimum concentration of additives.

The purpose of the experimental studies is to provide quantitative evidence of the effect of various operating conditions on product quality, to supply data for validating the mathematical models, and to provide product samples of UAl_3 for metallurgical testing. Tests are in progress to determine the most effective operating temperature for each reaction step, the change of U/Al ratio in each step, and the effect of aluminum nitrate, methanol, and CCl_4 concentration on product quality. Curves of experimentally determined reaction rate versus time and temperature are expected to indicate the nature of the process (gas film diffusion controlling, ash diffusion controlling, chemical

reaction controlling, etc). On-stream end-point indicators, such as chloride-ion detectors, are being investigated as an additional possibility for improving end point detection.

2.5 Fission Product Release from Heated Bulk Uranium Aluminide Fuels

(R. R. Hammer and D. E. Black; Reactor Safety Studies Section)

A series of tests are being conducted, in cooperation with the Analytical Chemistry Branch, to determine the release of noble gas and long-lived fission products (primarily Cs-137, Ru-106, and Sb-125) from irradiated, bulk, uranium aluminide fuel specimens. The releases are determined by heating a fuel specimen to progressively higher temperatures and collecting, quantitatively, the fission products released. A schematic flowsheet of the experiment is shown in Figure 33. The principal items of equipment, in sequence, are (a) the

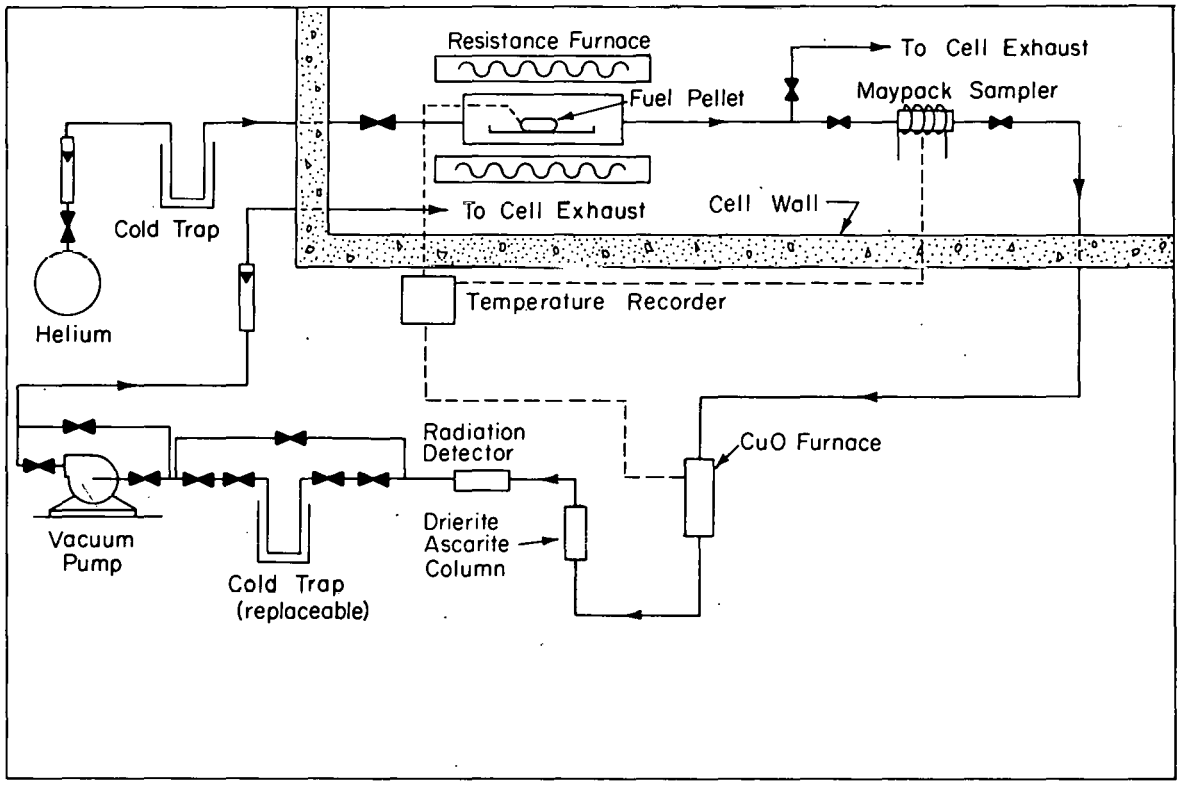

Fig. 33 Flowsheet of uranium-aluminide fission product release experiment.

furnace in which the fuel specimen is heated, (b) Maypack-type samplers containing high efficiency particulate filters and impregnated charcoal cartridges which retain the nonnoble gas fission products, (c) a CuO furnace which converts any organic materials (which interfere with the quantitative analyses of the noble gases) released from the fuel to CO_2, (d) a "Drierite-Ascarite" column which removes CO_2 and H_2O vapor from the gas stream, (e) a radiation monitor which determines the time at which Kr-85 is released from the fuel, and (f) replaceable cold traps cooled with liquid nitrogen and containing Linde type 5A Molecular Sieve which quantitatively retains the noble gases released from the fuel.

To date, four tests have been completed -- two on UAl_4 and two on UAl_3 bulk fuel specimens. Preliminary results indicate the major release of the noble gases and cesium occurs near the uranium aluminide peritectic reaction temperatures (~1350°C for UAl_3 and 730°C for UAl_4), both during heating and cooling of the fuel specimen. Smaller releases start at temperatures 100 to 200°C below the major release temperature and continue through the melting temperature of the fuel specimen. Releases of antimony and ruthenium, however, occur well below the peritectic temperatures. The magnitude of the noble gas and long-lived fission product releases has not yet been determined. Future tests will be conducted on UAl_3, UAl_4, UAl alloy, and UO_2 bulk fuel specimens.

IV. IDAHO NUCLEAR CORPORATION ORGANIZATIONAL CHART *

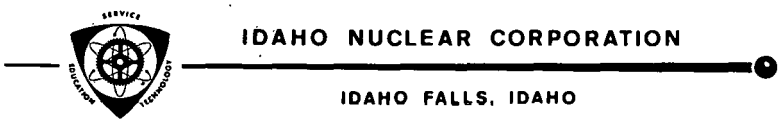

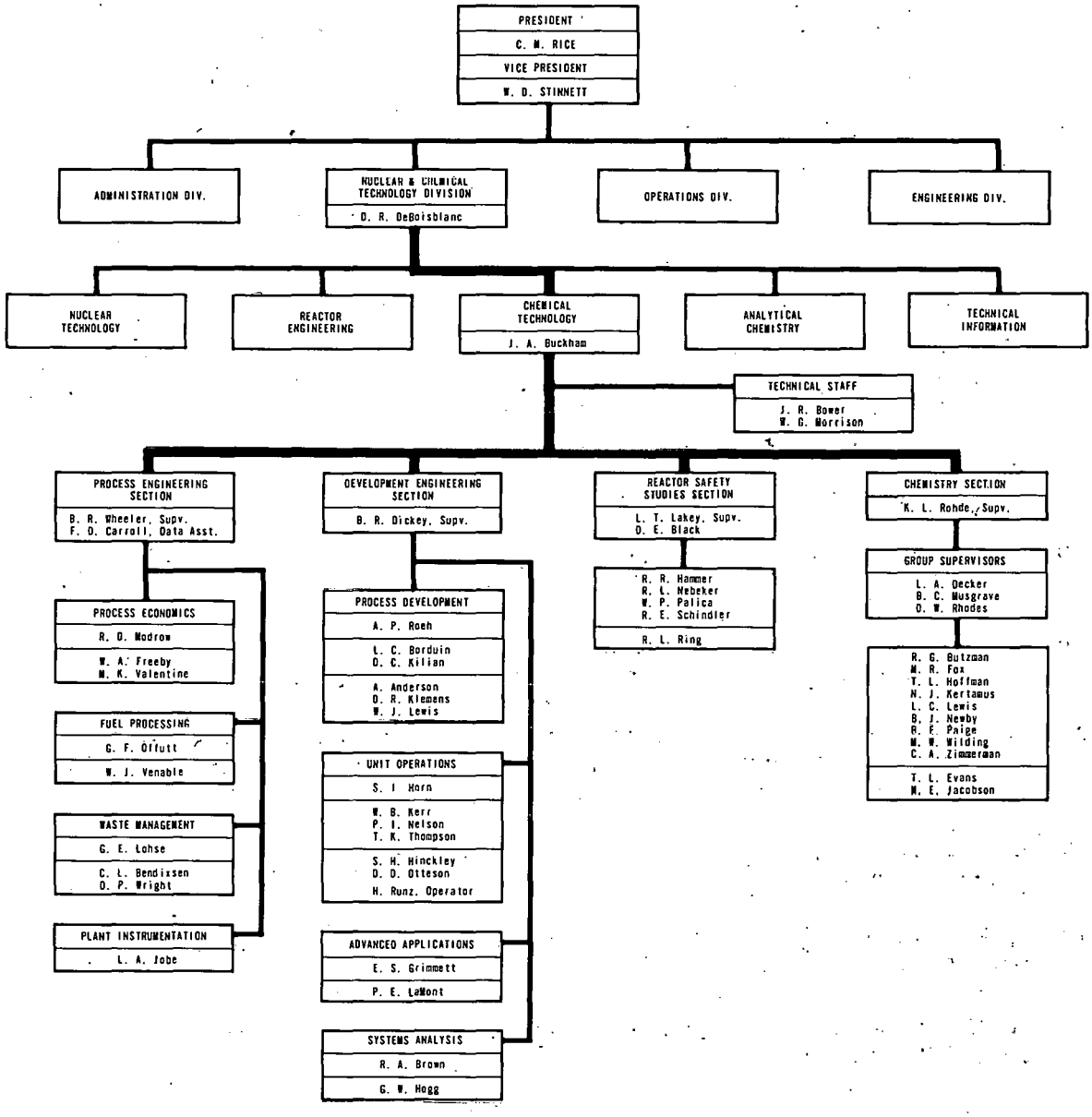

* ABBREVIATED CHART SHOWING THE RELATIONSHIP OF THE CHEMICAL TECHNOLOGY BRANCH WITHIN THE CORPORATION ORGANIZATION.

V. REFERENCES

1. J. R. Bower (ed.), Chemical Technology Branch Annual Report -- FY-1968, IN-1201 (October 1968).

2. B. E. Paige, G. W. Gibson, and K. L. Rohde, The Effect of Silicon on Fabrication and Reprocessing of Aluminum Alloy Reactor Fuels, IN-1194 (November 1968).

3. B. E. Paige, K. L. Rohde, and B. J. Newby, Emulsion Control in Liquid-Suspension Extraction, U. S. Patent 3,154,376 (October 1964).

4. H. J. Groh, Removal of Silica from Solutions of Nuclear Fuels, DP-293 (June 1958).

5. D. H. Cranney and B. C. Musgrave, Factors Influencing the Rate of Silica Gel Formation in High Acid-Salt Solutions, IN-1270 (February 1969).

6. G. W. Gibson, The Development of Powdered Uranium-Aluminide Compounds for Use as Nuclear Reactor Fuels, IN-1133 (December 1967).

7. U. S. Atomic Energy Commission, "Safety Standards for the Packaging of Radioactive and Fissile Materials", in AEC Manual, Book 2, Chapter 0529, Washington, D. C.: U. S. Atomic Energy Commission, revised 1969.

8. B. Elliot and J. Nelson, Process Development Quarterly Report, Part II, Pilot Plant Work, MCW-1411 (February 1958).

9. W. J. Venable, W. G. Morrison, and G. F. Offutt, Safety Analysis Report for the ICPP Denitration Process, IN-1293 (1969).

10. G. Pierini and J. Schmets, Some Aspects of Volatility Processes for Reactor Fuel Elements Containing Carbon, BLG-331 (June 1965).

11. E. Lopez-Menchero, G. Vermeulen, and E. Detilleux, Some Possibilities of Aqueous Processing of Graphite-Carbide Fuel Elements, Eurochemic Technical Report No. 172, NP-15753 (June 1965).

12. L. A. Decker, ICPP Laboratory Studies on a Combustion-Nitric Acid Leach Process for Rover Fuels (Classified), IDO-14659 (November 1965).

13. J. R. Bower (ed.), Chemical Technology Branch Annual Report -- FY-1967, IN-1087 (October 1967).

14. B. C. Musgrave (ed.), Chemical Development for EBR-II Fuel Processing, 1967-1969, IN-1285 (1969).

15. C. M. Slansky, K. L. Rohde, and H. T. Hahn, Review of Research and Development at the Idaho Chemical Processing Plant on the Electrolytic Dissolution of Nuclear Fuel, IDO-14535 (February 1961).

16. L. C. Lewis and B. C. Musgrave, Electrolytic Behavior of Cladding Alloys for Nuclear Fuels, IN-1295 (1969).

17. R. D. Fletcher, M. E. Jacobsen, and H. R. Beard, Effect of Alloying Constituents on Aluminum Dissolution Rates, IDO-14606 (April 1963).

18. D. H. Cranney, M. E. Jacobsen, and B. C. Musgrave, Clarification of Electrolytic Dissolver Solution Using a Hydrocyclone, IN-1276 (April 1969).

19. D. W. Rhodes, Measurement of Fission Product Leakage from Fuel Elements Stored in Water, IDO-14654 (March 1965).

20. J. T. Waber, An Analysis of Project Data on the Corrosion of Uranium in Various Media, LA-1381 (December 1948).

21. J. T. Waber, A Review of the Corrosion of Uranium and Its Alloys, LA-1524 (November 1952).

22. J. R. Bower (ed.), Chemical and Process Development Branch Annual Report -- FY-1966, IDO-14680 (October 1966).

23. C. L. Bendixsen and G. E. Lohse, Storage Facilities for Radioactive Calcined Waste Solids at the Idaho Chemical Processing Plant, IN-1155 (July 1968).

24. M. W. Wilding and D. W. Rhodes, Leachability of Zirconia Calcine Produced in the Idaho Waste Calcining Facility, IN-1298 (June 1969).

25. T. K. Thompson, Development of In-Bed Combustion Heating for Calcination of Radioactive Wastes, IN-1278 (1969).

26. L. T. Lakey, Plant Tests on the Decomposition of Nitrous Oxide Over a Heated Rhodium Catalyst, IDO-14545 (April 1961).

27. J. H. Zufall and H. S. Miller, Decomposition of Nitrous Oxide -- Final Report, IDO-14513 (July 1960).

28. R. C. Shank et al, Analytical Chemistry Branch Annual Report FY-1969, IN-1316 (September 1969).

29. R. E. Schindler et al, Development of a Continuous Sampler-Monitor for the LOFT Containment Atmosphere: Current Status, 1968, IN-1309 (1969).

30. K. A. Dietz (ed.), Quarterly Technical Report -- LOFT Program Office -- July 1 - September 30, 1968, IDO-17266 (February 1969).

31. B. J. Newby, Applicability of Chemically Removable Coatings to Reactor Containment Buildings, IN-1170 (August 1968).

32. J. J. DiNunno et al, Calculation of Distance Factors for Power and Test Reactor Sites, TID-14844 (March 1962).

33. U. S. Atomic Energy Commission, "Standards for Radiation Protection", in AEC Manual, Book 2, Chapter 0524, Washington, D. C.: U. S. Atomic Energy Commission, revised 1968.

34. U. S. Atomic Energy Commission, "Prevention, Control, and Abatement of Air and Water Pollution by Federal Activities", in AEC Manual, Book 2, Chapter 0510, Washington, D. C.: U. S. Atomic Energy Commission, revised 1968.

35. U. S. Atomic Energy Commission, Summary Report: AEC Reference Fuel-Processing Plant, WASH-743 (October 1957).

36. B. J. Newby, K. L. Rohde, and W. T. Jordan, Development of Testing Procedures for Protective Coatings to be Used in Nuclear Reactor Containment Structures, IN-1253 (February 1969).

37. G. W. Gibson, M. J. Graber, and W. C. Francis, Annual Progress Report on Fuel Element Development, IDO-16934 (November 1963).

VI. REPORTS AND PUBLICATIONS ISSUED DURING FY-1969

1. IDAHO NUCLEAR REPORTS

1. W. P. Palica and M. D. Gold, Uranium Recovery from Aluminum Alloyed Fuel at ICPP -- During FY-1966, IN-1153 (June 1969).

2. C. L. Bendixsen and G. E. Lohse, Storage Facilities for Radioactive Calcined Waste Solids at the Idaho Chemical Processing Plant, IN-1155 (July 1968).

3. B. J. Newby, Applicability of Chemically Removable Coatings to Reactor Containment Buildings, IN-1170 (August 1968).

4. W. A. Freeby, L. T. Lakey, and D. E. Black, Fission Product Behavior Under Simulated Loss-of-Coolant Accident Conditions in the Contamination-Decontamination Experiment, IN-1172 (January 1969).

5. T. L. Hoffman, Corrosion Experience with Type 316 Stainless Steel in Sodium-Potassium Eutectic Alloy at 1400 °F, IN-1185 (October 1968).

6. L. C. Lewis, The Physical Properties of Nitrate Solutions of EBR-II Fuel Elements, IN-1192 (August 1968).

7. B. E. Paige, G. W. Gibson, and K. L. Rohde, The Effect of Silicon on Fabrication and Reprocessing of Aluminum Alloy Reactor Fuels, IN-1194 (November 1968).

8. L. A. Decker and R. G. Butzman, Chemical Feasibility of Three Methods for Reprocessing Advanced Fuels (Classified), IN-1198 (August 1968).

9. G. F. Offutt and C. L. Bendixsen, Rare Gas Recovery Facility at the Idaho Processing Plant, IN-1221 (April 1969).

10. B. J. Newby, K. L. Rohde, and W. T. Jordan, Development of Testing Procedures for Protective Coatings to be Used in Nuclear Reactor Containment Structures, IN-1253 (February 1969).

11. D. H. Cranney and B. C. Musgrave, Factors Influencing the Rate of Silica Gel Formation in High Acid-Salt Solutions, IN-1270 (February 1969).

12. P. E. LaMont, Pilot-Plant Testing of a Two-Phase Vortex Fluid Amplifier for Liquid Flow Control, IN-1271 (March 1969).

13. D. H. Cranney, M. E. Jacobson, and B. C. Musgrave, Clarification of Electrolytic Dissolver Solution Using a Hydrocyclone, IN-1276 (April 1969).

14. M. W. Wilding and D. W. Rhodes, Leachability of Zirconia Calcine Produced in the Idaho Waste Calcining Facility, IN-1298 (June 1969).

2. PAPERS PRESENTED AT TECHNICAL SOCIETY MEETINGS

1. G. E. Lohse, B. M. Legler, and M. P. Hales, "Calcination of Zirconium Fluoride Wastes in Pilot and Plant-Scale Fluidized Beds", from Tripartite Chemical Engineering Conference, Montreal, Canada (September 1968).

2. C. L. Bendixsen and G. E. Lohse, "Experience with Non-Mechanical Solids Flow Control Devices in the Waste Calcining Facility", from Symposium on Storage, Flow, and Handling of Solids, Materials Handling Engineering Division of the ASME, Boston, Massachusetts (October 1968).

3. A. P. Roeh, D. C. Kilian, and B. R. Dickey, "Separation of Uranium from Graphite Based Fuels by Fluidized-Bed Combustion", from American Institute of Chemical Engineers Annual Meeting, New Orleans, Louisiana (March 1969).

4. B. J. Newby and K. L. Rohde, "Protective Coatings in Nuclear Reactor Containment Structures", from American Chemical Society 157th National Meeting, Minneapolis, Minnesota (April 1969).

5. J. A. Buckham, "Status of Reprocessing of Highly Radioactive Fuels in the USA", from IAEA Panel on Reprocessing of Highly Irradiated Fuels, Vienna, Austria (May 1969).

6. J. R. Bower and J. A. Buckham, "Control of Fission Product Activity During Short-Cooled Fuel Processing Connected with the ICCP RaLa Process", from IAEA Panel on Reprocessing of Highly Irradiated Fuels, Vienna, Austria (May 1969).

7. K. L. Rohde and J. A. Buckham, "Effect of Irradiation on the Dissolution Characteristics of Important Fuel and Cladding Materials", from IAEA Panel on Reprocessing of Highly Irradiated Fuels, Vienna, Austria (May 1969).

8. D. E. Black, "Radioactive and Fissionable Materials", from American Institute of Chemical Engineers Meeting, Cleveland, Ohio (May 1969).

9. L. T. Lakey and D. E. Black, Behavior of Iodine at Low Concentrations, presented at Spray Technology Symposium at meeting of ANS, Seattle, Washington (June 1969).

10. N. J. Kertamus and R. G. Butzman, "Behavior of Anodic Niobium and Cathodic Corrosion of Titanium, Both in Nitric Acid", from American Chemical Society Northwest Regional Meeting, Salt Lake City, Utah (June 1969).

3. OTHER PUBLICATIONS

1. B. E. Paige and K. L. Rohde, "Effect of Metallurgical Composition of Aluminum-Uranium-Silicon Fuels on Chemical Reprocessing", Nucl. Appl., 5 n 4 (October 1968) pp 218-223.

2. D. E. Black and S. J. Horn, "Radioactive Material in Pilot Plants", Chem. Eng. Prog., 64 n 10 (October 1968) pp 43-49.